



**Politecnico
di Torino**



COPPE
UFRJ
Instituto Alberto Luiz Coimbra de
Pós-Graduação e Pesquisa de Engenharia

Master Dissertation
Master of Science Program in Civil Engineering (LM-23)

An Experimental Campaign on the Use of Flax-TRMs for Seismic Strengthening of Masonry Structures

By

Iftiaz Hussain

Supervisors:

Prof. Alessandro Pasquale Fantilli, Supervisor
Prof. Romildo Dias Toledo Filho, Co-Supervisor

Politecnico di Torino
2023

Declaration

I hereby declare that the contents and organization of this dissertation constitute my own original work and do not compromise in any way the rights of third parties, including those relating to the security of personal data.

Iftiaz Hussain

2023

* This dissertation is presented in partial fulfillment of the requirements for **Master of Science Program in Civil Engineering** at Politecnico di Torino.

I dedicate this thesis to my parents.

Acknowledgments

First and foremost, I would like to thank the God Almighty for all the blessings that enabled me to be where I am today.

I would like to express my gratitude and thanks to my principal supervisor Prof. Alessandro Pasquale Fantilli for providing me with the platform and opportunity for Thesis Abroad and his thorough guidance throughout this experimental program.

I would also like to thank my co-supervisor Prof. Romildo Dias Toledo Filho for accepting me in his lab and welcoming me with open arms. His guidance and support regarding the development of the research program has been fundamental for in-time procurement of the materials and completion of the experiments.

I would also like to extend my special thanks to Dr. M'hamed Yassin da Gloria, Thais Sequeira, Joaquin H. Aquino Rocha and all the colleagues and staff at NUMATS lab for their continuous support throughout my stay at UFRJ, Brazil.

I would like to extend special gratitude to my friend Debora Bellu for her material support and my friend and colleague Navjit Kaur for her selfless support during the difficult times. It would not have been possible for me to go for thesis abroad if it was not for Navjit's efforts during the application procedure.

Last but not the least, my sincere thanks to my family and friends for all their prayers, always believing in me, and letting me be me.

ABSTRACT

Past earthquakes have shown that conventional masonry buildings are often most vulnerable to damage in case of an earthquake. Several approaches have been deployed in the past to strengthen the masonry structures against extreme loading events. One of the most widely used strengthening mechanisms is the application of externally bonded inorganic composite systems on masonry substrate. In recent years, with a focus on environmental conservation and sustainability, there are continuous efforts to use eco-friendly materials and innovative methods in construction instead of conventional materials and methods. Several studies have been conducted in the past to characterize such materials and to determine their suitability for short- and long-term applications. One such class of composite materials is the Natural Fiber Reinforced Cementitious Matrixes (NFRCMs) or Natural Textile Reinforced Mortars (N-TRMs). N-TRMs consist of layer/s of plant-based uni- or bi-directional textile embedded in the inorganic mortar matrix that can enhance the tensile and toughness properties of the substrate. Different studies have been conducted in the past on plant-based textiles such as jute, sisal, hemp, flax and other commonly produced natural textiles for their characterization and eventual determination of mechanical response of the composite systems in which they are embedded. However, there is still a considerable research gap to study the effects of textile pretreatment, mortar mix design and textile reinforcement amount on TRM performance.

This experimental campaign characterizes the plant-based bi-directional flax fabric locally produced in Italy and further studies the mechanical properties of flax-TRMs with different amounts of textile reinforcement. The inorganic matrix used in this study is designed keeping in view the sustainability principles to have the least environmental impact. The experimental plan reports the tensile properties of individual flax yarns, threads and subsequently the fabric strips while determining the change in these properties with a proposed pre-treatment. It further investigates the microscopic structure and pull-out behavior of pre-treated and untreated flax threads from the mortar while extending the study to introduce pretreated short jute fibers into the mortar matrix and reports its effect on the composite system's mechanical response. Eventually, masonry assemblages are prepared and reinforced with different flax-TRMs studied in the first phase to correlate the response of diagonal compression test on walls with tensile response of composite prisms.

The experimental results found that with pre-treatment, flax-TRM's mechanical performance in terms of peak tensile strength and reduced crack width is considerably improved. The study further compares the response of textile embedded in normal mortar to the textile embedded in fiber-reinforced mortar. The results show a considerable improvement of tensile strength and reduction in crack width of flax-TRMs embedded in fiber-reinforced mortar in comparison to conventional mortar. Additionally, the experimental test results on masonry wall assemblage prove the enhanced peak load capacity and a higher post peak strength gain of the masonry units reinforced with pretreated flax-TRMs in comparison to untreated flax-TRMs. Nonetheless, this study lays the foundation for further research to enhance the mechanical response of flax-TRMs adapting sustainable alternatives.

Table of Contents

1	Introduction	1
1.1.	Background	1
1.2.	Thesis Structure.....	2
1.3.	Research Context.....	3
2	Literature Review	4
2.1.	Textile Reinforced Mortars	5
2.2.	Tensile Test on TRM.....	7
2.3.	Diagonal Compression Test	11
2.4.	Plant Based/Natural Fibers in TRM Composites	12
2.4.1.	Plant Fibers	13
2.4.2.	Natural Textile Reinforced Mortars (N-TRMs).....	19
3	Characterization of Flax Textile	23
3.1.	Flax Fabric Pre-treatment.....	24
3.2.	Physical Characterization.....	25
3.3.	Mechanical Characterization.....	27
3.3.1.	Methods.....	27
3.3.2.	Results and Discussion.....	32
4	Characterization of Flax-TRMs.....	39
4.1.	Tensile Tests on Flax-TRM Prisms.....	39
4.1.1.	Materials	39
4.1.1.1.	Sand	39
4.1.1.2.	Jute Fibers.....	40
4.1.1.3.	Mortar	41
4.1.1.4.	Flax Fabric	42
4.1.2.	Methods.....	43
4.1.3.	Results and Discussion.....	46
4.2.	Pull-out Tests on Flax-Mortar Interface.....	54
4.2.1.	Materials & Methods	54
4.2.2.	Results & Discussion	56
5	Mechanical Behavior of Masonry Assemblage Externally Bonded with Flax-TRMs.....	58
5.1.	Materials and Methods	58
5.2.	Results and Discussion.....	62
6	Conclusions and Recommendations	73
6.1.	Main Conclusions.....	73

6.2. Recommendations	74
References.....	1

List of Figures

Figure 2.1 - Basalt textile grid application on masonry wall [3].	6
Figure 2.2 - PBO mesh used for intradoxal strengthening of concrete arch bridge [3].	6
Figure 2.3 - Masonry vault intradoxal strengthening with AR Glass fiber grid & mortar [3].	6
Figure 2.4 - Column confinement with AR Glass fiber grid & mortar [3].	7
Figure 2.5 - Beam shear strengthening with PBO fiber grid embedded in mortar [3].	7
Figure 2.6 - Tensile test specimen geometry [9].	8
Figure 2.7 - Tensile test arrangement [9].	9
Figure 2.8 - Tensile response curve of a classical TRM [11].	10
Figure 2.9 - Failure mechanisms of a classical TRM [11].	11
Figure 2.10 - Diagonal cracking of clay brick wall [13].	12
Figure 2.11 - Flax fiber schematic macro- and nano-scopic structure [18].	15
Figure 2.12 - Flax fiber schematic macro- and nano-scopic structure [21].	17
Figure 2.13 - E-Glass versus Natural fibers: a) cost per unit weight of fibers; b) cost per quantity of fibers having capacity to take 100 kN tensile load [22].	17
Figure 2.14 - Tensile strength versus embodied energy of fibers and composites [21].	18
Figure 2.15 - Pull-out test setup of a natural fiber from mortar [23].	19
Figure 2.16 - Tensile response of flax-TRMs with different layers of textile [29].	20
Figure 2.17 - Tensile response of flax-TRMs with one and two layers of textile [30].	21
Figure 2.18 - No. of cracks in uniaxial tensile test vs. P_{max} (a), parameter A_f representing fracture toughness (b), residual strength y_1 (c), residual strength y_2 (d) [27].	22
Figure 3.1 - Bidirectional Flax fabric 100 cm wide roll (a); magnified texture of the fabric (b)	23
Figure 3.2 - Saturated solution of $Ca(OH)_2$ in water (a); flax fabric immersed in solution (b)	24
Figure 3.3 – Optical Microscopic image of untreated flax thread (a); Optical Microscopic image of flax thread treated with $Ca(OH)_2$ solution (b).	25
Figure 3.4 - SEM image of representative untreated flax thread	26
Figure 3.5 - SEM image of representative pre-treated flax thread	26
Figure 3.6 - Tensile test sample of Yarn (Untreated) series (a); Tensile test sample of Yarn (Treated) series (b).	28

Figure 3.7 - Tensile test sample of Thread (Warp) series (a); Tensile test sample of Thread (Weft) series (b)	29
Figure 3.8 - Tensile test sample of Thread (Untreated) series (a); Tensile test sample of Thread (Treated) series (b).....	29
Figure 3.9 - Tensile test sample of Fabric (Untreated) series (a); Tensile test sample of Fabric (Treated) series (b).....	30
Figure 3.10 - Thread's tensile test sample in Microforce Testing Machine (During Test)	30
Figure 3.11 - Tensile test sample in Microforce Testing Machine (During Test)	31
Figure 3.12 - Bidirectional flax fabric (Warp & Weft directions).....	31
Figure 3.13 - Force versus displacement graph of flax yarn (Untreated vs Treated)	32
Figure 3.14 - Force versus displacement graph of flax thread (Warp vs Weft).....	33
Figure 3.15 - Force versus displacement graph of flax thread (Untreated vs Treated)	33
Figure 3.16 - Stress-strain graph of flax yarn (Untreated vs Treated).....	35
Figure 3.17 - Stress-strain graph of flax thread (Warp vs Weft)	35
Figure 3.18 - Stress-strain graph of flax thread (Untreated vs Treated)	36
Figure 3.19 - Force-displacement graph of flax textile strip (Untreated vs Treated)	37
Figure 3.20 - Stress-strain graph of flax textile strip (Untreated vs Treated)	37
Figure 4.1 - Sand particle size distribution curve	40
Figure 4.2 - Raw jute fibers as procured (a); treated & sized fibers to be used in mortar (b) .	40
Figure 4.3 - Mortar during mixing (a); fresh state consistency measurement (b)	41
Figure 4.4 - Mortar prism in flexure testing (a); mortar cube under compression testing (b) .	42
Figure 4.5 - Empty TRM mold (a); mortar spreading and levelling with roller (b); embedding the flax fabric strip and final rolling (c).....	44
Figure 4.6 - TRM specimen being connected with steel plates with epoxy (a); TRM tensile specimen ready for testing (b); Tensile test setup (c)	45
Figure 4.7 - Load versus displacement response of TRM-U1L and TRM-T1L.....	46
Figure 4.8 - Load versus displacement response of TRM-U2L and TRM-T2L.....	47
Figure 4.9 - Load versus displacement response of TRM-FU1L and TRM-FT1L	47
Figure 4.10 - Phase-1 development of 1st crack in TRM specimen (a); Phase-2 development of multiple cracking (b); Slippage & ultimate failure of the flax textile (c).....	48
Figure 4.11 - Stress-strain response of TRM-U1L and TRM-T1L.....	51
Figure 4.12 - Stress-strain response of TRM-U2L and TRM-T2L.....	51
Figure 4.13 - Stress-strain response of TRM-FU1L and TRM-FT1L	52

Figure 4.14 - Splitting of TRM-T2L specimens in the gripping area (a); close-up of the grips (b).....	52
Figure 4.15 - Stress-strain response comparison of TRM-T1L versus TRM-FT1L.....	53
Figure 4.16 - Peak tensile strength comparison of different TRMs.....	53
Figure 4.17 - Ultimate strain comparison of different TRMs.....	54
Figure 4.18 - Molds preparation for pull-out samples (a); close-up of a freshly cast sample (b)	55
Figure 4.19 - Pull-out samples (a); test set-up (b)	56
Figure 4.20 – Force versus displacement graph of pull-out test	57
Figure 5.1 - Brick compression test set-up (a); test set-up for modulus of rupture (b)	59
Figure 5.2 - Brick wall during construction (a); fully constructed (b).....	59
Figure 5.3 - Application of 1st mortar layer (a); embedding of flax-fabric (b); application of 2nd mortar layer (c); smoothed final assemblage (d)	61
Figure 5.4 - Diagonal compression test set-up.....	62
Figure 5.5 - Force versus displacement graph of Wall-Ref series.....	63
Figure 5.6 - Development of crack in Wall-Ref-1 (a); Wall-Ref-2 (b)	63
Figure 5.7 - Force versus displacement graph of Wall-U1L series	64
Figure 5.8 - Force versus displacement graph of Wall-T1L series.....	65
Figure 5.9 - Force versus displacement graph of Wall-U2L series	66
Figure 5.10 - Force versus displacement graph of Wall-T2L series.....	66
Figure 5.11 - Comparison of peak load bearing capacity of all series of walls.....	67
Figure 5.12 - Comparison of post-peak load bearing capacity of all series of walls.	67
Figure 5.13 - Crack development in representative samples of Wall-U1L (a); Wall-T1L (b); Wall-U2L (c); Wall-T2L (d).....	68
Figure 5.14 - Walls shear strength comparison	70
Figure 5.15 - Wall diagonal compression result: a) load vs. displacement (P-d) diagram; b) post-peak curve; c) idealized bilinear post-peak curve to determine TRM effect [37].	71
Figure 5.16 - Wall fracture toughness parameter A_f versus number of cracks in TRM (a); y_1 vs number of cracks (b); y_2 vs number of cracks (c); P_{max} vs number of cracks developed in TRM tensile test.....	72

List of Tables

Table 2.1 - Plant fibers' approximate global production [18].	14
Table 2.2 - A comparison of plant and synthetic fibers' mechanical properties [18].....	16
Table 3.1 - Physical parameters of untreated and pre-treated flax threads	27
Table 3.2 - Summary of mechanical properties of flax yarn, thread, and fabric	38
Table 4.1 – Summary of mortar properties.	42
Table 4.2 - Summary of mechanical properties of flax fabric strips used in TRM.	42
Table 4.3 - Summary of mechanical properties of flax-TRMs.....	48
Table 4.4 - Summary of fabric exploitation ratio for different TRM composites.	50
Table 5.1 - Summary of shear strength of walls.	69
Table 5.2 - Summary of fracture toughness parameters of all walls.	71

Chapter 1

Introduction

1.1. Background

Italy, being at the junction of African and Eurasian plates, is susceptible to very high seismic risk among the countries in the Mediterranean. The historical analysis of seismic events highlights a considerable damage to the socio-economic situation of the area specifically due to the fact that most of the structures were built in an era when there was a negligible to no presence of knowledge for prevention against earthquakes. In the current situation, although there is sufficient knowledge about prevention or dissipating the effects of earthquakes in terms of earthquake resistant design of new structures and seismic strengthening of existing structures, there are still risks to human life. These risks exist mainly because of the fact that the historic city centers are predominantly built in the eras when the earthquake design principles and methods were not enforced. Thus, the medium-high seismic risk due to the geographical position, an extreme vulnerability due to the type of infrastructures and a very high exposure due to importance of human life, historic and strategic infrastructures, classifies the Italian peninsula as high seismic risk.

The city centers in most of the Italian cities are characterized by historical brick or stone masonry structures designed solely to undertake vertical gravitational loads with no consideration of seismic horizontal forces. Intervention of seismic strengthening of these structures is of utmost importance to prevent human casualties and to ensure safe habitats for all in case of a seismic event.

With a continuous focus on sustainability, there is a continuous demand to develop and use eco-friendly materials and methods not only in construction but in general. These demands are continuously taking attention and are being transformed into policies by the governments on the recommendations of environmentalists and agencies concerned. Researchers and industry professionals are thus continuously developing materials and testing methods that have long lasting positive ecological impacts and contribute towards sustainability.

Professionals and researchers in the construction industry are following the suite and have in recent years developed innovative solutions to help respond to sustainability requirements. Thus, developing alternative materials and methods referred to as green building materials and green construction practices.

Natural Textile Reinforced Mortars (N-TRMs) also referred as Natural Fiber Reinforced Composite Matrixes (N-FRCMs) are one such class of materials, composed of natural/plant-based textile/fabric embedded in an inorganic mortar matrix, used as innovative material for seismic strengthening of masonry structures [1]. In recent years, there have been extensive studies to characterize such plant based TRMs to respond to the common concerns about their applicability and effectiveness. Various types of plant fibers, such as hemp, flax, sisal, jute, coconut, and curaua, have already been recognized for their potential as reinforcement in composites in various industries, including aeronautics, naval, and automotive. These fibers offer several desirable properties such as availability, favorable mechanical parameters, economy, high strength-to-weight ratio, and environment sustainability [2]. Recently, a number of plant-based fiber-based composites have been studied and are being successfully applied in the construction materials domain. The adoption of textiles made from plant fibers in TRM composites has surfaced as a highly auspicious reinforcement mechanism with noteworthy possibilities, yet it still faces various challenges that hinder its widespread adoption in the market compared to more commonly used synthetic-based composites [3]. In this context, comprehensive research has been carried out on flax-TRMs (specifically flax fabric embedded in a lime-based mortar), by Ferrara et al., for their qualification and use in masonry strengthening applications.

However, there is still a huge research potential to improve the performance of plant based TRMs either by efficient use of reinforcement amount or by different proposed pre-treatments of plant fibers. In addition, there is a need to study the adaptation of more sustainable inorganic matrixes in TRMs instead of 100% cement or lime-based mortars. In order to realize these needs, this study focuses on the development of a more sustainable mortar matrix and enhancement of flax-TRMs by a proposed pre-treatment of flax textile.

Finally, the study highlights the need for further research on different pretreatments on flax textiles and their potential benefits on flax-TRMs based on the experimental evidence shown in the current study.

1.2. Thesis Structure

The dissertation is composed of the procedure and results of an experimental campaign performed from constituent scale of flax-TRMs to the structural element scale of masonry assemblage. Each chapter of the dissertation explains a different scale of study starting from physical and mechanical characterization of flax textile to the mechanical characterization of flax-TRMs and further correlates the response of flax-TRM prisms to the performance of

masonry assemblage externally strengthened by flax-TRMs. The overall structure of the dissertation is discussed below:

- Chapter 1: This chapter consists of the introduction and background context of the research.
- Chapter 2: This chapter comprises the literature review with details of the information present in the literature about plant/natural fibers and textiles and their subsequent use in composite systems. It also includes results of experimental campaigns conducted on flax-TRMs in the past.
- Chapter 3: This chapter describes the methods and results of the experimental investigations for physical and mechanical characterization of flax textile. It also includes the pre-treatment methodology employed in this research.
- Chapter 4: This chapter reports the materials, methods and experimental investigations carried out for characterization of flax-TRMs. It describes the tensile tests carried out on TRM prisms and the pullout tests of flax fibers from mortar matrix.
- Chapter 5: This chapter defines the external application of flax-TRMs to masonry assemblage and the diagonal compression test on masonry units. It verifies the system performance in in-plane shear after strengthening mechanism by flax-TRMs.
- Chapter 6: This chapter reports the main conclusions which can be drawn based on this experimental campaign and its future implications.

1.3. Research Context

This research is part of the Master thesis in which the experimental campaign is carried out entirely at “Núcleo de Ensino e Pesquisa em Materiais e Tecnologias de Baixo Impacto Ambiental na Construção Sustentável (NUMATS)” of Federal University of Rio de Janeiro (UFRJ). The research thesis is funded by Politecnico di Torino under the foreign mobility of “Tesi su proposta per studenti 2021/2022”.

Chapter 2

2 Literature Review

Due to its geographical position in the Mediterranean and morphological characteristics associated with its strata, Italy is most prone to the seismic phenomenon compared to its neighboring countries. Additionally, most of the city centers of major cities are constructed with masonry from the times when there were little to no guidelines/laws governing the seismic design of buildings. Hence, these existing structures and infrastructures are designed solely to withstand the vertical gravitational loads. The earthquakes which occurred in the Mediterranean have underscored the importance of enhancing the seismic performance of existing buildings, which are primarily constructed with masonry. These buildings typically have significant capacity to withstand vertical static loads but are substantially unsuitable to withstand large earthquake loads. As a result, walls have experienced both in-plane and out-of-plane failures due to catastrophic seismic events, usually due to limited shear capacity [2].

Typically, there are two methods envisaged to reduce the vulnerability of structures to seismic phenomenon. First described as reducing the seismic demand of the structures by means of base isolation or dampers or redistribution of mass etc. Second, by enhancing the capacity of the structures by retrofitting techniques such as confinement with steel jacketing, FRP, pointing, grouting, installation of internal reinforcement in masonry etc.

Hence, many buildings that already exist require strengthening measures, and various technical solutions have been created for this purpose. One such solution is the utilization of textile-reinforced mortar (TRM) composites, which has gained widespread approval as a technically feasible and economically advantageous alternative [1].

TRM systems are typically composed of two components, referred to as "phases." The first phase is an inorganic matrix, which is commonly made from a cement- or lime-based mortar. The second phase is an internal reinforcement, which is made from a low-density textile composed of various types of fibers, including glass, basalt, carbon, high-strength steel, PBO, and aramid [3]. These inorganic composite systems have however shown some drawbacks when applied to masonry substrates such as their non compatibility with the masonry substrate, lack of fire resistance and limited ductility etc.

With a continuous focus on sustainability and an urge to use the eco-friendly materials and methods across all disciplines, there is a continuous struggle in the construction industry to employ more sustainable and environment friendly alternatives in the construction sector. Hence, the use of plant based/natural fibers has gained much attention in the recent decades due to their potential as an innovative and eco-friendly alternative to conventional fibers.

Natural Textile Reinforced Mortar (NTRM), which involves incorporating plant fibers into inorganic composite systems as reinforcement, presents a novel approach that offers a more environmentally friendly option compared to conventional high-strength inorganic fibers [2]. Recent studies involving jute and flax textiles embedded in inorganic mortar matrixes have shown promising results when applied to masonry structures. Results from these studies indicate that the use of Flax-TRM reinforcement improves both the strength and ductility of masonry structures, validating the practical application of these materials [2].

2.1. Textile Reinforced Mortars

Textile Reinforced Mortar composite systems, commonly known as TRMs incorporating layer/s of high strength textile embedded in lime or cement based inorganic mortar matrix, commonly adapted for use in masonry strengthening applications in the form of thin externally bonded layers. In the literature, different terminologies have been adapted for such systems such as Fiber Reinforced Cementitious Matrix (FRCM), Textile Reinforced Concrete (TRC), Cementitious Matrix Grid (CMG), Inorganic Matrix Grid (IMG), Composite Reinforced Mortar (CRM) etc [4]. Due to their better compatibility with masonry substrate, TRMs are preferred over conventional FRPs in strengthening applications involving masonry. FRPs possess very high strength and are applied in the form of thin laminates but they experience lack of adhesion with masonry substrate due to high stress concentrations. On the other hand, the presence of fine aggregates in the mortar matrix in TRMs requires a thinner textile mesh. TRMs are commonly used to cover the full masonry units to ensure an even distribution of stress on the surface. Additionally, TRMs have better compatibility with masonry substrates compared to FRPs due to the material's affinity and permeability [5].

The adoption of Textile Reinforced Matrix (TRM) systems is becoming increasingly accepted as a viable technical approach to reinforce masonry structures. When considering sustainability-related factors, such as renewability, recyclability, biodegradability, and cost-effectiveness, the utilization of natural fabrics (such as those composed of flax) instead of synthetic materials can yield positive results [6]. The composites can be applied in numerous applications such as masonry walls (Figure 2.1) arches (Figure 2.2), vaults (Figure 2.3), beams (Figure 2.4) and columns (Figure 2.5). In masonry walls they are applied as bi-directional fabric to increase the shear strength against in-plane and out of plane failure. By using a FRCM strengthening system on the surfaces of a masonry wall and implementing either a continuous or discontinuous layout, it is possible to enhance the wall's capacity for shear as well as combined axial and bending moments.



Figure 2.1 - Basalt textile grid application on masonry wall [3].



Figure 2.2 - PBO mesh used for intradoxal strengthening of concrete arch bridge [3].



Figure 2.3 - Masonry vault intradoxal strengthening with AR Glass fiber grid & mortar [3].



Figure 2.4 - Column confinement with AR Glass fiber grid & mortar [3].



Figure 2.5 - Beam shear strengthening with PBO fiber grid embedded in mortar [3].

TRMs have been used in numerous applications since their inception although the studies to accurately determine their short- and long-term properties are still underway. Research committees were formed to determine the guidelines for TRM qualification and thus on their recommendation certain types of mechanical tests are reported in order to qualify a TRM. Specifically, the determination of TRMs effective usage and the procedures to improve composite's performance are gaining more and more attention from the researchers.

2.2. Tensile Test on TRM

TRMs typically reinforce elements that are exposed to multiple load conditions, including compression, bending moments, and shear. However, the composite's primary strength lies in its ability to withstand tension. As a result, the qualification process involves conducting direct

tensile tests to determine the fundamental mechanical properties of the material [7]. The mechanical behavior of materials is heavily influenced by various factors such as the specimen geometry, the test configuration, and the monitoring techniques used to measure mechanical parameters [8]. To address this issue, RILEM TC 232-TDT is a scientific technical committee established with the specific objective of offering recommendations on the testing method for assessing the load-bearing capacity of textile reinforced concrete specimens subjected to tensile forces [9]. The TRM specimens shall conform to a minimum length to width ratio of 5:1 and should be at least 500 mm in length, 60 mm in width and 6 mm in thickness with a minimum of 200 mm as free length for displacement measurement during the tensile test (Figure 2.6). The specimens are prepared with alternating layers of mortar and textile with at least a 3 mm thick mortar layer on each side of the sandwiched fabric layer. Along the length of the specimen, each end is fixed with steel gripping plates up to a length of at least 100 mm. The tensile force is applied by pulling these steel gripping plates in a tensile testing machine. Displacement and crack development is measured by means of LVDT or strain gauges applied in the vicinity of the transition area between grips and the free length (Figure 2.7). Utilizing Digital Image Correlation (DIC) technique in conjunction with conventional equipment can yield valuable insights into the deformation distribution on the specimen's exterior face, thereby facilitating a precise assessment of the crack pattern [10].

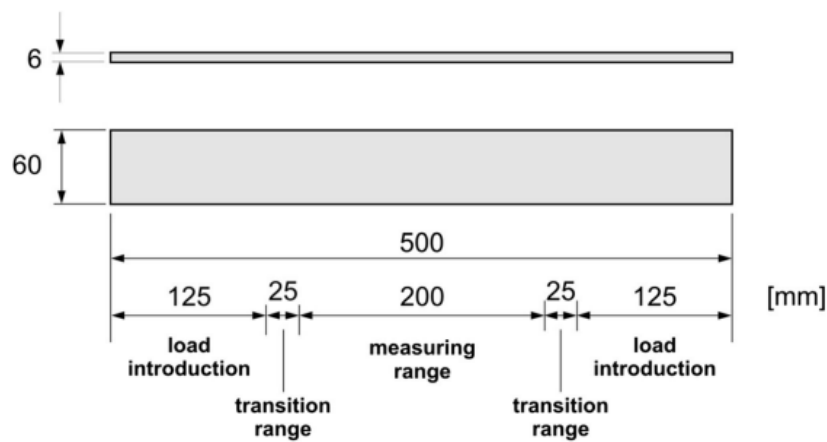


Figure 2.6 - Tensile test specimen geometry [9].

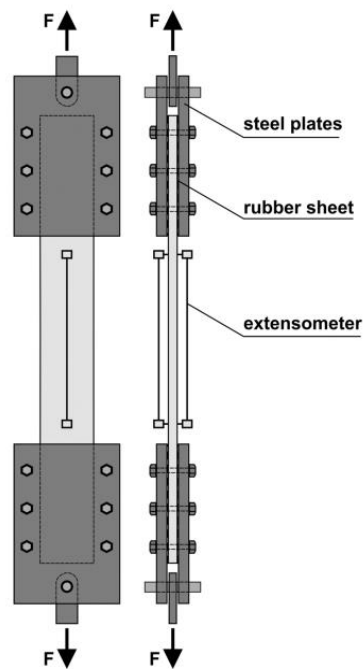


Figure 2.7 - Tensile test arrangement [9].

The stress versus strain graph of a classical TRM is identified as a three-phase response (Figure 2.8). In which the first phase represents a linear-elastic branch till the appearance of the first crack in the TRM specimen. This phase is identified with a stiffness E_1 and it is representative of a perfect bond between the textile and the inorganic mortar matrix. The first crack appearance in the matrix is identified as the tensile strength of the matrix. The stiffness in this phase is determined by considering a perfect textile to matrix bond.

The second phase, after the development of the first crack, is identified as a series of cracks appearing one after another whose dependence is varied in nature heavily based upon the mortar compressive/tensile strength and mortar to textile bond strength among other factors. The transition zone between phase1 and phase2 is observed with a pair of stress-strain values σ_1 and ϵ_1 . At the development of each crack in phase2, a sudden drop of load is observed, thus the values of stiffness E_2 are estimated by interpolation in a representative range of the curve. There should be enough cracks for correct interpolation of stiffness value. The distribution and number of cracks development in the specimen is dependent upon textile grid spacing, mortar to textile bond, textile deployment ratio etc.

Once all the possible cracks have occurred, there is a second transition zone which identifies the difference between phase2 and phase3. This second transition zone is characterized by another pair of values σ_2 and ϵ_2 . After the second transition phase, the third phase, represented by an almost linear hardening branch, is mainly defined by the textile tensile behavior. This phase reflects the widening of existing cracks without development of any further cracks and the response is comparable to the tensile response of dry textile. If the textile yarns fail under tension, the composite's stress-bearing capacity is comparable to the dry textile's tensile strength [11].

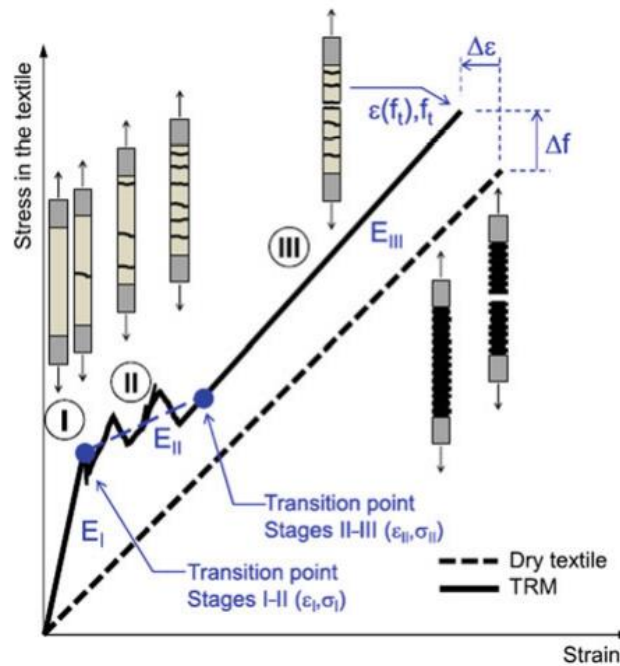


Figure 2.8 - Tensile response curve of a classical TRM [11].

The ultimate failure of TRM specimens is governed by one of the three failure modes 1) failure of textile near the gripping 2) failure of textile within the free length 3) slippage of textile within the matrix (Figure 2.9). The failure mechanism is highly dependent upon the boundary conditions of the test specimens. In general, two types of boundary conditions have been adapted in TRM tensile tests. First commonly known as Clamping method in which the gripping portion of the specimen is subjected to a lateral pressure, second is Clevis method in which the steel plates are attached to the specimens by the help of an epoxy glue and no lateral pressure is applied. In the clamping method, the failure is predominantly caused by a rupture of the textile within the specimen. However, in the Clevis method since the forces are transferred by means of a glue between the steel plates and the specimen, hence the length of the glued portion, the mortar to textile bond and the tensile strength of textile governs the overall failure mechanism which might be the slippage of textile in the transition zone.

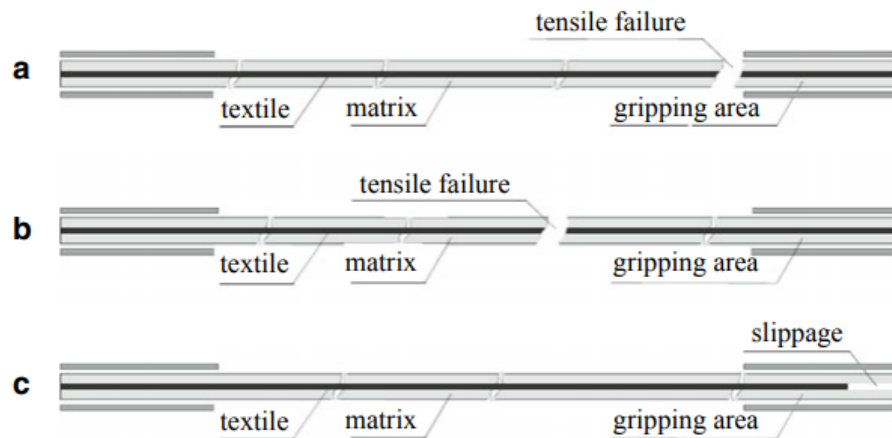


Figure 2.9 - Failure mechanisms of a classical TRM [11].

The direct tensile test on TRM specimens gives valuable information about the design parameters for composite systems to be adapted in strengthening applications: such as the crack spacing and the stress corresponding to the development of the first crack (σ_1) are essential parameters for Serviceability Limit State design, likewise the stiffness in phase 3 of the tensile curve, the ultimate stress and corresponding strain are essential design parameters for Ultimate Limit State design [11, 12]. The results obtained from response to tension indicate that the Flax-TRM system exhibits a visible composite behavior, which is characterized by the familiar three stages comprising the elastic response, crack formation, and the reinforcement response until failure [1].

2.3. Diagonal Compression Test

Tensile test analysis of the TRM specimens, described in the previous chapter, gives significant parameters to accurately determine and design the TRMs for strengthening mechanisms. However, to verify the accuracy of results obtained by these small-scale tests and to correlate the response of small-scale tensile prisms with that of large-scale masonry assemblage externally bonded with TRM performance, it is pertinent to perform large scale experiments on masonry assemblage. In literature, seismic performance of masonry is related to the in-plane shear capacity of the masonry assemblages which can be determined by applying static or cyclic loading in direct shear tests or by diagonal compression test. Diagonal compression tests have frequently been employed to assess the mechanical effectiveness of TRM systems in strengthening masonry structures including walls with single or double leaf composed of tuff volcanic elements and utilizing different TRM systems with varying characteristics such as geometry, type of mortar, and textile, due to the reliability and reproducibility of the results (Figure 2.10).

Diagonal compression tests are generally carried out on square masonry assemblage of size 120 cm x 120 cm by compression loading along one of the two diagonals as per the standard [14]. The compressive load is applied at a rate recommended by the standard and

horizontal & vertical displacements are measured with suitable LVDTs during the test. The sample fails in diagonal splitting in tension with cracks propagating perpendicularly to the direction of applied compressive load. These displacements and applied compressive load can be used to determine stiffness, shear strength and strain in the center of the wall specimen.

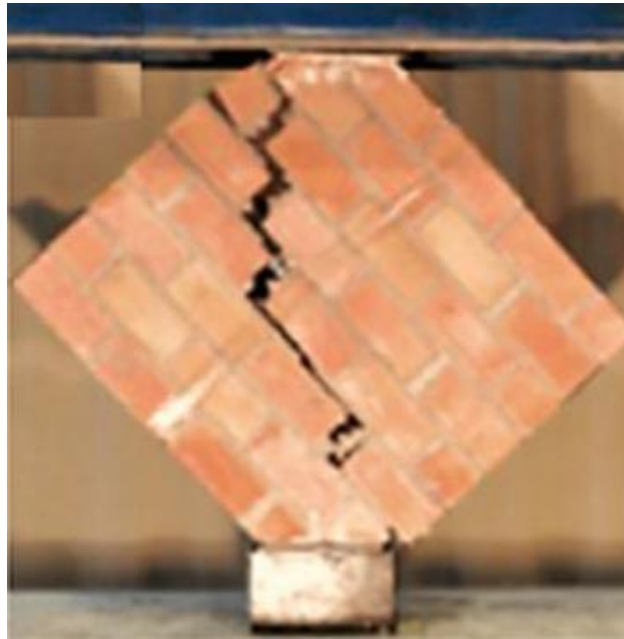


Figure 2.10 - Diagonal cracking of clay brick wall [13].

The effectiveness of TRM systems in improving the in-plane shear capacity of masonry panels is heavily influenced by numerous parameters, including the mechanical and geometric properties of the matrix and textile reinforcement, the presence of mechanical anchors, and the properties of the masonry substrate. The peak capacity of the panel is significantly impacted by the mechanical properties of the TRM matrix [8]. In addition, the peak load bearing capacity is also affected by the elastic modulus of the textile employed such that when lower elastic modulus textiles are utilized, a smaller enhancement is obtained compared to textiles with higher axial stiffness [13].

The inelastic post peak behavior was always significantly enhanced no matter if the textile increased the strength capacity or not [15].

2.4. Plant Based/Natural Fibers in TRM Composites

With a continuous focus on the environment and to preserve the natural resources, there is an ongoing focus on the use of renewable materials in construction just like other fields. In order to have the least environmental impact, different scientific committees are working across the board to develop and characterize such materials and methods which contribute towards the preservation of depleting virgin resources. The reduction of the environmental "impact" of human activities has become a crucial factor in all industrial domains, including the building

domain such that to achieve greater environmental sustainability, the construction industry must focus on reducing energy and raw material demand, as well as minimizing the emission of greenhouse gasses [16]. To ensure sustainability, there is a growing trend in developing new building materials and promoting the reuse of waste materials and utilizing raw materials from replenishable sources, which have minimal environmental impact [17].

One such class of materials is composites which incorporate different strategies to include more sustainable options. For example, the use of natural fibers also commonly referred to as plant fibers as a replacement for traditional industrial fibers in the development of bio composites represents a promising approach towards creating environmentally friendly and durable materials [8]. Hence, it can be conveniently stated that bio composites are the innovative materials keeping sustainability at the core of their development. Due to their sustainable nature and replenishable properties, scientists and researchers are more and more focused to study their mechanical properties and to further improve them for structural applications.

2.4.1. Plant Fibers

Plant fibers are classified as either wood fibers or non-wood fibers depending upon their place of origin. The non-wood fibers are extracted from various parts of the parent plants such as leaves, fruit, stem, straw, grass. Due to their abundant presence, economy, and low density, they have gained interest as advantageous raw materials (Table 2.1).

Plant fibers have often proved to possess mechanical properties comparable to those of synthetic fibers apart from advantages of being sustainable in nature. However, they have still not been completely commercialized for use in actual applications due to certain uncertainties surrounding their long-term properties and application complexities. Another major setback is the large variability of their mechanical and physical properties which are strongly dependent on various factors such as chemical composition, filament physical properties and surface roughness [18].

Table 2.1 - Plant fibers' approximate global production [18].

Fibre type	Production per year (Million tonnes)	Main producer countries
Abaca	0.10	Philippines, Equator
Cotton	25	China, USA, India, Pakistan
Coir	0.45	India, Sri Lanka
Flax ^a	0.50–1.5	China, France, Belgium, Ukraine
Hemp ^b	0.10	China
Henequen	0.03	Mexico
Jute	2.5	India, Bangladesh
Kenaf	0.45	China, India, Thailand
Ramie	0.15	China
Silk	0.10	China, India
Sisal	0.30	Brazil, China, Tanzania, Kenya

^aThe real production of flax was underestimated because the production of Canada is not considered

^bChina has announced plan to substantially increase the hemp production for textiles in the coming years to 1.5 million tonnes of fibres per year

Plant fibers are composed of cellulose, hemicellulose and lignin which make themselves a composite material [8]. Cellulose, being the main structural unit of the fiber, has a major role in deciding the mechanical properties such as strength, stiffness, and stability of the plant fibers. The chemical composition of plant fibers determines their classification, based on the proportion of different components such as cellulose. Fibers like cotton, hemp, flax, sisal, and ramie, which contain around 70% cellulose in their chemical composition, are considered cellulose-rich fibers. The chemical composition and thus the mechanical properties of plant fibers may also be influenced by a combination of various other factors such as geo-climatic conditions, plant type, soil type, plant maturity and the fiber production process [19]. A typical schematic diagram of flax fiber structure is presented in (Figure 2.11).

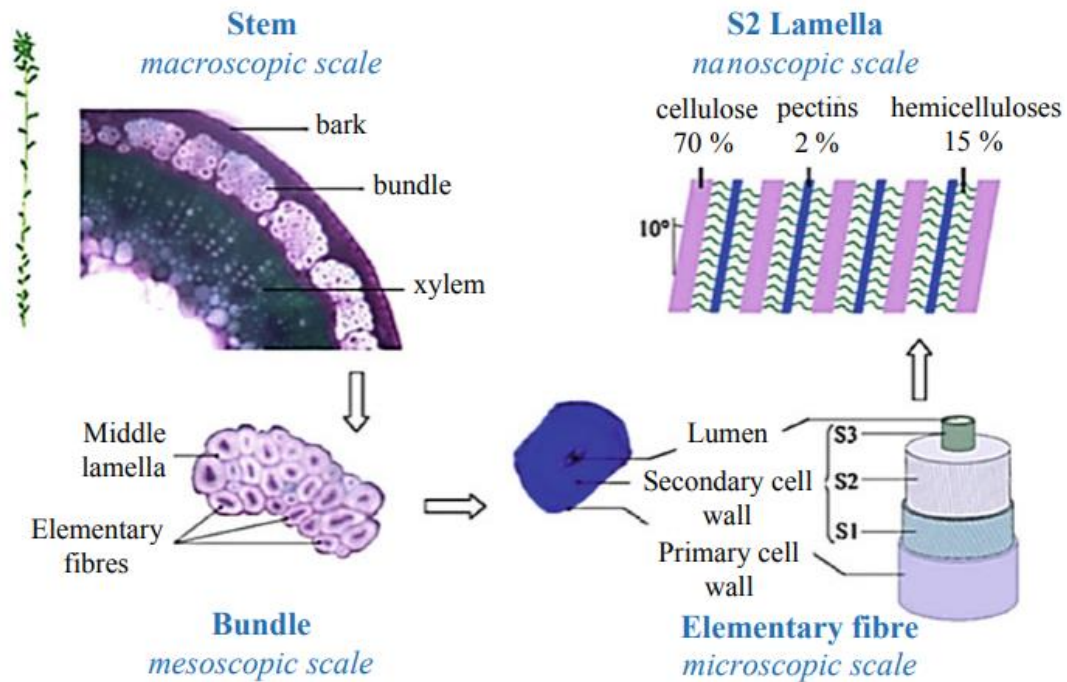


Figure 2.11 - Flax fiber schematic macro- and nano-scopic structure [18].

Plant fibers' mechanical performance is also linked with their physical properties in such a way that longer fibers contribute towards reducing the tensile strength of the fibers and the explanation lies in the fact that the longer fibers have a higher probability of imperfections which may lead to a premature failure compared to shorter fibers [18]. Important mechanical properties of natural fibers in comparison with synthetic fibers are presented in (Table 2.2).

Table 2.2 - A comparison of plant and synthetic fibers' mechanical properties [18].

Fibre type	Relative density (g/cm ³)	Tensile strength (MPa)	Elastic modulus (GPa)	Specific modulus (GPa \times cm ³ /g)	Elongation at failure (%)
Abaca	1.5	400–980	62–20	9	1.0–10
Alfa	0.89	35	22	25	5.8
Bagasse	1.25	222–290	14–27.1	18	1.1
Bamboo	0.6–1.1	140–800	11–32	25	2.5–3.7
Banana	1.35	500	12	9	1.5–9
Coir	1.15–1.46	95–230	2.8–6	4	15–51.4
Cotton	1.5–1.6	287–800	5.5–12.6	6	3–10
Curaua	1.4	87–1150	11.8–96	39	1.3–4.9
Flax	1.4–1.5	343–2000	27.6–103	45	1.2–3.3
Hemp	1.4–1.5	270–900	23.5–90	40	1–3.5
Henequen	1.2	430–570	10.1–16.3	11	3.7–5.9
Isora	1.2–1.3	500–600	–	–	5–6
Jute	1.3–1.49	320–800	30	30	1–1.8
Kenaf	1.4	223–930	14.5–53	24	1.5–2.7
Piassava	1.4	134–143	1.07–4.59	2	7.8–21.9
Palf	0.8–1.6	180–1627	1.44–82.5	35	1.6–14.5
Ramie	1.0–1.55	400–1000	24.5–128	60	1.2–4.0
Sisal	1.33–1.5	363–700	9.0–38	17	2.0–7.0
Aramid	1.4	3000–3150	63–67	46.4	3.3–3.7
Carbon	1.4	4000	200–240	157	1.4–1.8
E-glass	2.5	1000–3500	70–76	29	0.5
S-glass	2.5	4570	86	34.4	2.8

It is evident from the tensile strength and elastic modulus values of flax, hemp and ramie that these plant fibers have a mechanical resistance comparable to some synthetic fibers such as glass fibers. However, plant fibers' strain/elongation at failure is significantly different from the synthetic fibers due to the fact that plant fibers represent a lower stiffness in the first part of ascending branch in tensile test while the overall response is more relatable to an elasto-visco-plastic behavior in which the cellulosic microfibrils realign themselves to the tensile axis during the test [20].

Tensile strength versus density of some plant based and synthetic fibers is presented on logarithmic scale in Ashby plot in (Figure 2.12). The graph shows that the flax fibers present a tensile strength comparable to some synthetic fibers such as glass.

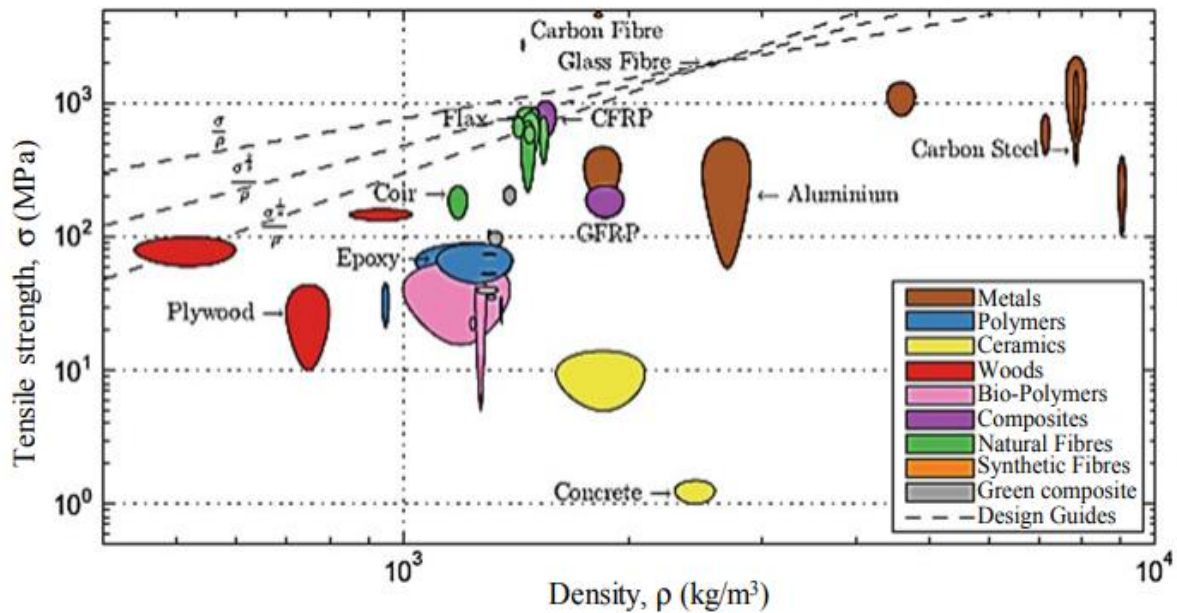


Figure 2.12 - Flax fiber schematic macro- and nano-scope structure [21].

Apart from the mechanical performance of the plant fibers, another important factor is their economic performance compared to synthetic fibers. In order to understand this aspect (Figure 2.13a) represents a comparison of a number of natural fibers with glass fiber as cost per unit weight. (Figure 2.13b) refers to a more performant economic criteria in terms of cost of the fibers' quantity having capacity to take a tensile load of 100 kN.

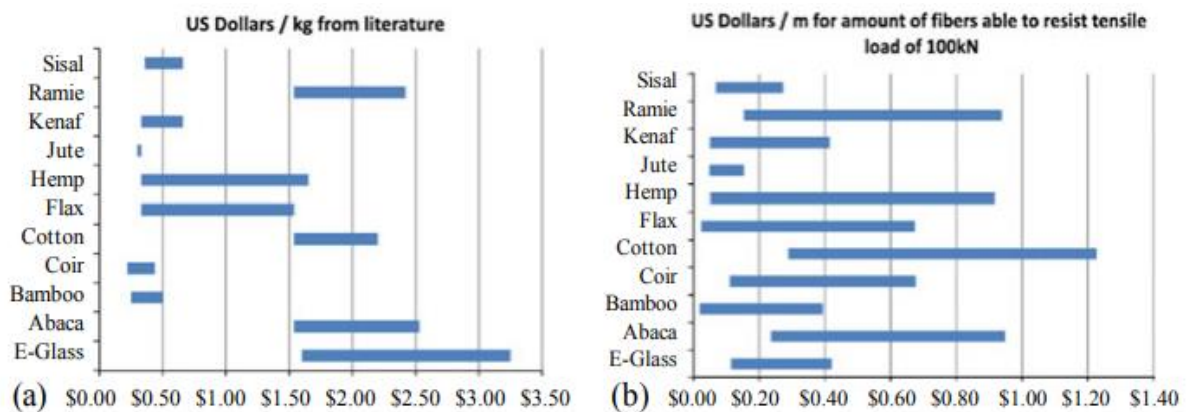


Figure 2.13 - E-Glass versus Natural fibers: a) cost per unit weight of fibers; b) cost per quantity of fibers having capacity to take 100 kN tensile load [22].

As per the (Figure 2.13b) the difference in cost between E-Glass and other natural fibers is more regular. Furthermore, the cost associated with the plant fibers is susceptible to a

considerable variability if additional treatments to improve the mechanical properties of these fibers are performed. Nevertheless, the economic component alone cannot decide the usefulness of a certain class of fibers unless an environmental impact assessment in terms of embodied energy is carried out. Plant fibers are recognized for their relatively low embodied energy, which refers to the total energy consumed during the production of a building material or a structure, starting from the extraction of raw materials to production and transportation. By examining this parameter in conjunction with tensile strength across a broad range of fiber types and fiber-based composites, a comprehensive comparison can be established (Figure 2.14).

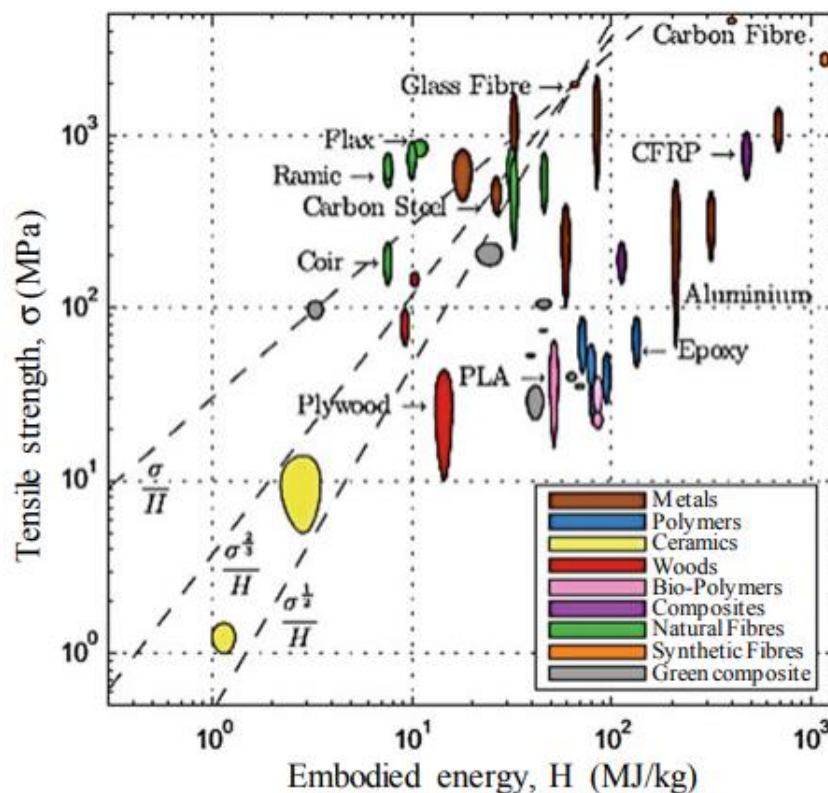


Figure 2.14 - Tensile strength versus embodied energy of fibers and composites [21].

The production energy required for synthetic fibers is roughly 10 times higher than that of plant fibers when measured in absolute terms. Additionally, it has been noted that the production of composite materials using synthetic fibers demands around five times more energy compared to plant based composites [21]. Based on all these factors discussed above and taking into account the sustainability advantages associated with the use of plant-based fibers and their derivatives, it is evident that flax, sisal, jute and hemp are among potentially viable alternatives to synthetic fibers.

2.4.2. Natural Textile Reinforced Mortars (N-TRMs)

Natural fibers are intrinsically different from synthetic fibers and thus their behavior in the composite systems is also varied in nature. Due to which, the rules governing the performance of synthetic fibers as established by the researchers in the previous decade cannot be directly applied to the natural fiber-based composites. Several studies have been conducted in recent years to qualify the natural TRMs (N-TRMs) and to establish a basis for the design of such composites for strengthening applications. Different types of tests have been conducted at various scales to determine the design parameters such as mortar to matrix bond, N-TRM to masonry bond and strength enhancement by application on masonry assemblage [8].

The bond at fiber-matrix interface fundamentally governs the response of the N-TRM and its effectiveness in strengthening applications. The pullout tests conducted on natural fibers/threads embedded in mortar matrix cylinder (Figure 2.15) provide an insight into the resisting force (which can be converted into shear stress) versus slip of the thread from the matrix. The graph of shear stress versus slip shows an initial linear branch with a subsequent friction phase. The peak stress and the residual stress strongly depend upon the fiber morphology, matrix properties and the fiber embedment length. The critical embedment length of 10 mm was observed in an experimental study performed on jute fiber embedded in cement mortar cylinder [23]. The fiber-mortar bond can be enhanced by specific fiber pre-treatments [24].

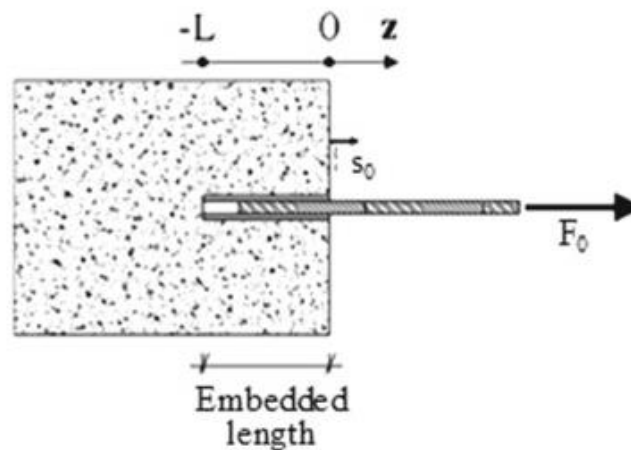


Figure 2.15 - Pull-out test setup of a natural fiber from mortar [23].

Various procedures can be adopted to improve the strength of fibers, such as hornification, alkaline treatment, polymer impregnation, and hybrid treatments (that combine hornification and polymer impregnation). Hornification involves subjecting fibers to cycles of wetting and drying in hot water, while alkaline treatment requires immersing the fibers in low alkaline concentration solutions for 50 minutes and then drying them for 24 hours. Polymer impregnation involves saturating the fibers with a polymer solution. When these treatments were applied to sisal fibers embedded in a cement-based matrix, the tensile strength of the

fibers and the bond between the fibers and the matrix were observed to increase significantly [25].

It has been observed that alkaline treatment of fibers tends to remove the amorphous components (Hemicellulose and lignin) of the fiber structure [26], thus regularizing the cellulosic structure of the fiber which is a fundamental component contributing towards the strength of fibers. The studies suggest that although the alkaline treatment with $\text{Ca}(\text{OH})_2$ reduces the tensile strength of vegetal fibers, the fiber to matrix bond improves [27].

Ferrara et al. applied an XSBR epoxy coating on flax textile and observed a marginal reduction in the tensile strength of the textile while the ultimate strain was sufficiently reduced. They also observed a reduction of bond strength at fiber to mortar interface due to the presence of a thin layer of epoxy [33].

Ferrara et al. studied the response of flax textile embedded in lime-based mortar matrix at different scales [2], [6]. They further studied a comparative response of TRMs reinforced with flax and jute textile and reported that the physical and mechanical properties of natural textile threads such as the transverse area and stiffness play a pivotal role in mechanical performance of N-TRMs and thus verified the better performance of flax-TRMs in comparison to jute-TRMs [1].

N-TRMs are represented by a three-phase tensile response similar to the synthetic fiber-based TRMs [28]. In contrast to the former, Natural TRMs exhibit a secondary phase during which a notable decrease in load occurs upon the appearance of a crack which can be attributed to a difference in the axial stiffness of the textile and the mortar (Figure 2.16).

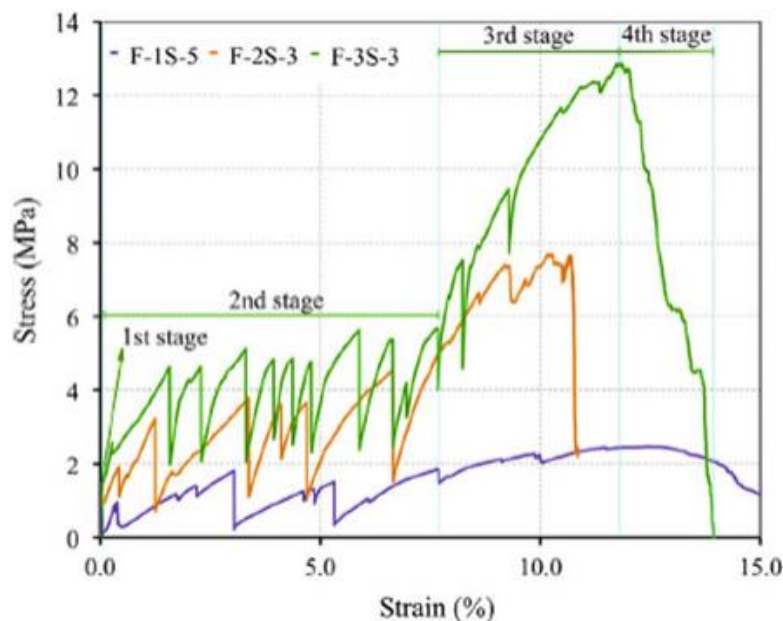


Figure 2.16 - Tensile response of flax-TRMs with different layers of textile [29].

The mechanical performance of N-TRMs is highly dependent on the volume percentage of fibers in the composite (Figure 2.17). An ideal volume fraction is therefore paramount for effective TRM performance.

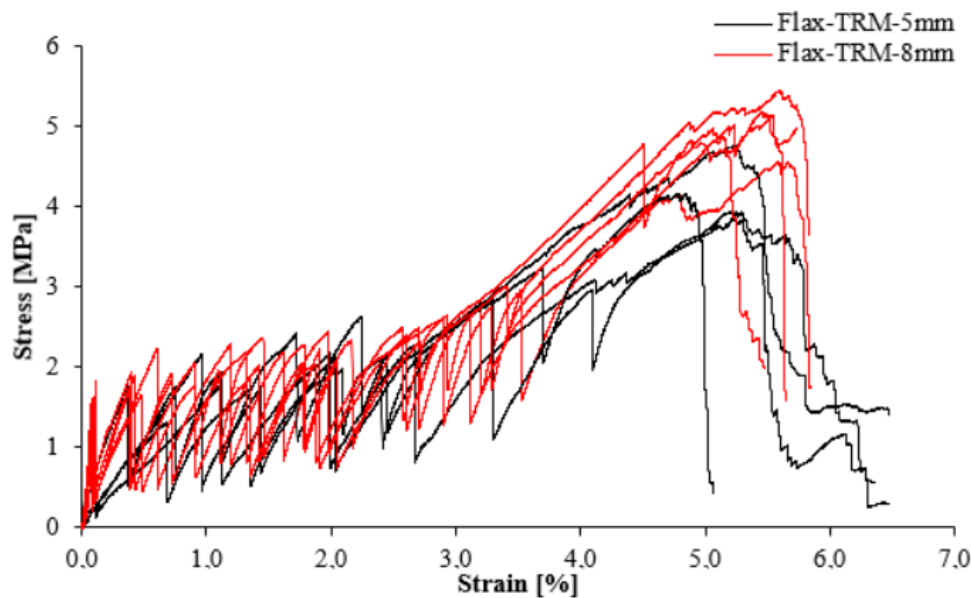


Figure 2.17 - Tensile response of flax-TRMs with one and two layers of textile [30].

Mercedes et al. used an epoxy and polyester coating respectively on natural textiles and observed that the tensile response of the textile was magnified. In comparison, the N-TRMs embedded with epoxy-coated textile represented a better exploitation ratio compared to polyester-coated textile [31]. Ferrara et al. studied the behavior of flax textile embedded in curauá-fiber-based inorganic mortar matrix and observed an increase of stress corresponding to the occurrence of first crack as well as overall strength gain specifically in stage II, despite no specific change in the deformability of the composite [32].

Ferrara et al. studied the change in shear capacity of clay brick walls externally strengthened with single and double ply flax-TRMs in diagonal compression test. Shear capacity of walls strengthened with single and double layers of flax fabric was observed to increase by 118% and 136% respectively of the strengthened wall [2]. Bonfanti et al. reported the performance of brick walls strengthened with jute- and flax-TRMs and observed that the increase of toughness and ductility of the strengthened walls was directly proportional to the number of cracks developed during tensile tests of N-TRM specimens (Figure 2.18).

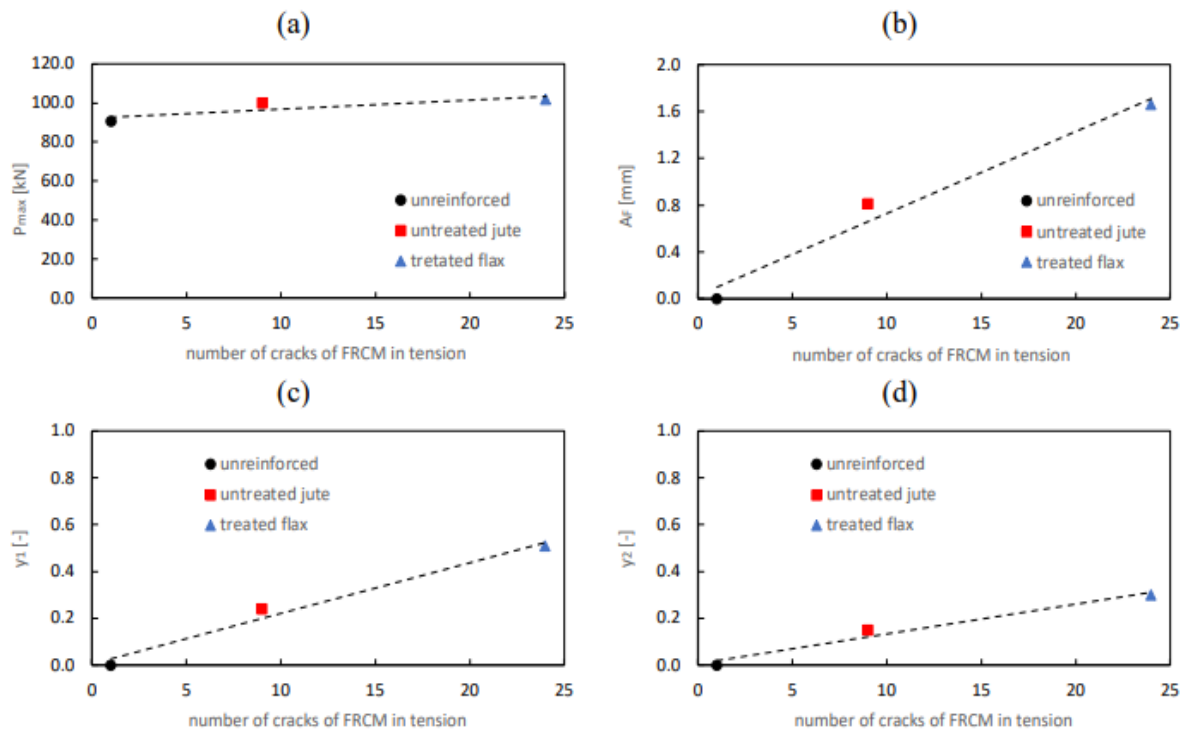


Figure 2.18 - No. of cracks in uniaxial tensile test vs. P_{max} (a), parameter A_f representing fracture toughness (b), residual strength y_1 (c), residual strength y_2 (d) [27].

Based on the extensive literature review, there is sufficient gap in research involving the enhancement of N-TRMs efficiency in terms of textile treatments or mortar improvements to reduce the N-TRM deformability and to increase the textile-mortar bond behavior.

Chapter 3

3 Characterization of Flax Textile

In order to determine the behavior of flax-TRMs, it is necessary to first perform physical and mechanical characterization of flax textile. The study starts with the physical characterization at constituent-scale and eventually leads to the mechanical characterization at fabric scale. This study starts with the microscopic analysis of yarn and thread's morphology and leads to the determination of mechanical properties of yarn, thread, and textile in terms of tensile strength and stiffness.

The flax textile used in this study was purchased locally in Italy, sold as “FIDFLAX GRID 300 HS20®” by FIDIA srl (Figure 3.1). The fabric is supplied in rolls of 50m in length and a width of 20, 50 or 100 cm. The fabric employed in this study had a width of 100 cm. A pre-treatment of fabric in a saturated alkaline solution has also been used in this study and subsequently its effects on physical and mechanical properties of the textile have been reported. The experiments for the characterization of physical and mechanical parameters were performed at the lab NUMATS/POLI/COPPE of Federal University of Rio de Janeiro (UFRJ), Brazil.



Figure 3.1 - Bidirectional Flax fabric 100 cm wide roll (a); magnified texture of the fabric (b)

3.1. Flax Fabric Pre-treatment

Plant fibers are constituted by cellulose, hemicellulose, and lignin among which the first represents the main structural component of the fiber while hemicellulose and lignin dissolve in presence of alkaline solution [1]. Past studies have found improvement in mechanical response of N-TRMs embedded with plant/natural fibers subjected to pre-treatment with alkaline solution of water.

It has been reported in the literature that the immersion of plant fibers in alkaline solution of water for less than an hour does not degrade the fibers. Instead, positive enhancement of mechanical properties of fibers have been observed in certain studies.

Bonfanti et al. performed alkaline treatment on flax fabric by first washing the fabric for 3 hours in hot water at 80°C and then drying for at least 24 hours at 40°C. Subsequently, the fabric was immersed in a saturated alkaline solution of $\text{Ca}(\text{OH})_2$ for 50 minutes and again dried for at least 24 hours at 40°C [37].

The flax fabric in the current study was immersed in a saturated solution of $\text{Ca}(\text{OH})_2$ in the proportion of 1.85g/l of water for 50 minutes at laboratory controlled temperature of 24°C and then dried in a forced airflow chamber at 40°C for at least 24 hours (Figure 3.2).



Figure 3.2 - Saturated solution of $\text{Ca}(\text{OH})_2$ in water (a); flax fabric immersed in solution (b)

3.2. Physical Characterization

The flax textile used in this study was purchased locally in Italy, sold as “FIDFLAX GRID 300 HS20®” [1]. This bi-directional textile is characterized by 4.3 threads/cm in both directions, hereinafter referred as warp and weft direction. The textile is simply woven in both directions with two threads running parallel to each other. Each thread is composed of two yarns intertwined in a spiral like pattern. Each yarn consists of a bundle of fiber filaments integrally combined in a haphazard manner. The yarn, however, is considered as the smallest unit for textile characterization in this study. Several samples of yarn, thread and fabric were analyzed in Optical Microscope (OM) and then in Scanning Electron Microscope (SEM) to deeply inspect the fiber morphology (Figure 3.3).

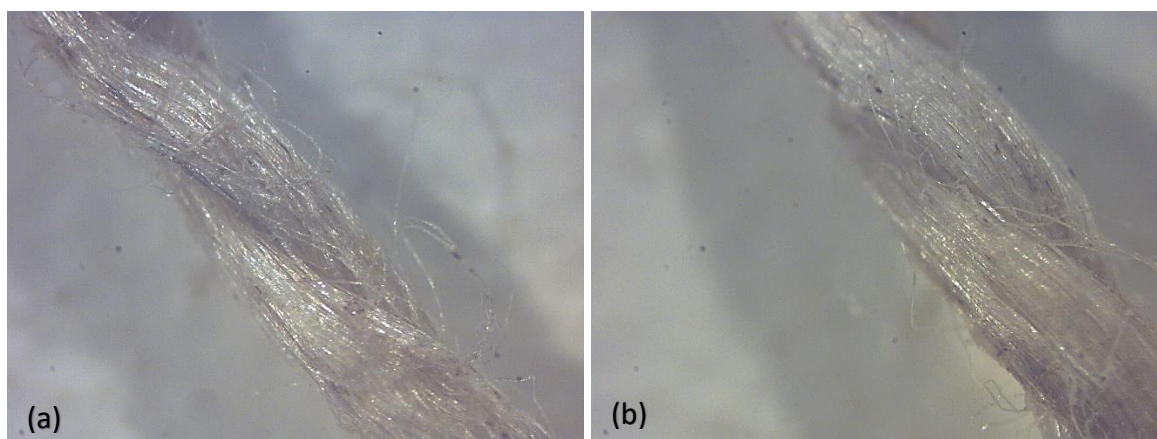


Figure 3.3 – Optical Microscopic image of untreated flax thread (a); Optical Microscopic image of flax thread treated with Ca(OH)₂ solution (b)

The resulting images obtained from OM show the presence of a smooth and shiny thin layer on the untreated fabric threads. On the other hand, the images of treated fabric represent that the treatment has considerably removed the shiny layer and hence it shows comparatively rough texture (Figure 3.3).

To determine the mechanical properties of flax thread, it is necessary to obtain the thread cross-section, several samples were analyzed in SEM and the resulting images obtained were post-processed in an image enhancement software (ImageJ) to determine the thread cross-section and perimeter. The representative image obtained from SEM analysis of untreated flax thread is shown in Figure 3.4. Similarly, a representative image of pre-treated flax thread obtained by SEM is shown in Figure 3.5.

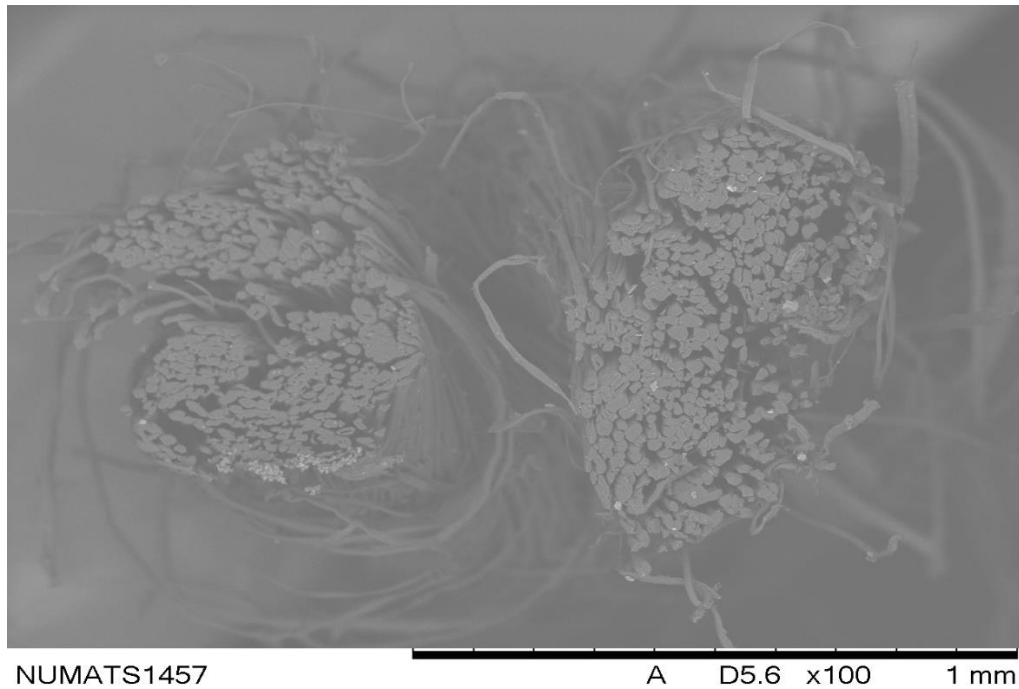


Figure 3.4 - SEM image of representative untreated flax thread

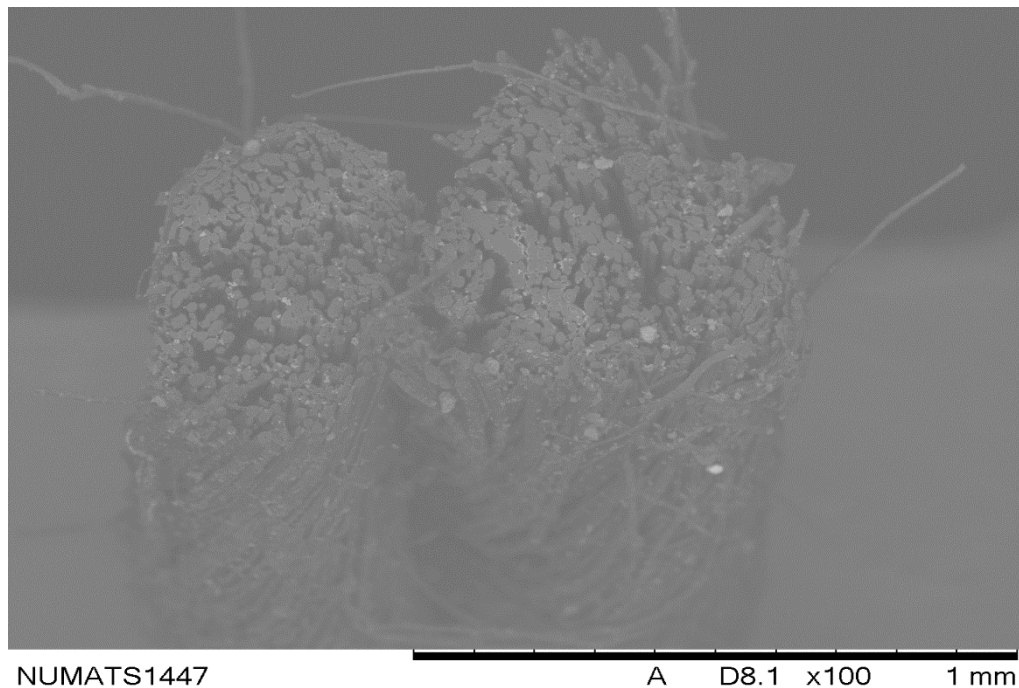


Figure 3.5 - SEM image of representative pre-treated flax thread

A total of 4 images of untreated flax threads and 7 images of pre-treated flax threads were analyzed to determine the physical properties such as bulk cross section area and perimeter. The mean values of cross-section area and perimeter are reported in Table 3.1.

Table 3.1 - Physical parameters of untreated and pre-treated flax threads

Parameter	Untreated Thread	Treated Thread
Cross-section Area (mm ²)	0.27	0.26
COV (%)	11	6
Perimeter (mm)	2.98	3.39
COV (%)	16	11

As per the first observation, the values of cross-section area are reduced, and perimeter are increased as reported in Table 3.1 after the pre-treatment procedure on the flax textile. The mean cross-section area of flax thread reduced by 4% from 0.27 mm² (COV 11%) for untreated flax threads to 0.26 mm² (COV 6%) for treated flax threads. Alternatively, the perimeter increased by 14% from an untreated flax thread perimeter of 2.98 mm (COV 16%) to treated flax thread perimeter of 3.39 mm (COV 11%). This behavior can be attributed to the fact that with alkaline treatment, the fibers' hemicellulose and lignin are decomposed thus creating voids in the already closed packing of filaments which reduces the cross-section area but due to the creation of voids the perimeter increases.

On the contrary, the variation in these properties among different samples from the same fabric has considerably reduced. The decrease in coefficient of variation of cross-section area and perimeter from untreated to treated flax threads has been calculated as 45% and 31% respectively. These results show a more homogeneous structure of the fibers, thus fulfilling the purpose of removing the non-structural impurities from the fibers by alkaline treatment.

3.3. Mechanical Characterization

Mechanical performance of plant-based textiles/fabrics represents a large variability due to physical and chemical characteristics associated with their origin and subsequent manufacturing processes involved in production of such textiles. Thus, the determination of mechanical parameters with acceptable coefficient of variation is the first step before their practical application in composites.

3.3.1. Methods

For mechanical characterization, the plant-based fibers are generally tested in tensile. Hence, different samples of yarn, thread and fabric are prepared and tested in uniaxial tensile to determine their resistance. Considering the nature of the plant-based fibers, a large natural variability of their properties has been reported in the literature. In order to compare the response of the textile under study, samples like previous similar studies are prepared and tested in tension. Thread, being the main structural unit of the textile, has been considered as the fundamental unit for mechanical characterization of the flax-textile under study. Different series of samples tested in this experimental campaign are listed below:

- *Yarn (Treated & Untreated):* It consists of one of the two subunits intertwined to make a thread. The yarns are extracted from the treated and untreated fabric in warp direction with a total length of 70mm (Figure 3.6).
- *Thread (Warp & Weft):* The main structural element woven to make the fabric is thread. Threads are extracted from both warp and weft direction of a total length of 70mm (Figure 3.7).
- *Thread (Treated & Untreated):* Threads extracted from warp direction of a total length of 70mm have been taken (Figure 3.8).
- *Fabric (Treated & Untreated):* Flax fabric strips of 60mm width and 500mm length have been extracted in such a way that the length is parallel to the warp direction (Figure 3.9).

The yarn and thread samples were glued to the paper molds with the help of a quick setting epoxy glue (TekBond Super Glue 793) and silver tape (commonly referred as duct tape, locally sold by the name silver tape in Brazil) by a length of 10 mm on both ends with a 50 mm free length. These paper molds were prepared specifically for the purpose of keeping the yarn/thread in line with the testing-machine axis (Figure 3.6, Figure 3.7, Figure 3.8). Once the sample has been axially aligned with the machine axis, before testing, the paper was cut transversally with the help of a scissor (Figure 3.10). At least 11 samples of Yarn (Untreated) series and 9 samples of Yarn (Treated) series were prepared and tested. 11 samples of each of the series Thread (Warp) and Thread (Weft) were prepared and tested. Warp and weft directions are represented in the Figure 3.12. Similarly, 11 samples of Thread (Untreated) and 10 samples of Thread (Treated) series were prepared and tested. The tests were conducted in the microforce testing machine (MTS Tytron 250) with a maximum load cell of 1 kN in displacement control rate of 4 mm/minute.

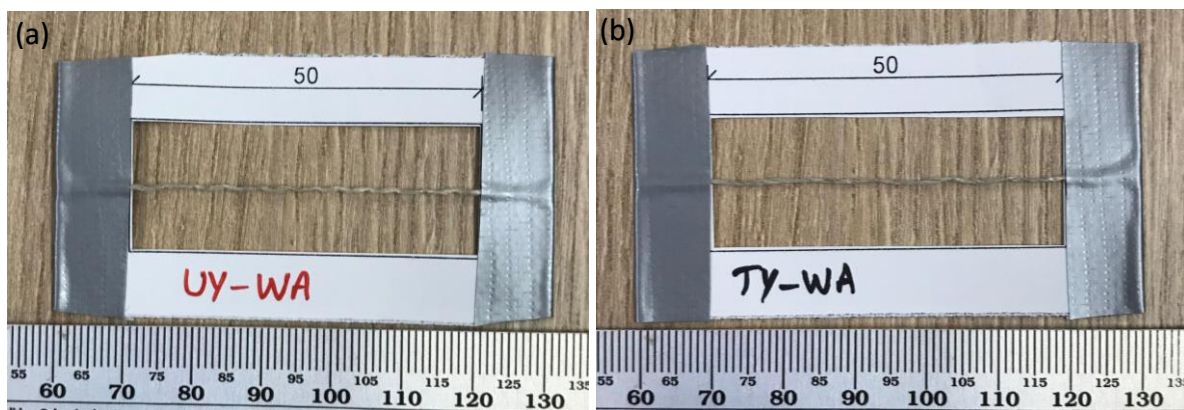


Figure 3.6 - Tensile test sample of Yarn (Untreated) series (a); Tensile test sample of Yarn (Treated) series (b)

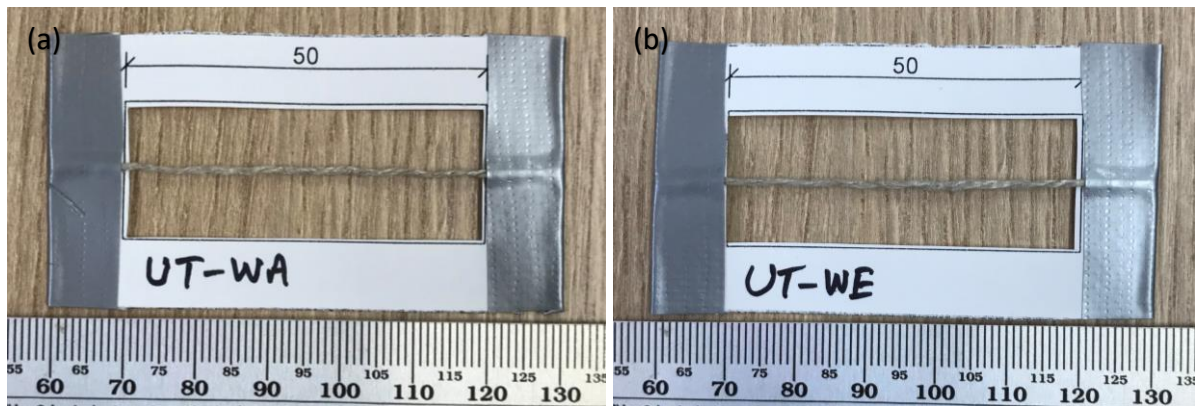


Figure 3.7 - Tensile test sample of Thread (Warp) series (a); Tensile test sample of Thread (Weft) series (b)

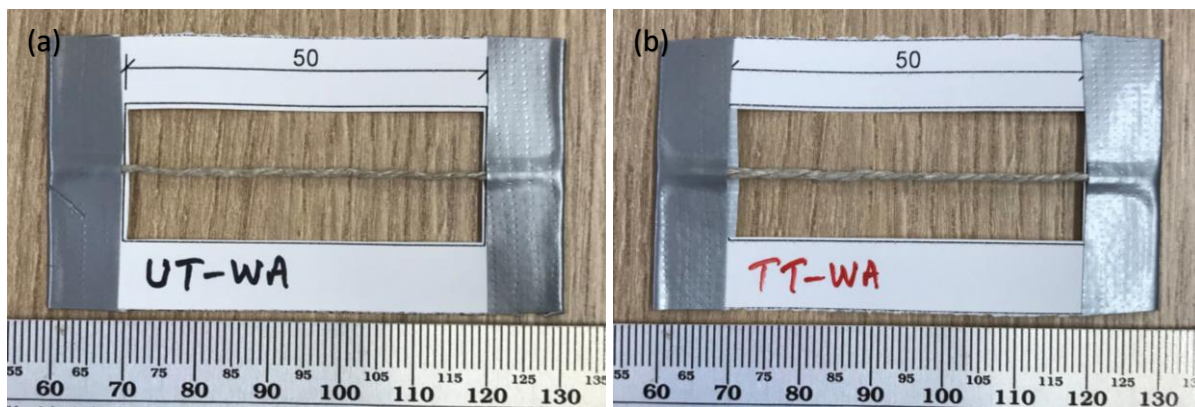


Figure 3.8 - Tensile test sample of Thread (Untreated) series (a); Tensile test sample of Thread (Treated) series (b)

The series Fabric (Treated & Untreated) had a total of 5 samples of untreated fabric and 4 samples of treated fabric. The fabric specimens were glued to steel plates of 2 mm thickness with an epoxy resin (locally purchased in Brazil with the name Sikadur[®]-32) and let it dry for at least 24 hours for proper bonding. The specimens were glued to a length of 100 mm on each edge with a 300 mm free length between the steel grips (Figure 3.9). The tensile test was performed in a tensile universal testing machine (Shimadzu AG-X) with a load cell of 100 kN at a displacement control rate of 4 mm/minute (Figure 3.11).

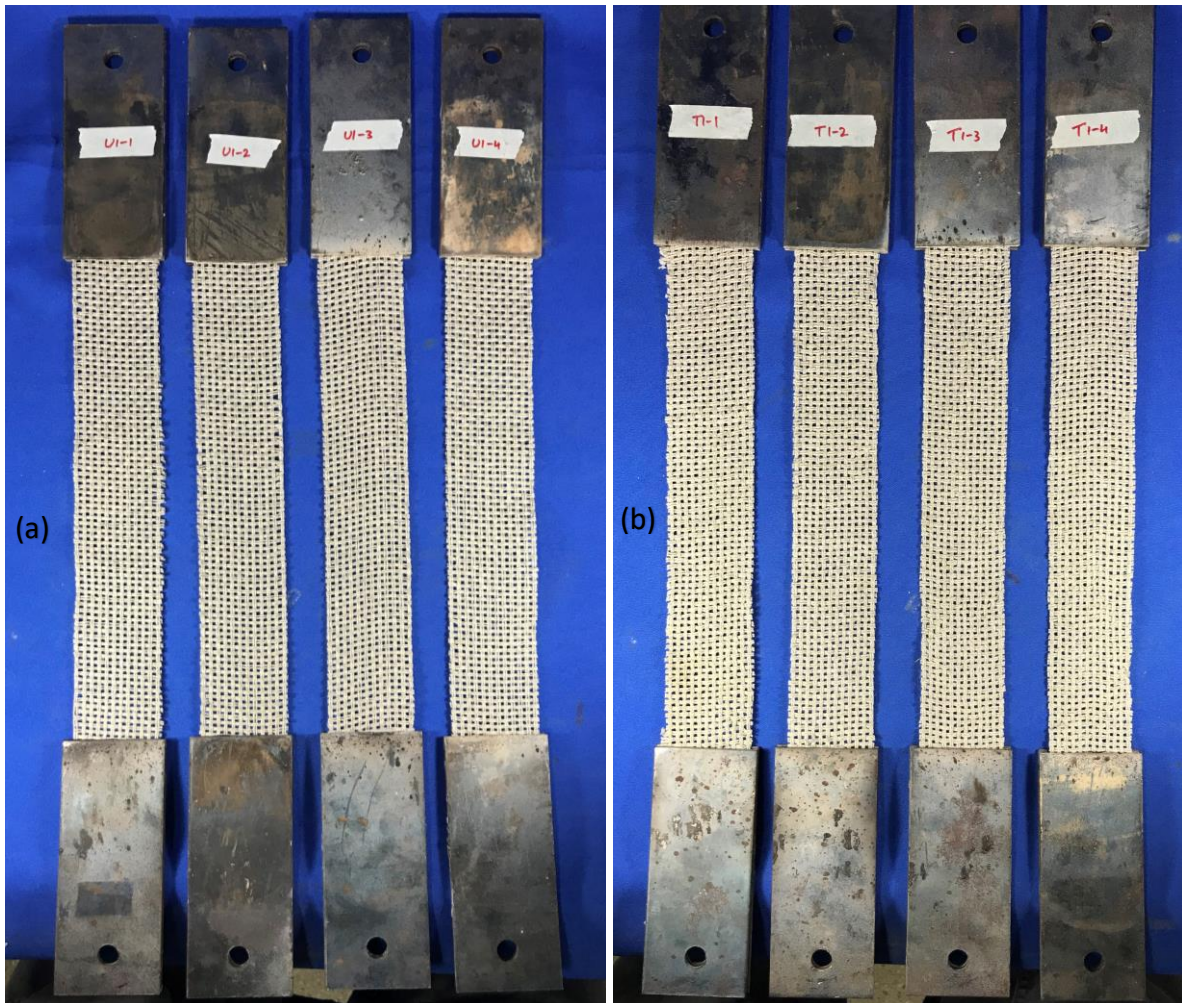


Figure 3.9 - Tensile test sample of Fabric (Untreated) series (a); Tensile test sample of Fabric (Treated) series (b)

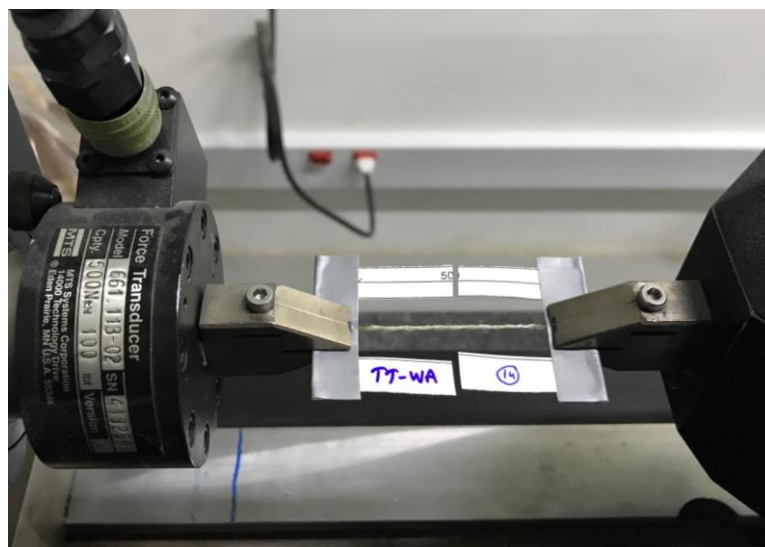


Figure 3.10 - Thread's tensile test sample in Microforce Testing Machine (During Test)



Figure 3.11 - Tensile test sample in Microforce Testing Machine (During Test)

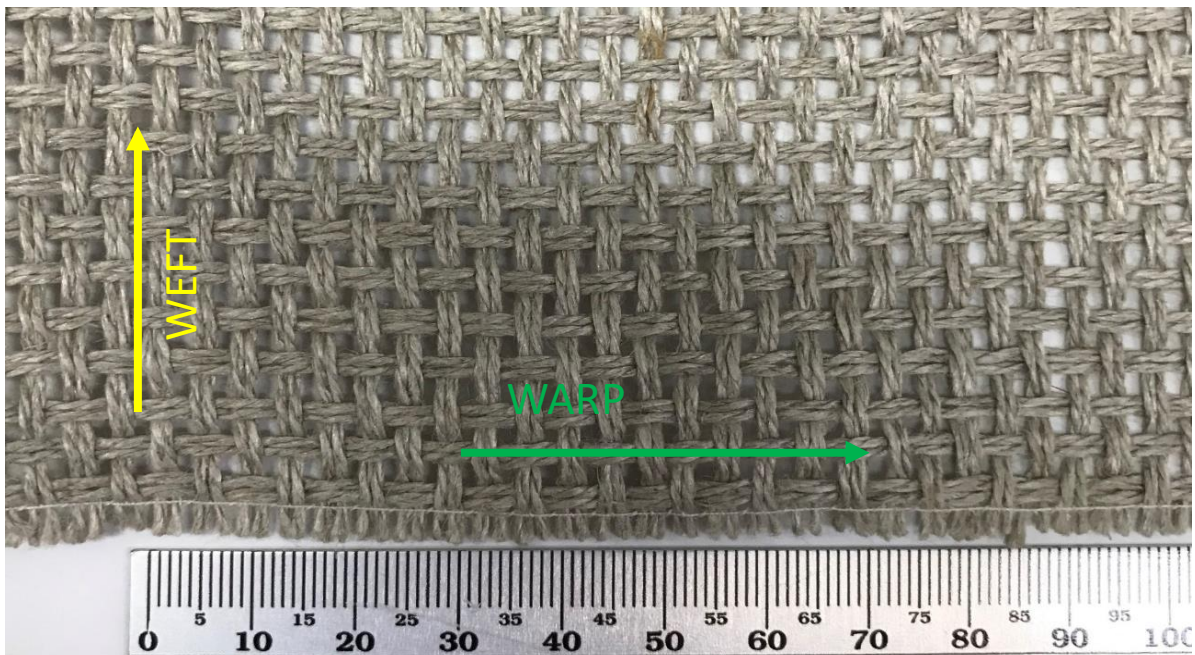


Figure 3.12 - Bidirectional flax fabric (Warp & Weft directions)

3.3.2. Results and Discussion

Axial displacement and force were automatically recorded by the Microforce testing machine for the tested series of samples of Yarn and Thread (Figure 3.13, Figure 3.14, Figure 3.15). A large variability in the tensile test results of flax yarn is observed with some samples failing at a load value as low as 15 N while others reaching an ultimate load value of up to 55 N. Axial displacement and force values are then converted to stress and strain respectively using the cross-section area determined in previous topic of physical characterization. The cross-section area of a yarn is half of the cross-section area of a thread since each thread is composed of two yarns.

The graphs of stress and strain show a typical behavior of natural fibers with a relatively small stiffness in the beginning, then a quasi-linear phase in the ascending branch before ultimate failure (Figure 3.16). The low initial stiffness of natural/plant-based fibers can be attributed to haphazard arrangement of fiber filaments during the rowing operation of thread manufacturing process. As in the literature, the stiffness E of threads in this study is defined as the slope of the curve in the range of 20% to 50% of ultimate strength.

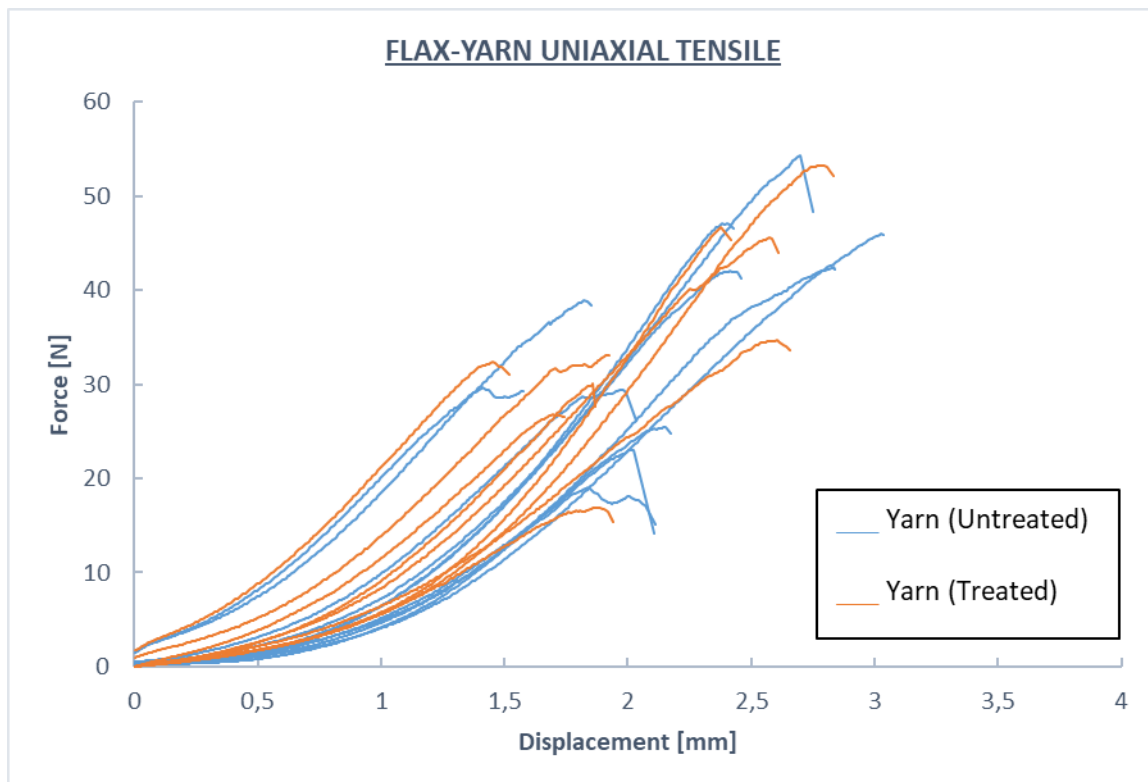


Figure 3.13 - Force versus displacement graph of flax yarn (Untreated vs Treated)

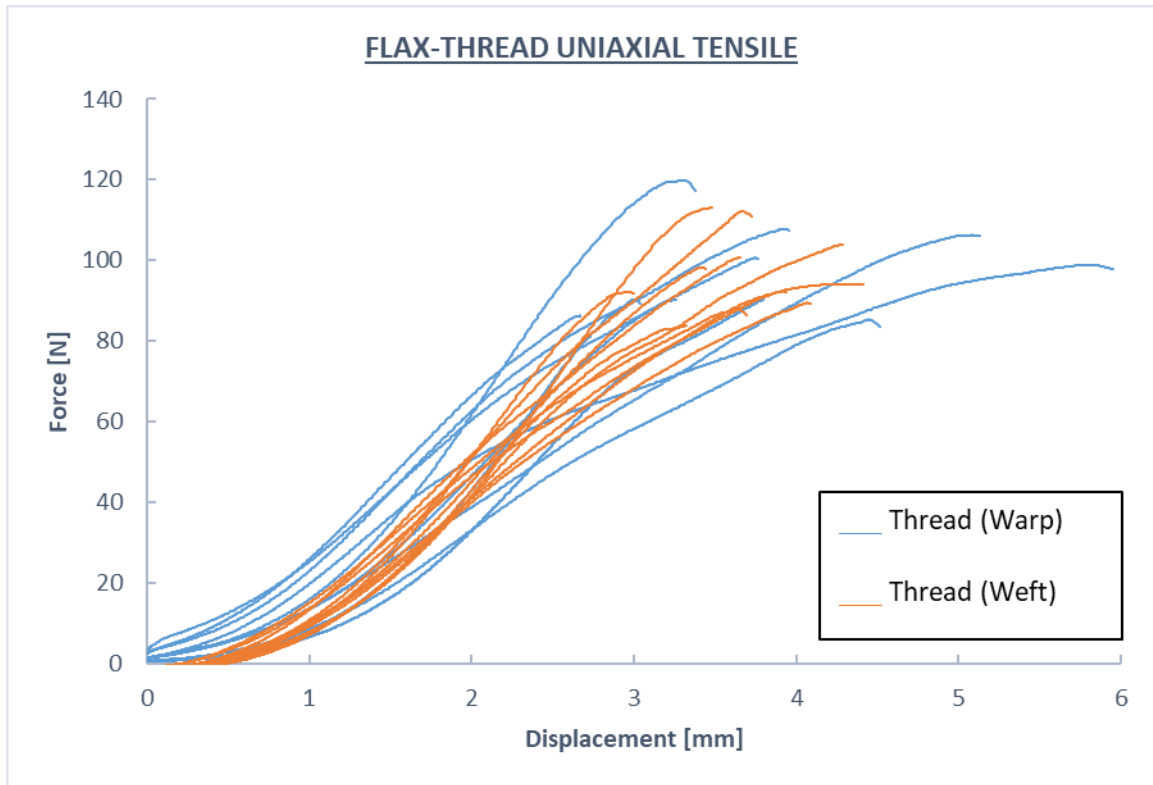


Figure 3.14 - Force versus displacement graph of flax thread (Warp vs Weft)

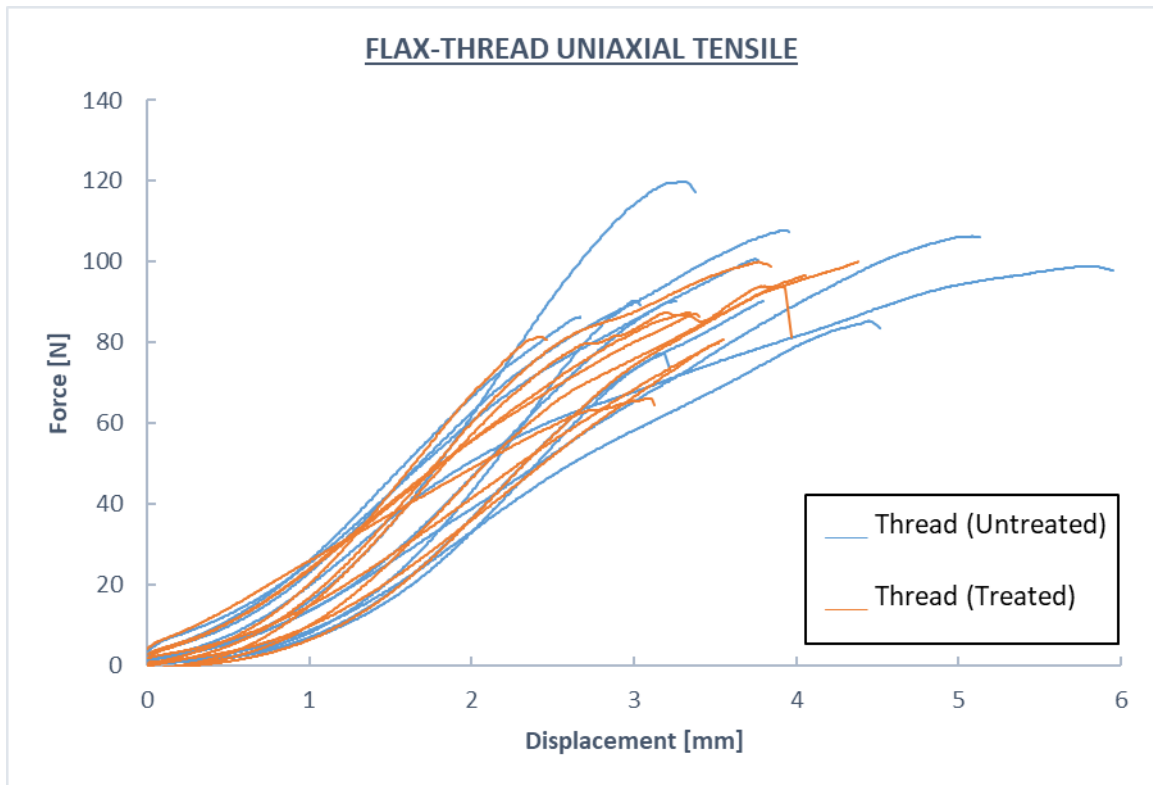


Figure 3.15 - Force versus displacement graph of flax thread (Untreated vs Treated)

The stresses in yarn, thread and fabric are determined by dividing the force by the transversal cross-section area determined by SEM analysis in the physical characterization chapter, considering such that a thread is made of two yarns and the fabric strip comprises 12 duals of threads making a total of 24 threads per strip under testing. Three main parameters; ultimate strength f_t , strain at failure ε_t and stiffness E ; have been reported to characterize the response of Yarn, Thread and Fabric series of samples. A considerable variability in the mechanical properties of flax was observed comparable to similar studies in the literature. The stress-strain response of Yarn (Treated & Untreated) series of samples is presented in the Figure 3.16.

Yarn (Untreated) series shows an average peak stress of 267 MPa (COV 32%) and average strain corresponding to maximum stress of 4.5% (COV 20%) while the Yarn (Treated) series is represented by an average peak stress of 273 MPa (COV 32%) and corresponding average strain of 4.2% (COV 22%). The elastic modulus of untreated and treated yarn samples is averaged at 7.7 GPa (COV 22%) and 7.9 GPa (COV 25%) respectively. Mechanical properties marginally change pre- and post-treatment with a slight increment of yarn strength of about 2%. The values of stress of Yarn (Untreated & Treated) series vary in the range 134 – 403 MPa and 130 – 410 MPa respectively. The huge variability in the measured mechanical properties suggests that yarn cannot solely be considered as a fundamental unit to determine the mechanical response of flax fabric.

The stress-strain graph of Thread (Warp & Weft) series of samples is presented in Figure 3.17. Thread (Warp & Weft) series demonstrate the average peak strength of 355 MPa (COV 13%) and 360 MPa (COV 10%) with corresponding ultimate strain values of 7.7% (COV 25%) and 7.4% (COV 11%) respectively. The mean values of elastic modulus of threads in warp and weft direction are 6.7 GPa (COV 18%) and 7.3 GPa (COV 13%) respectively. Strength values of both series of samples show a comparable behavior while the ultimate strain corresponding to peak stress slightly increases for thread in weft direction and the reason may be attributed to the manufacturing process in which the warp threads are kept stretched into place while the weft threads are woven in. Warp direction has been considered as the governing direction for all later tests in this study.

Compared to Yarn series of samples, the variability of mechanical properties of Thread series of samples is considerably reduced (Yarn peak-stress COV 32% versus Thread peak-stress COV 13%) hence the thread has been considered as the primary unit of flax textile under study.

The stress-strain graph of Thread (Untreated & Treated) series of samples is presented in Figure 3.18. The treated threads displayed mean peak-strength value 5% lower and corresponding ultimate strain value 8% lower than the untreated threads. The elastic modulus is however observed to marginally increase from 6.7 GPa (COV 18%) to 6.8 GPa (COV 2%) for untreated versus treated threads respectively. It is observed that the alkaline treatment tends

to slightly reduce the strength of the flax fibers, however, it also positively reduces the deformability of the threads at peak stress. The strain corresponding to peak strength for untreated and treated series of samples is measured as 7.7% and 7.1% respectively.

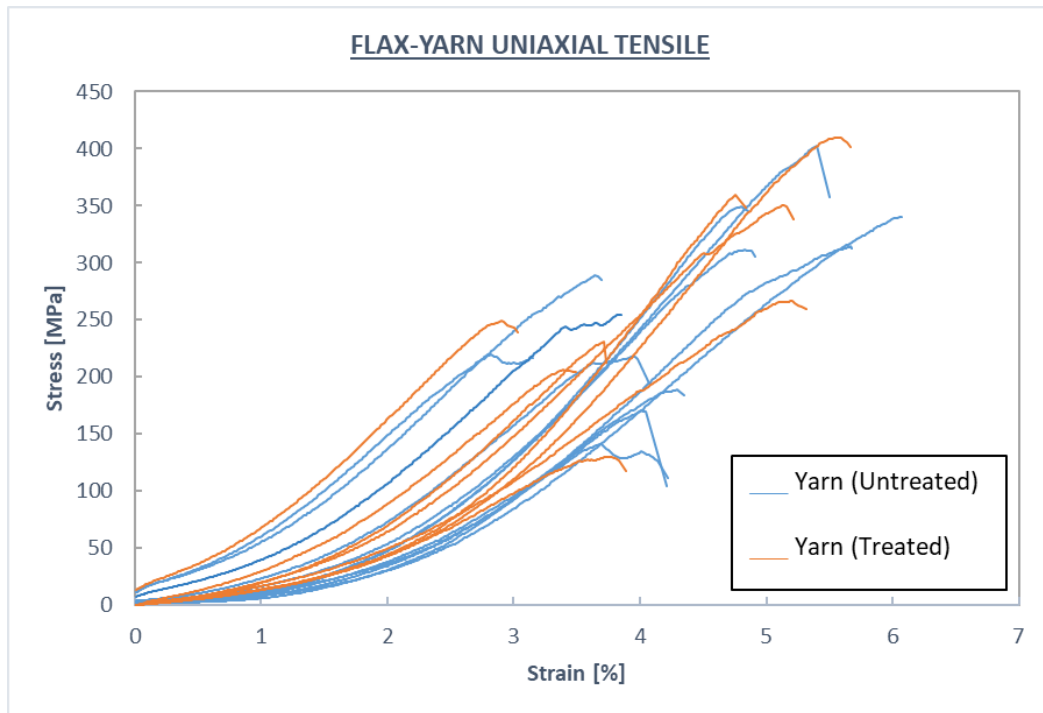


Figure 3.16 - Stress-strain graph of flax yarn (Untreated vs Treated)

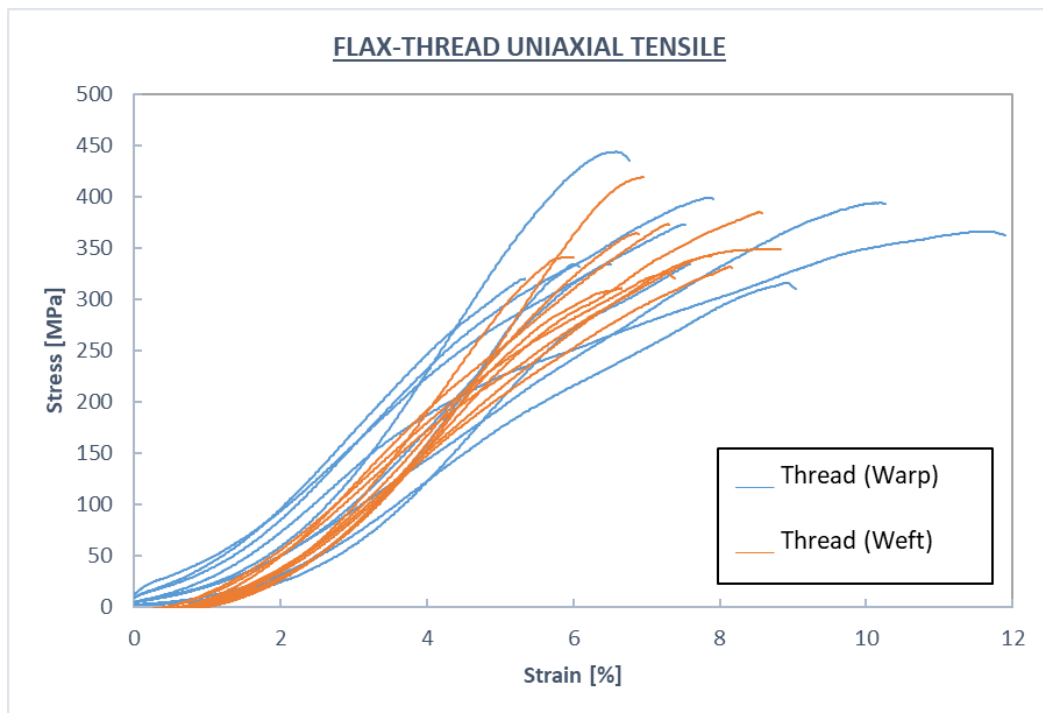


Figure 3.17 - Stress-strain graph of flax thread (Warp vs Weft)

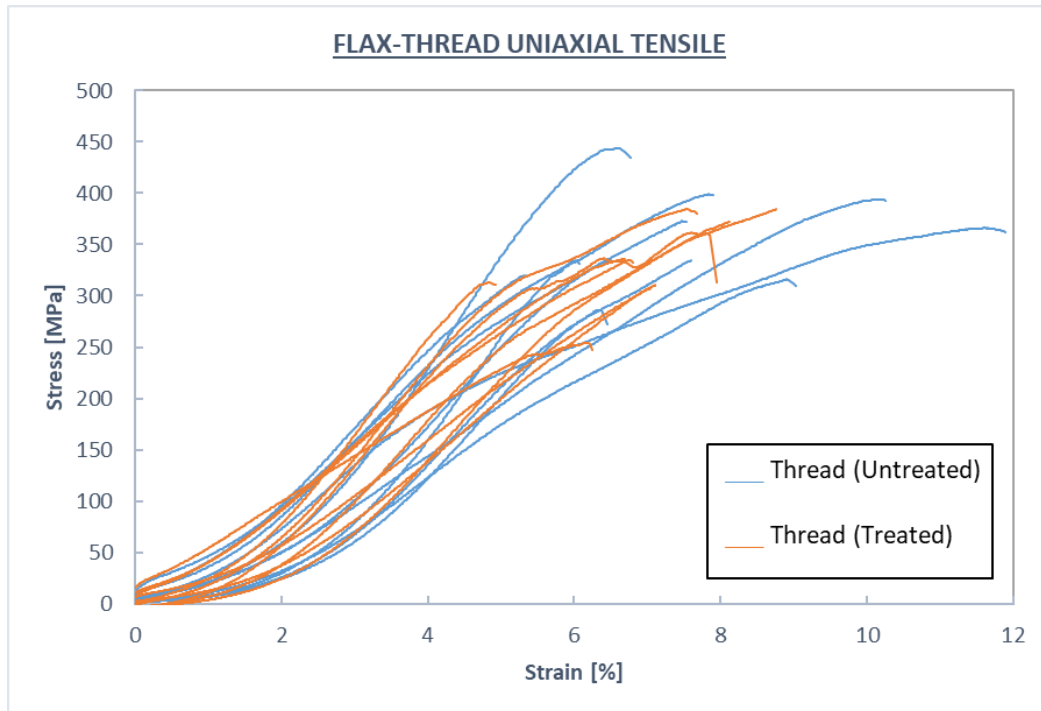


Figure 3.18 - Stress-strain graph of flax thread (Untreated vs Treated)

The flax textile strips of 60 mm width and 300 mm gauge length were tested in Shimadzu (AG-X) tensile testing machine and the crosshair movement of machine was recorded for the strain calculation. The load values were automatically recorded by the machine and later converted to stress by dividing with the gross cross-section area of the threads contained in the strip i.e., 24 threads. The force-displacement and stress-strain graphs of Fabric (Untreated & Treated) series of samples are presented in Figure 3.19 and Figure 3.20.

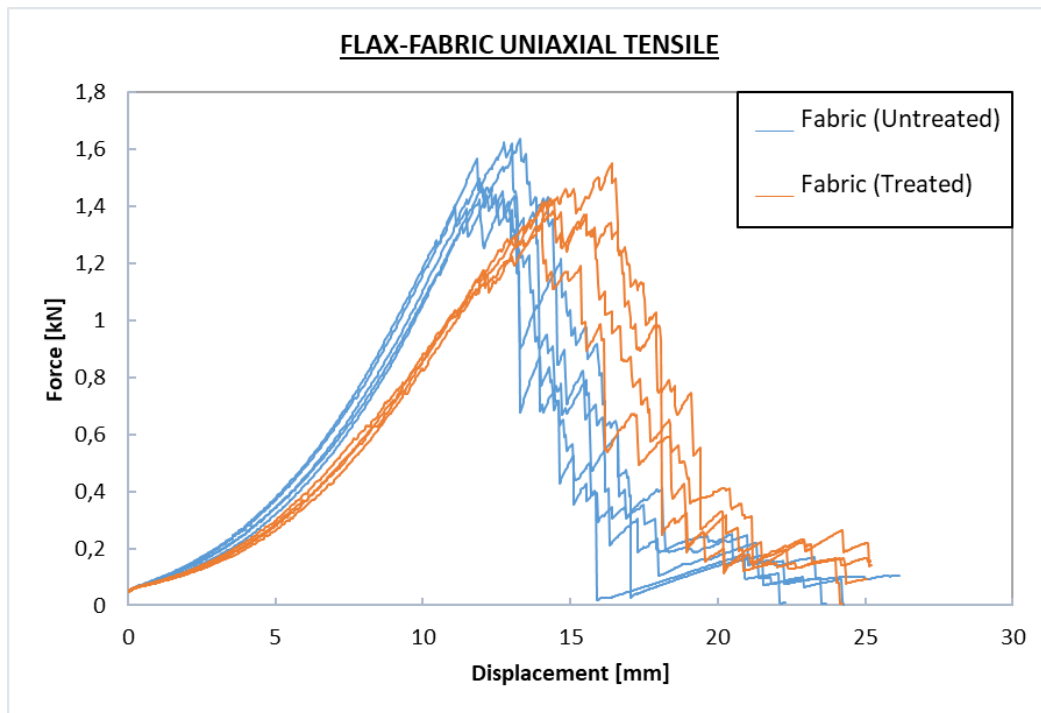


Figure 3.19 - Force-displacement graph of flax textile strip (Untreated vs Treated)

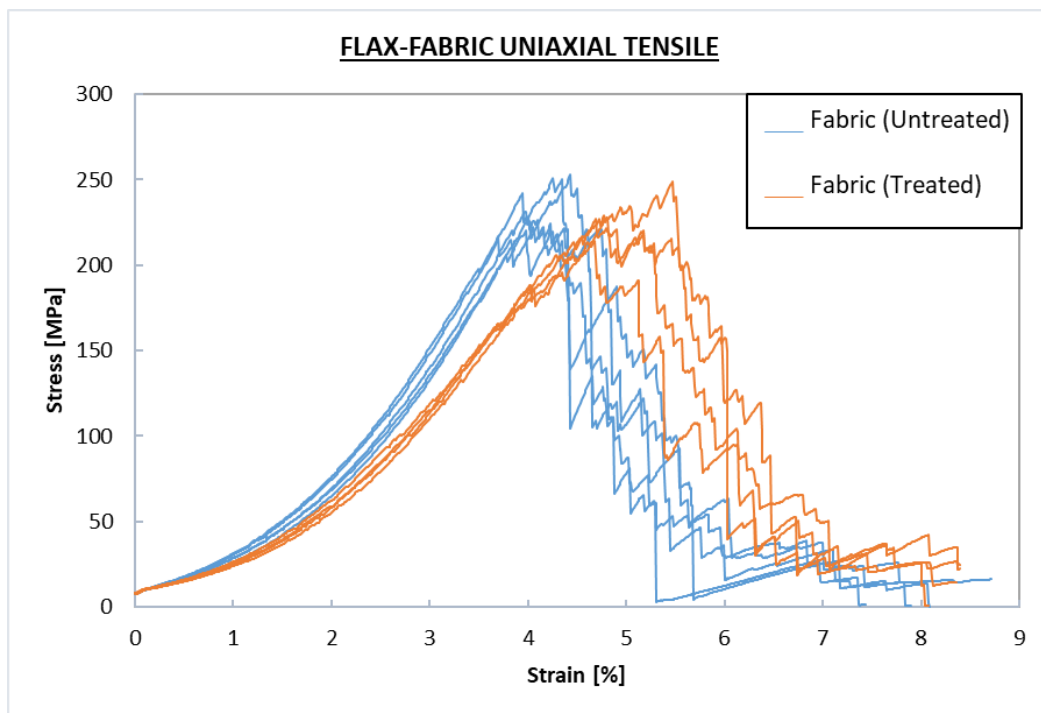


Figure 3.20 - Stress-strain graph of flax textile strip (Untreated vs Treated)

The mean peak-strength of Fabric (Untreated & Treated) series of samples is 238 MPa (COV 6%) and 230 MPa (COV 6%) respectively. Corresponding strain at peak for both series are determined as 4.2% (COV 5%) and 4.9% (COV 8%). The elastic modulus of untreated and treated fabric samples is measured as 5.9 GPa (COV 5%) and 5.3 GPa (COV 5%) respectively.

The stiffness of the fabric reduces with alkaline treatment by as much as 10%. This reduction in stiffness can be explained by the fact that the amorphous constituents (Hemicellulose and Lignin) of the fibers disintegrate with alkaline treatment creating a less compacted fiber cross-section. Due to the removal of these constituents by treatment, a 3% reduction in mean peak strength of the flax fabric has also been observed. The main mechanical properties of all series of samples are reported in Table 3.2.

Table 3.2 - Summary of mechanical properties of flax yarn, thread, and fabric

Series	P_{max} (N)	σ_{max} (MPa)	COV (%)	δ_u (mm)	ε_u (%)	COV	E (MPa)	COV
Yarn (Untreated)	36.0	266.7	32	2.3	4.5	20	7.7	22
Yarn (Treated)	35.5	273.1	32	2.1	4.3	22	7.9	25
Thread (Warp)	95.7	354.5	13	3.8	7.7	25	6.7	18
Thread (Weft)	97.1	359.5	10	3.7	7.4	11	7.3	13
Thread (Untreated)	95.7	354.5	13	3.8	7.7	25	6.7	18
Thread (Treated)	87.3	335.9	12	3.5	7.1	15	6.8	21
Fabric (Untreated)	1541.5	237.9	6	12.7	4.2	5	5.9	5
Fabric (Treated)	1432.3	229.5	6	14.7	4.9	8	5.3	5

Chapter 4

4 Characterization of Flax-TRMs

After mechanical characterization of the constituents i.e., flax fabric and mortar, the study has been extended to flax-TRMs in this section. This is in line with the previous studies to qualify a fabric to be used in TRMs. Hence, the experimental program advances from material scale to the composite scale, specifically the TRM prisms are prepared and tested in tensile for composite qualification.

4.1. Tensile Tests on Flax-TRM Prisms

4.1.1. Materials

Two mortars were prepared to be employed in the current research, one being the conventional mortar (hereinafter referred to as Mortar-1) and the other fiber-based mortar (hereinafter referred to as Mortar-2). Constituent materials in both the mortars were identical except that treated jute fibers of 2 cm length were added by 0.5% of the dry weight of the binder in Mortar-2.

4.1.1.1. Sand

Particle size distribution is of utmost importance when preparing mortar to be used in TRMs, the maximum particle size was ensured to be less than the nominal fabric mesh opening. Sand, being the inert coarse material, was used with a maximum aggregate size of 1.18 mm to allow for a good penetration of matrix through fabric mesh. The specific density of the sand was calculated as 2468 g/cm³. Particle size distribution of sand obtained by a vibrating test sieve machine is presented in Figure 4.1.

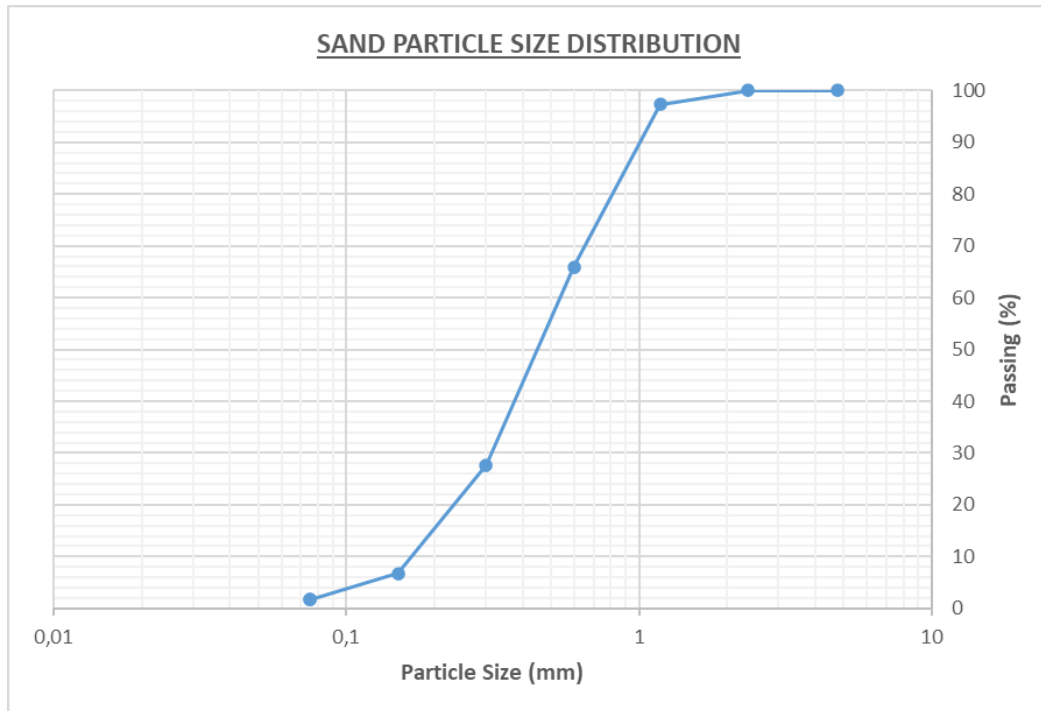


Figure 4.1 - Sand particle size distribution curve

4.1.1.2. Jute Fibers

The jute fibers, procured in Brazil, obtained in raw form, were washed by immersing in hot water at 80°C for 3 hours to remove any impurities and then the fibers were let dry for at least 24 hours in hot air flow chamber at 40°C. Subsequently, the washed fibers were then immersed in saturated solution of $\text{Ca}(\text{OH})_2$ in water (1.85 g per liter of water) at ambient temperature for 50 minutes and again dried in hot air flow chamber at 40°C for 24 hours. The resulting fibers were then cut into 2 cm pieces to be used in fiber-based mortar (Figure 4.2).



Figure 4.2 - Raw jute fibers as procured (a); treated & sized fibers to be used in mortar (b)

4.1.1.3. Mortar

The mortars were designed considering the fundamentals of sustainability and their suitability for application on existing structures. Specifically, instead of using 100% cement, we adapted partial replacement of cement with industrial by-products including Metakaolin, Fly Ash and Lime, hence promoting ecofriendly product development. Multiple mortar mix designs were prepared to determine the optimum mix-design in terms of low environment impact and desirable fresh and hardened state properties. The final mix design contained the binder quantities in a proportion of 35% cement, 35% metakaolin, 15% fly ash and 15% lime. The specific density of each of these constituents are 3048 g/cm^3 , 2728 g/cm^3 , 1920 g/cm^3 , 2538 g/cm^3 respectively. A reduction of 65% of cement in the mix-design compared to conventional cement-based mortars was obtained. The cement used in this study was purchased locally in Brazil with the brand name of CP-II-F.

The mortars were mixed as per EN 196-1 [38] with a binder to sand ratio of 1:2 and a water to cement ratio of 0.55 with a 0.55% Gelinium used as a superplasticizer. The consistency of mortar-1 and mortar-2 at fresh state was measured as 238 mm (Figure 4.3) and 170 mm respectively, as per EN 1015-3 [39]. The reduction in spread from 238 mm to 170 mm is attributed to the fact that addition of dry jute fibers absorbs a considerable amount of water of the fresh mortar. At least 5 specimens of each type of mortar were cast for mechanical characterization of mortars. The specimens were de-molded after at least 24 hours of casting and cured in a humid chamber for 28 days before testing.



Figure 4.3 - Mortar during mixing (a); fresh state consistency measurement (b)

Hardened state mechanical properties i.e., flexure and compressive strength of both mortars were determined at 28 days in Shimadzu (AG-X) machine (Figure 4.4) in compression testing configuration as per EN 196-1 [38]. Mortar-1 exhibited a flexure strength of 1.93 MPa and a compressive strength of 12.4 MPa at 28 days of wet curing. On the other hand, Mortar-2 showed a flexure strength of 2.33 MPa and a compressive strength of 13.8 MPa. The

enhancement of mechanical properties from Mortar-1 to Mortar-2 is in line with similar studies in literature. Inclusion of fibers in the mortar matrix increases the flexure as well as compressive strength of the mortar. Main properties of both mortars are summarized in Table 4.1.

Table 4.1 – Summary of mortar properties.

Type	Consistency (mm)	COV (%)	Flexure Strength (MPa)	COV (%)	Compressive Strength (MPa)	COV (%)
Mortar-1	238	5	1.93	13	12.4	24
Mortar-2	170	4	2.33	12	13.8	4

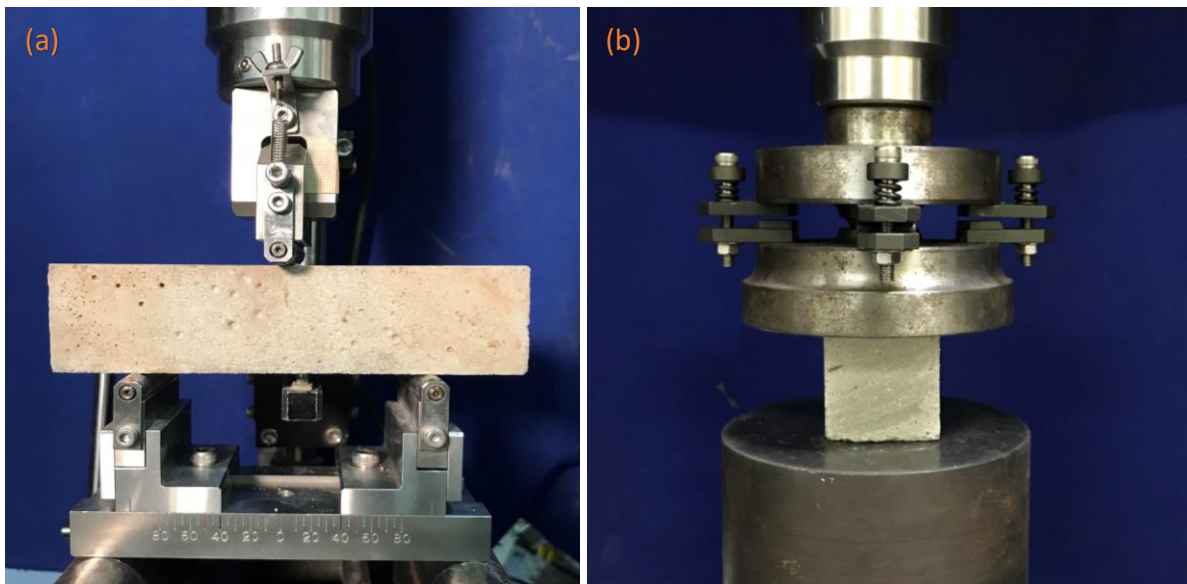


Figure 4.4 - Mortar prism in flexure testing (a); mortar cube under compression testing (b)

4.1.1.4. Flax Fabric

The natural textile used in this study is the flax fabric available locally in Italy sold as “FIDFLAX GRID 300 HS20®” whose physical and mechanical characterization is detailed in chapter 3. The properties of flax strips used as reinforcement in flax-TRMs are described in the Table 4.2. The tensile strength of a single thread, being the fundamental constituent of flax fabric, untreated and treated is measured as 304.9 MPa & 272.9 MPa respectively, the elastic modulus as 5.7 MPa and 5.5 MPa respectively and strain corresponding to peak strength as 7.8% and 7.1% respectively.

Table 4.2 - Summary of mechanical properties of flax fabric strips used in TRM.

Series	Size (mm)	P_{max} (N)	σ_{max} (MPa)	COV (%)	δ_u (mm)	ϵ_u (%)	COV	E (MPa)	COV
Flax Fabric (Untreated)	60x500	1541.5	237.9	6	12.7	4.2	5	5.9	5
Flax Fabric (Treated)	60x500	1432.3	229.5	6	14.7	4.9	8	5.3	5

4.1.2. Methods

To prepare flax-TRM specimens, the wet lay-up procedure was adapted as per ACI 549.4R-13 [40]. Purpose specific molds, of size 60 x 500 x 10 mm with the possibility to manually stretch the fabric in major axis direction during casting, were prepared (Figure 4.5). For ease of demolding the specimens after casting, oiling of the surface of the molds was done. Flax-TRM specimens embedded with a single layer of flax textile were prepared in three layers such that the two layers of mortar have the equivalent thickness around the central textile strip. The first layer of mortar was laid and leveled with the help of a roller (Figure 4.5), then the flax textile strip was embedded with the help of a roller while keeping the strip stretched at both ends manually (Figure 4.5), eventually the final layer of mortar was applied and leveled with roller before conveniently smoothing it (Figure 4.5). Flax-TRM specimens embedded with a double layer of flax textile were prepared such that there is an equivalent layer of mortar between both the textile strips. Hence, three layers of mortar of equivalent thickness were applied following the same procedure as in the case of a single layer but with repetition of the procedure for double layer.

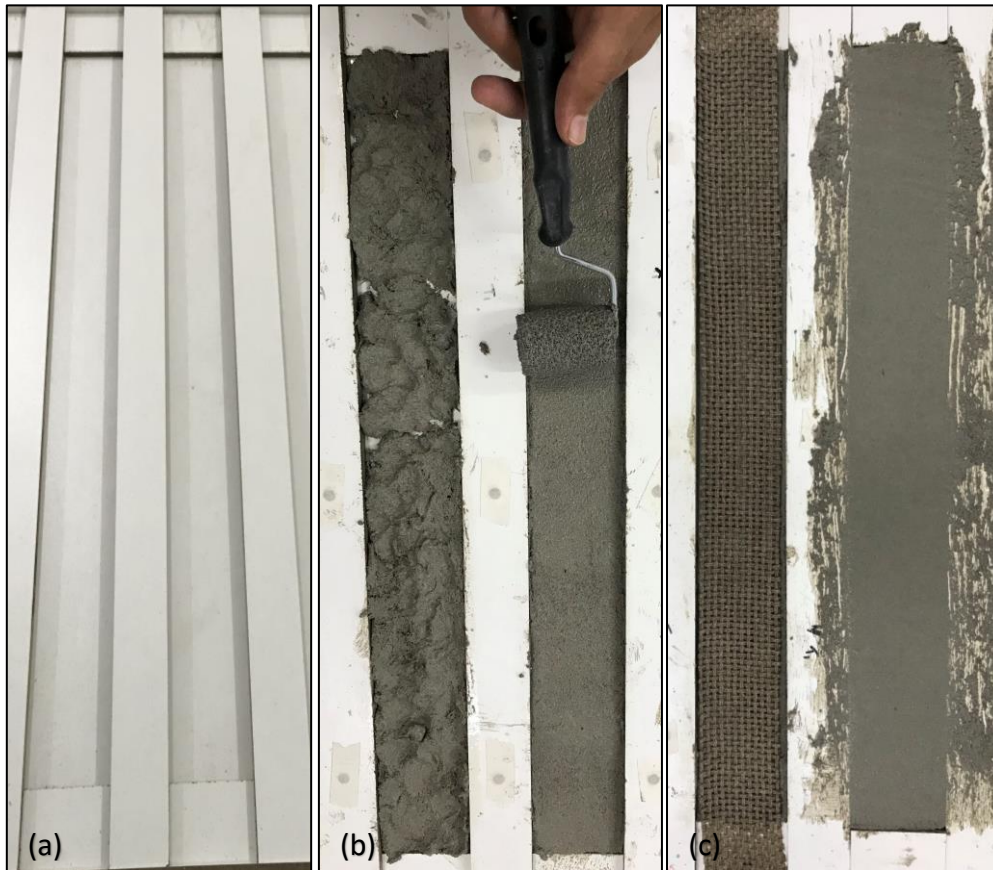


Figure 4.5 - Empty TRM mold (a); mortar spreading and levelling with roller (b); embedding the flax fabric strip and final rolling (c)

Four series of flax-TRM specimens were prepared with Mortar-1 as the inorganic matrix with a total thickness of 1 cm and a width of 6 cm as described below.

- *TRM-U1L: series of specimens consisting of flax-TRM prisms with normal mortar embedded with single layer of untreated flax textile.*
- *TRM-U2L: series of specimens consisting of flax-TRM prisms with normal mortar embedded with two layers of untreated flax textile.*
- *TRM-T1L: series of specimens consisting of flax-TRM prisms with normal mortar embedded with single layer of pretreated flax textile.*
- *TRM-T2L: series of specimens consisting of flax-TRM prisms with normal mortar embedded with two layers of pretreated flax textile.*

Two series of flax-TRM specimens were prepared with Mortar-2 as the inorganic matrix with a total thickness of 1 cm and a width of 6 cm as described below.

- *TRM-FU1L: series of specimens consisting of flax-TRM prisms with fiber-based mortar embedded with single layer of untreated flax textile.*

- *TRM-FTIL: series of specimens consisting of flax-TRM prisms with fiber-based mortar embedded with single layer of pretreated flax textile.*

The samples were prepared and kept in the mold under ambient conditions by covering with blanket to control dehydration of mortar for at least 24 hours before demolding. After demolding the samples were kept in humidity chamber for 28 days to allow for proper hydration.

After 28 days, the specimens were removed from the humid chamber and dried in ambient conditions before testing. The TRM specimens were tested, and results have been reported as per AC434 [41]. Each series of specimens has a total length of 50 cm in which 10 cm on each side are glued to the steel plates during the tensile testing phase of flax-TRM prisms. These steel plates eventually transfer the tensile force to the specimens during testing (Figure 4.6). Tensile tests on TRM specimens were performed at the lab NUMATS/POLI/COPPE of Federal University of Rio de Janeiro in a tensile universal testing machine (Shimadzu AG-X) with a load cell of 100 kN at a displacement control rate of 0.3 mm/minute. The force and crosshair displacement of the machine were measured at each step of the test.

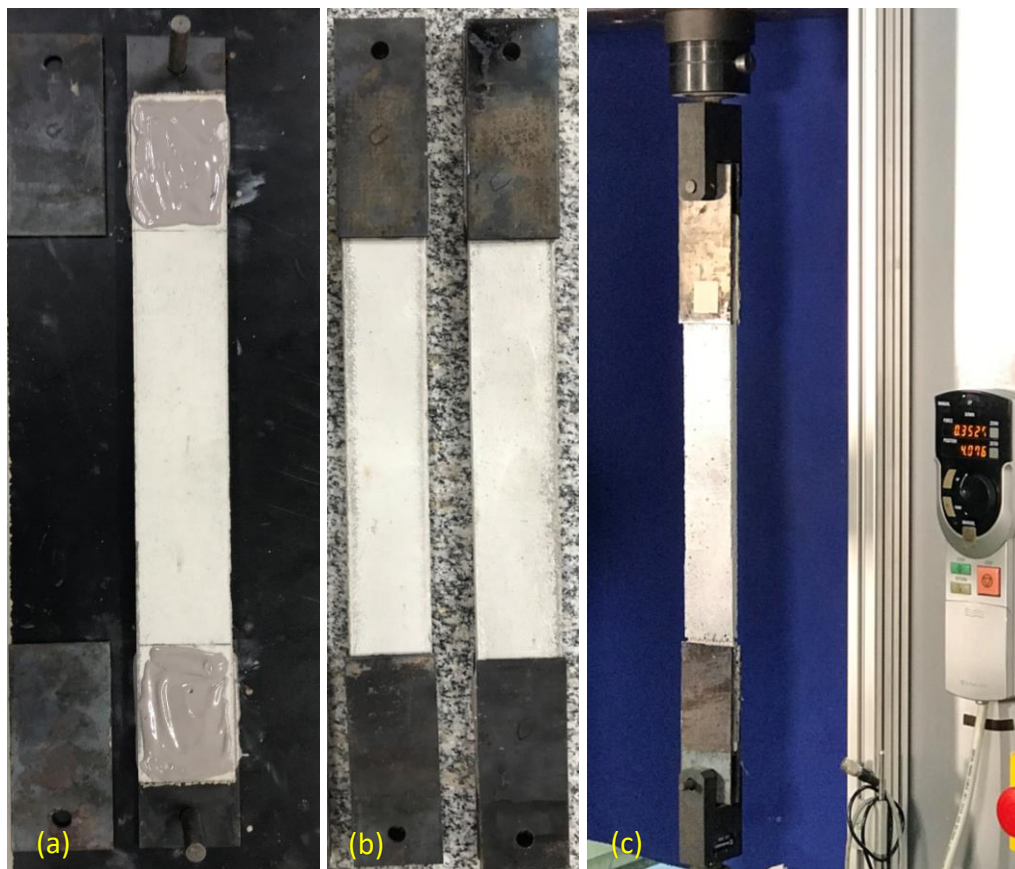


Figure 4.6 - TRM specimen being connected with steel plates with epoxy (a); TRM tensile specimen ready for testing (b); Tensile test setup (c)

4.1.3. Results and Discussion

The load at each step of the displacement-controlled test was measured by the machine automatically. The load-displacement graphs of tensile tests on flax-TRM specimens are presented in Figure 4.7, Figure 4.8, and Figure 4.9. Subsequently, the calculation of stress and strain was performed considering the gross cross-section area of the TRM specimens for stress evaluation and free length of the specimen (300 mm) for strain evaluation. Resulting stress-strain graphs are presented in Figure 4.11, Figure 4.12, and Figure 4.13. As expected, all the series of samples present a typical three-phase response hereinafter referred to as Phase-1, Phase-2 and Phase-3, in-line with similar studies in the literature.

The first phase represents the linear branch of stress-strain curve and corresponds to the development of first transversal crack in the mortar matrix (Figure 4.10a). At the development of the first crack, there is a transition zone between phase-1 and phase-2 with a sudden drop of load. Phase-2 is identified by the development of series of transversal cracks in the TRM specimen (Figure 4.10b) and is characterized by multiple loading and unloading patterns in the stress-strain curve. After all the possible cracks have occurred, the TRM response is identified by slippage of fabric threads inside the mortar and the ultimate breakage of the threads in the vicinity of any of the developed crack (Figure 4.10c). In the stress-strain response curve, Phase-3 is represented with a strain hardening branch.

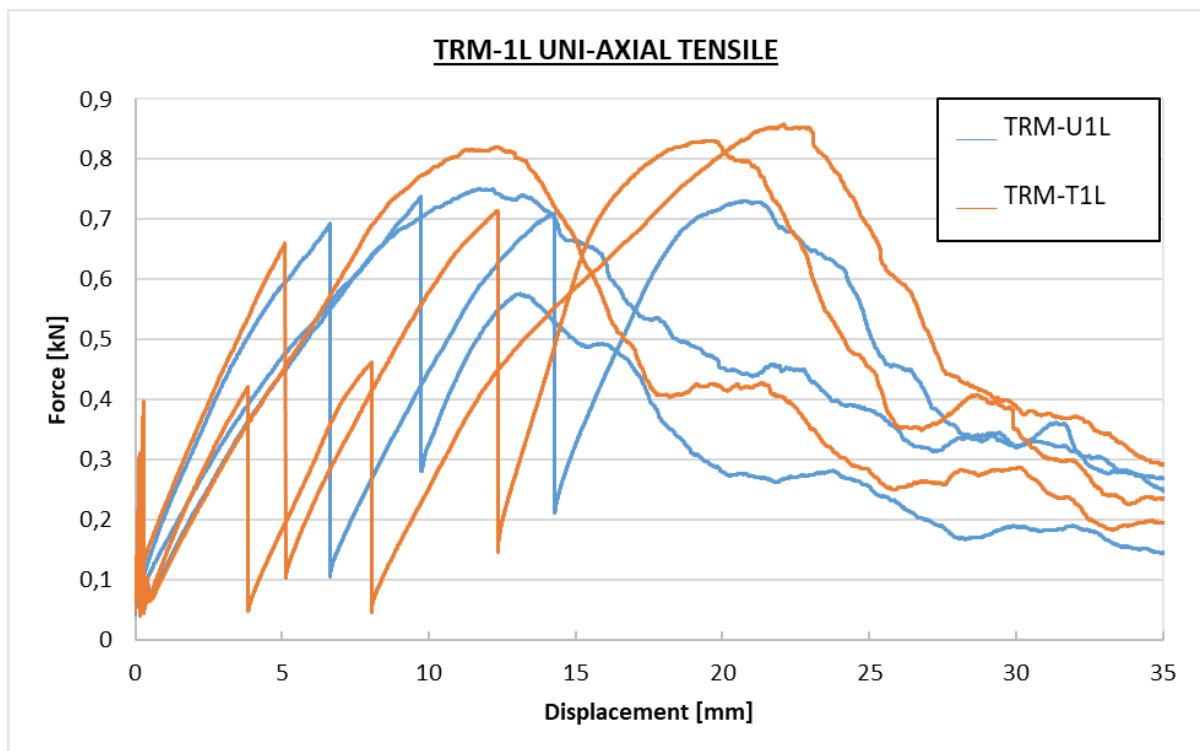


Figure 4.7 - Load versus displacement response of TRM-U1L and TRM-T1L

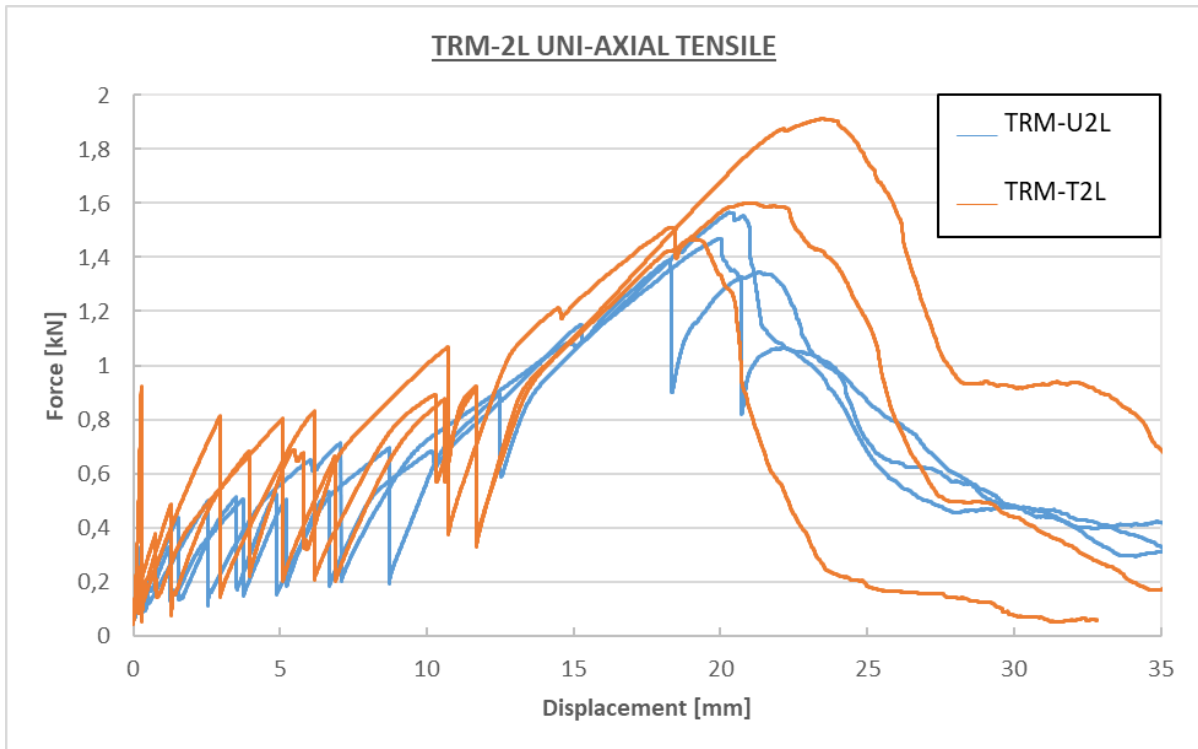


Figure 4.8 - Load versus displacement response of TRM-U2L and TRM-T2L

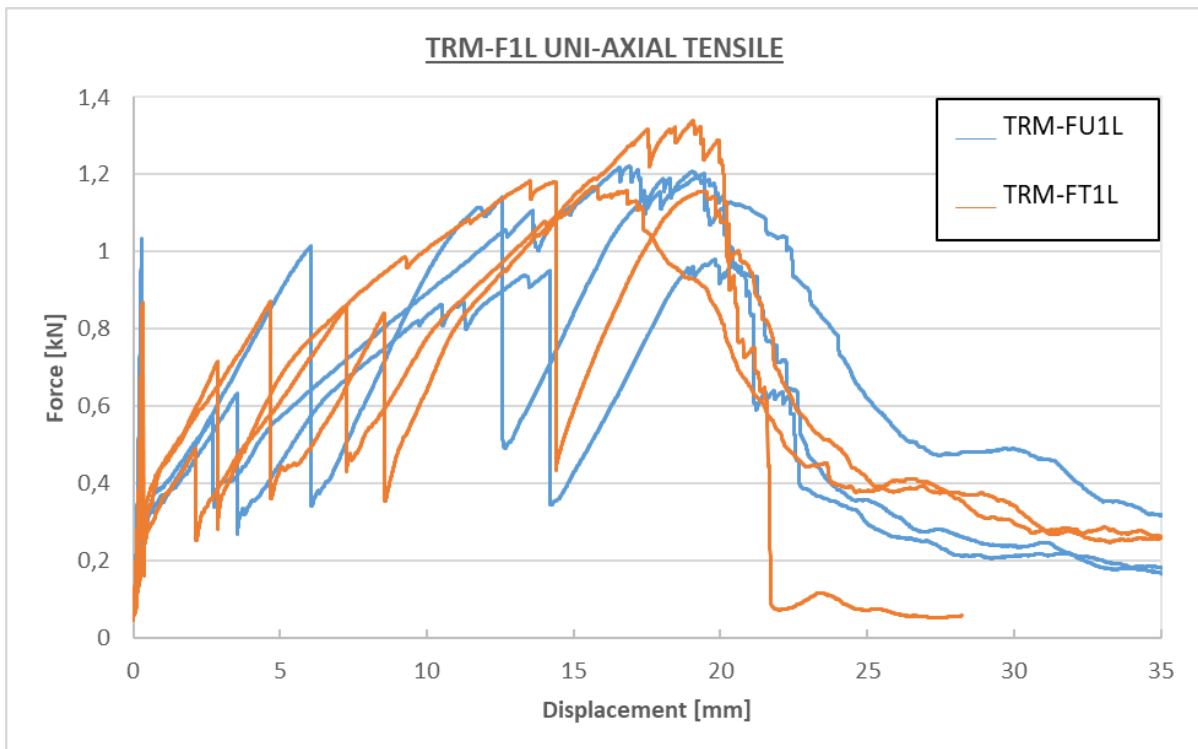


Figure 4.9 - Load versus displacement response of TRM-FU1L and TRM-FT1L

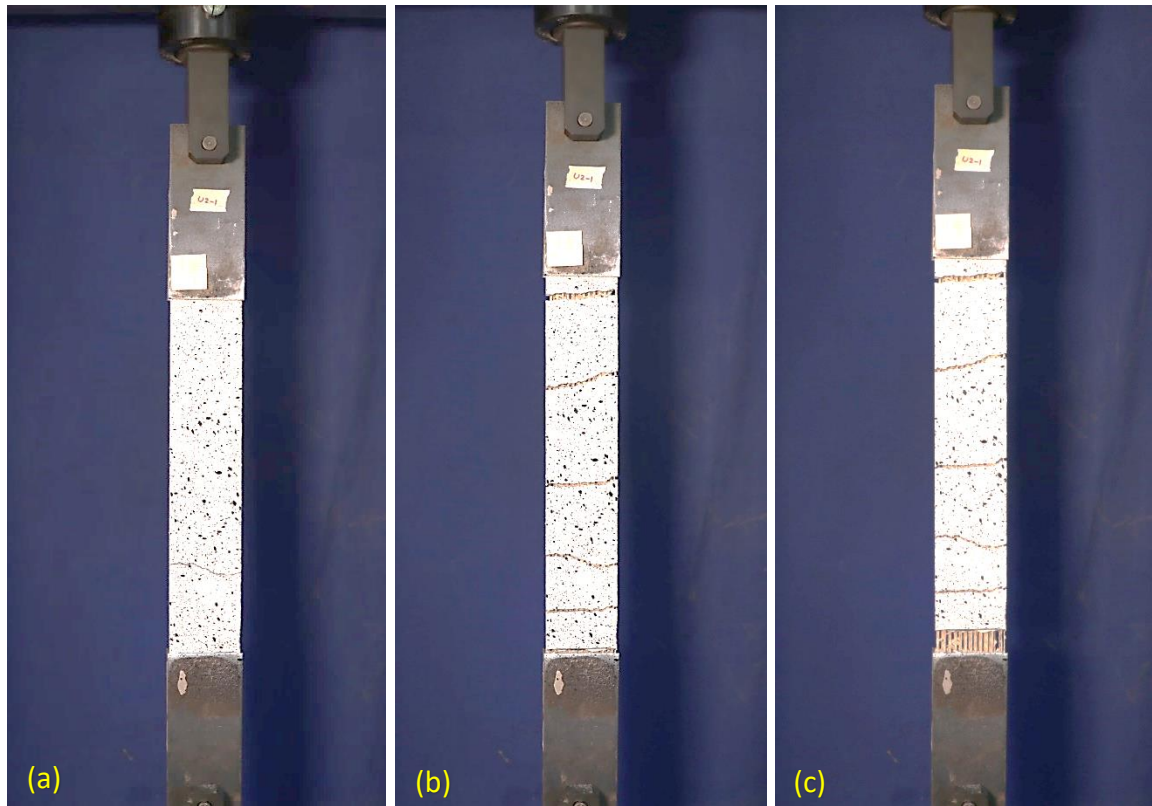


Figure 4.10 - Phase-1 development of 1st crack in TRM specimen (a); Phase-2 development of multiple cracking (b); Slippage & ultimate failure of the flax textile (c)

Three specimens for each series were tested and the mean values of maximum load, maximum stress, displacement & strain corresponding to maximum stress are reported in Table 4.3.

Table 4.3 - Summary of mechanical properties of flax-TRMs.

Series	P_{\max} (N)	σ_{\max} (MPa)	COV (%)	δ_u (mm)	ϵ_u (%)	COV
TRM-U1L	740.0	1.23	1	15.2	5.1	32
TRM-T1L	836.6	1.39	2	18.0	6.0	28
TRM-U2L	1474.5	2.46	6	20.5	6.8	3
TRM-T2L	1675.1	2.79	13	20.9	7.0	12
TRM-FU1L	1134.5	1.89	12	18.7	6.2	8
TRM-FT1L	1231.0	2.05	8	18.1	6.0	11

TRM-U1L series has the least resistance in terms of mean ultimate stress calculated as 1.23 MPa (COV 1%) which is exactly half of the peak stress of 2.46 MPa (COV 6%) taken by TRM-U2L series. This shows a 100% increase in the peak resistance thus doubling the number of flax layers embedded in the TRM matrix doubled the peak tensile load capacity of the TRM. This contrasts with what Ferrara et. al. has reported [29] that the change in volume fraction of fabric embedded in TRM does not significantly affect the TRM mechanical properties. Additionally, deformability of the composite matrix has also increased in TRM-U2L compared to TRM-U1L by 33%. The mean ultimate strain values of TRM-U1L and TRM-U2L are measured as 5.1% (COV 32%) and 6.8% (COV 3%) respectively.

A similar trend is observed in TRMs embedded with treated single and double layers of flax fabric. TRM-T1L and TRM-T2L demonstrate mean peak strength of 1.4 MPa (COV 2%) and 2.8 MPa (COV 13%) and corresponding ultimate strain values of 6% (COV 28%) and 7% (COV 12%) respectively. An increment of 100% in the peak strength from single to double layer and an increment of 17% in the ultimate strain value has been observed.

Comparing the response of TRMs embedded with untreated flax fabric to the ones embedded with treated flax fabric shows a considerable enhancement of mechanical properties in terms of mean peak strength as well as increasing the deformability of the matrix composite. TRM-T1L series shows an increase of 13% and 19% in the values of peak stress and ultimate strain corresponding to peak stress respectively when compared to TRM-U1L series. The increase of peak strength and corresponding strain of TRM-T2L series is measured as 13% and 2% respectively, in comparison to TRM-U2L series. Comparatively lesser increase in ultimate strain measured in TRM-T2L series in current study can be explained by the fact that two of the TRM-T2L samples experienced splitting at the tabs (Figure 4.14) triggering premature failure due to loss of matrix-fabric bond.

The values of peak strength are directly dependent on the fabric to matrix bond behavior and the response of the dry matrix in tension. This shows that the alkaline treatment not only improves the fabric to matrix bond behavior but also contributes towards extra deformability of the composite system. Further, measuring the value of stress taken by the composite system at a given value of strain shows a higher strength gain by the TRM specimens embedded with treated flax fabric compared to untreated ones.

TRM-FU1L and TRM-FT1L series present a very unique response in terms of the ultimate strength gain and the corresponding deformability of the matrix. The mean peak strength and corresponding mean ultimate strain of TRM-FU1L is measured as 1.89 MPa (COV 12%) and 6.2% (COV 8%) respectively. TRM-FT1L series experienced a mean peak strength value of 2.05 MPa (COV 8%) which is 8% in excess of TRM-FU1L series. The mean ultimate strain of TRM-FT1L series, however, has experienced a reduction of 3% from the corresponding mean ultimate strain value of TRM-FU1L. This reduction in deformability from

untreated to treated fabric can be attributed to the casting anomalies of specimens due to lesser workability of Mortar-2.

A comparison of mechanical properties of all series of TRM specimens is reported in Figure 4.16 and Figure 4.17. In terms of peak tensile strength and ultimate strain, TRM-T2L series represent the best combination of results.

The comparison of stress-strain graph of TRM-T1L series with TRM-FT1L series is reported in Figure 4.15. The mechanical response of the latter shows a much-improved response due to the presence of short jute fibers in the mortar matrix. An increase of 48% in the peak strength of TRM-FT1L series with no change in the ultimate strain has been observed in comparison to TRM-T1L series. A comparison of the exploitation ratio of the flax fabric in all series of TRMs is presented in Table 4.4. It is the ratio of mean peak tensile stress taken by the flax fabric strip in the composite to the flax fabric strip measured in dry condition [29].

Table 4.4 - Summary of fabric exploitation ratio for different TRM composites.

Series	Composite P_{\max} (N)	Composite σ_{\max} (MPa)	Dry Fabric P_{\max} (N)	Dry Fabric σ_{\max} (MPa)	Fiber Exploitation Ratio (%)
TRM-U1L	740.0	114.2	1541.5	237.9	48
TRM-T1L	836.6	134.1	1432.4	229.5	58
TRM-U2L	1474.5	113.8	1541.5	237.9	48
TRM-T2L	1675.1	134.2	1432.4	229.5	59
TRM-FU1L	1134.5	175.1	1541.5	237.9	74
TRM-FT1L	1231.0	197.3	1432.4	229.5	86

TRM-FT1L series demonstrates the maximum exploitation of the flax fabric measured at 86% followed by slightly lower exploitation ratio of TRM-FU1L series at 74%. The composites with conventional mortar matrix show much lower values of exploitation ratios measured as 48% for the single layered flax composites and 58% for double layered flax composites.

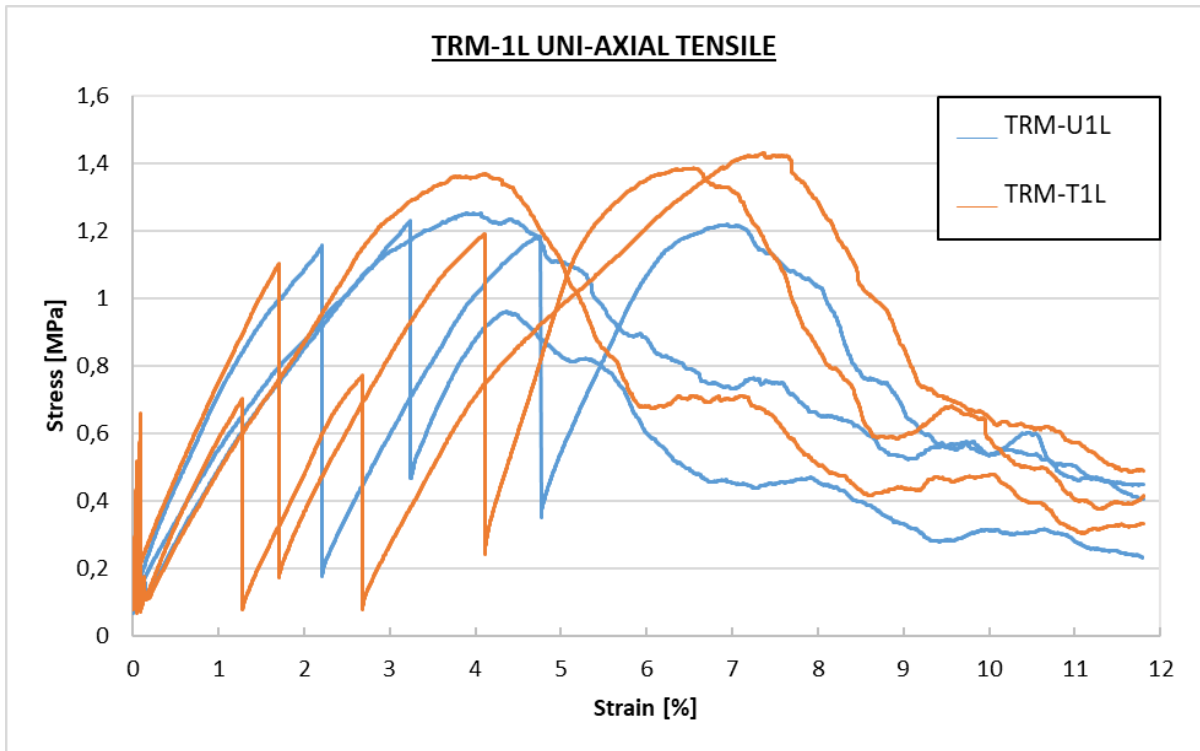


Figure 4.11 - Stress-strain response of TRM-U1L and TRM-T1L

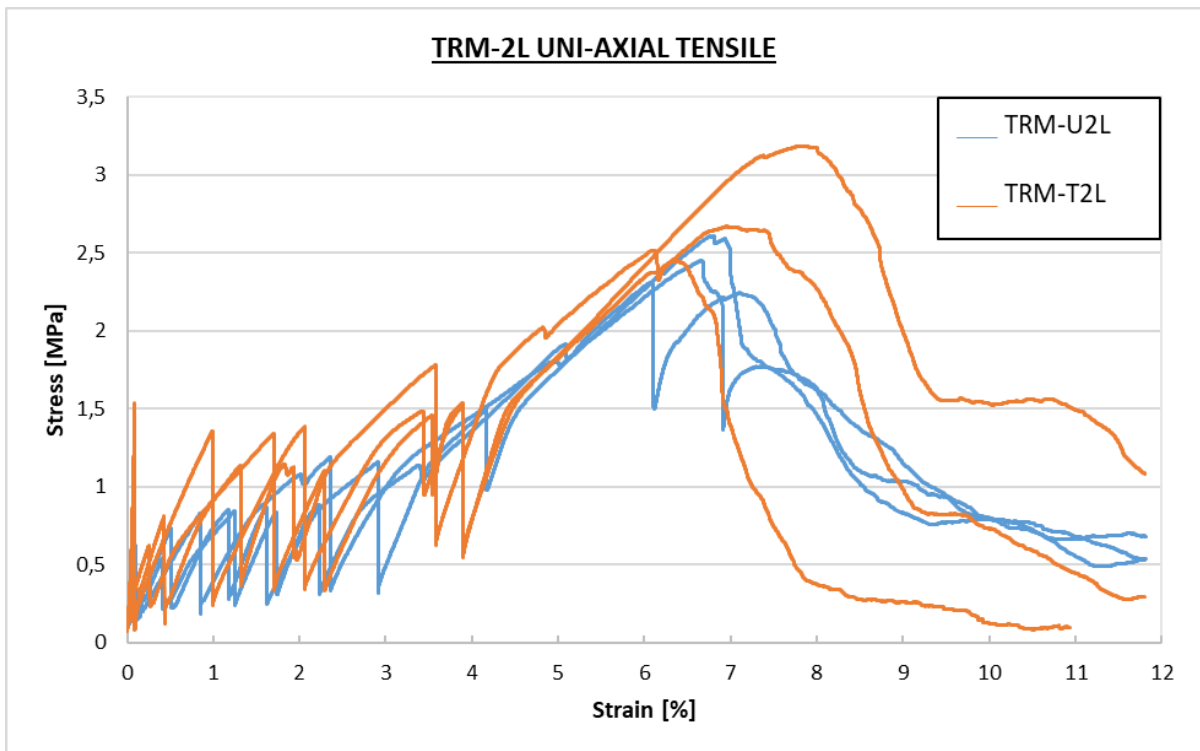


Figure 4.12 - Stress-strain response of TRM-U2L and TRM-T2L

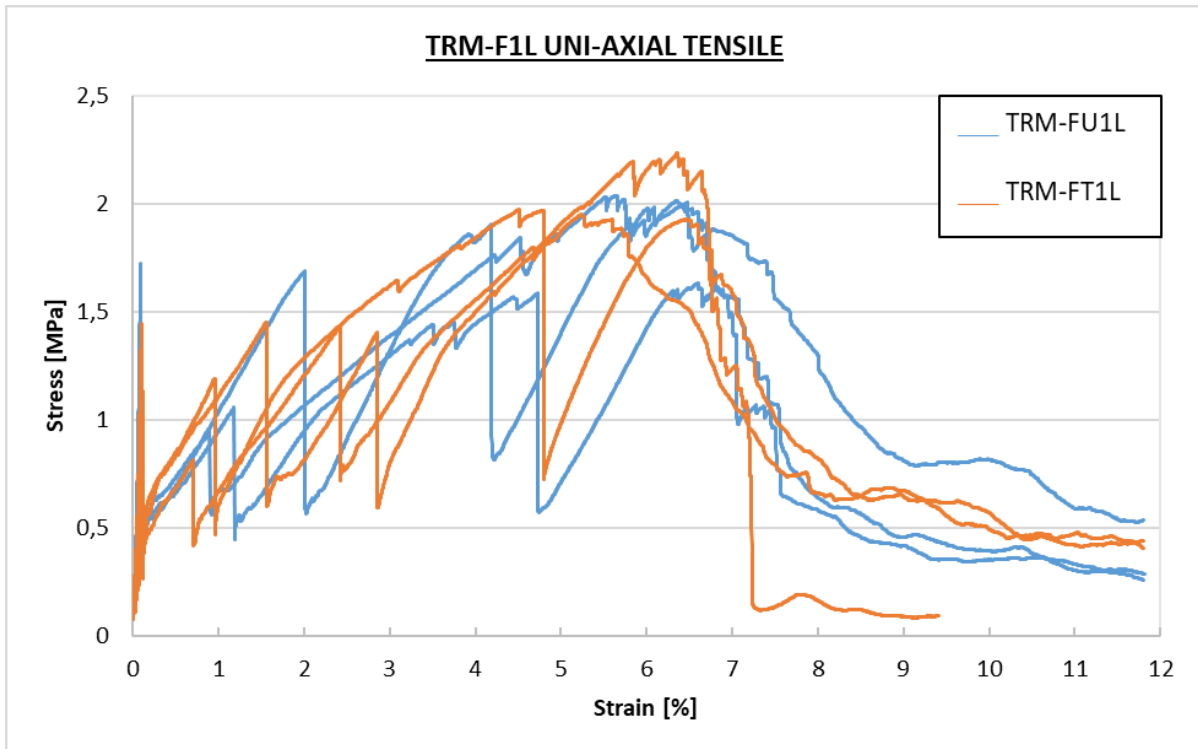


Figure 4.13 - Stress-strain response of TRM-FU1L and TRM-FT1L

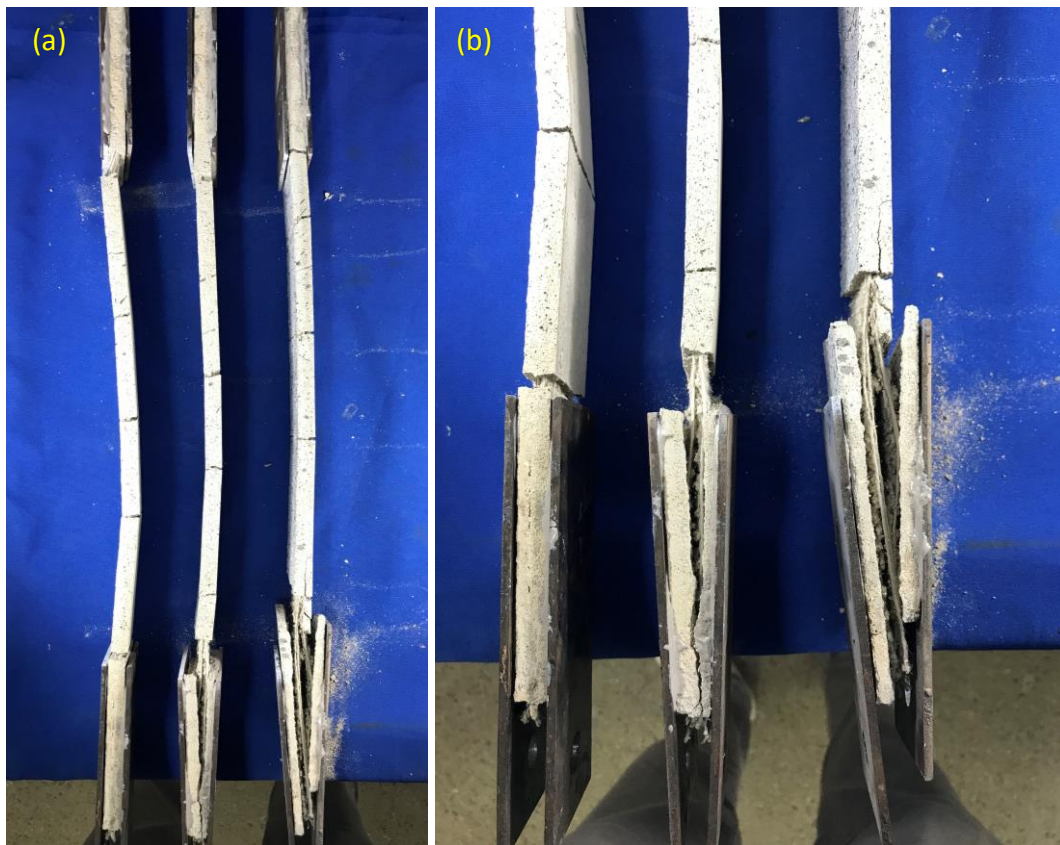


Figure 4.14 - Splitting of TRM-T2L specimens in the gripping area (a); close-up of the grips (b)

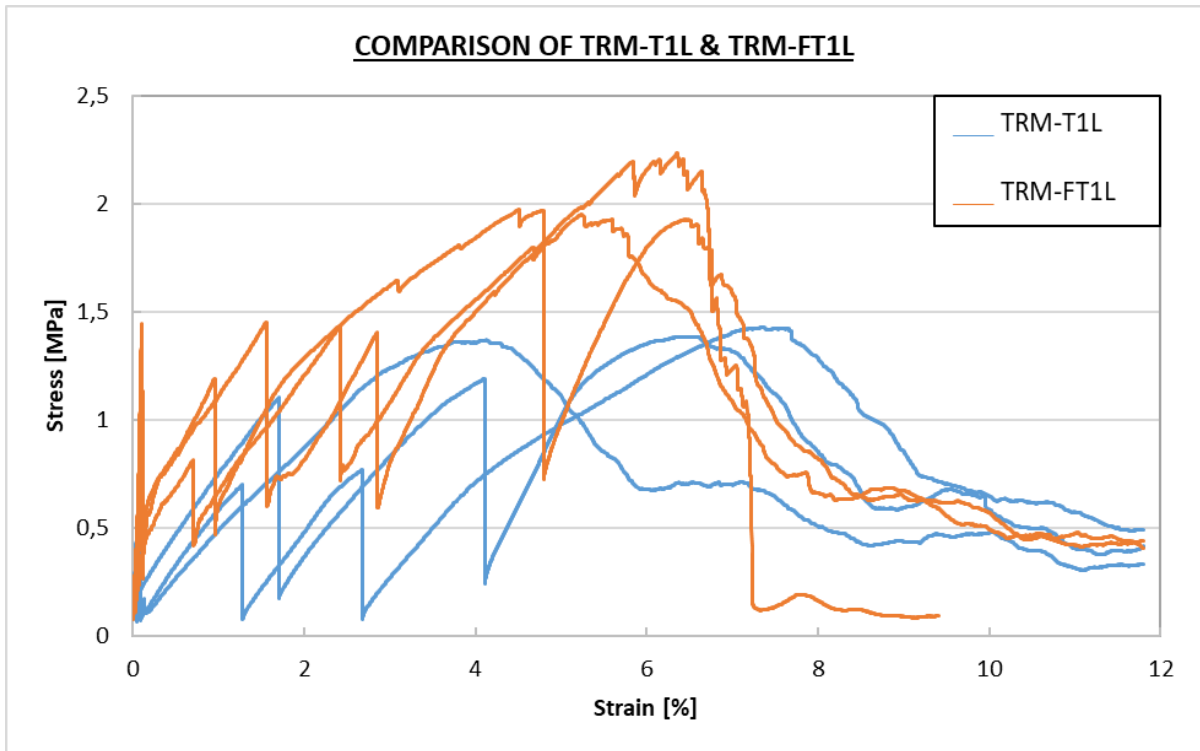


Figure 4.15 - Stress-strain response comparison of TRM-T1L versus TRM-FT1L

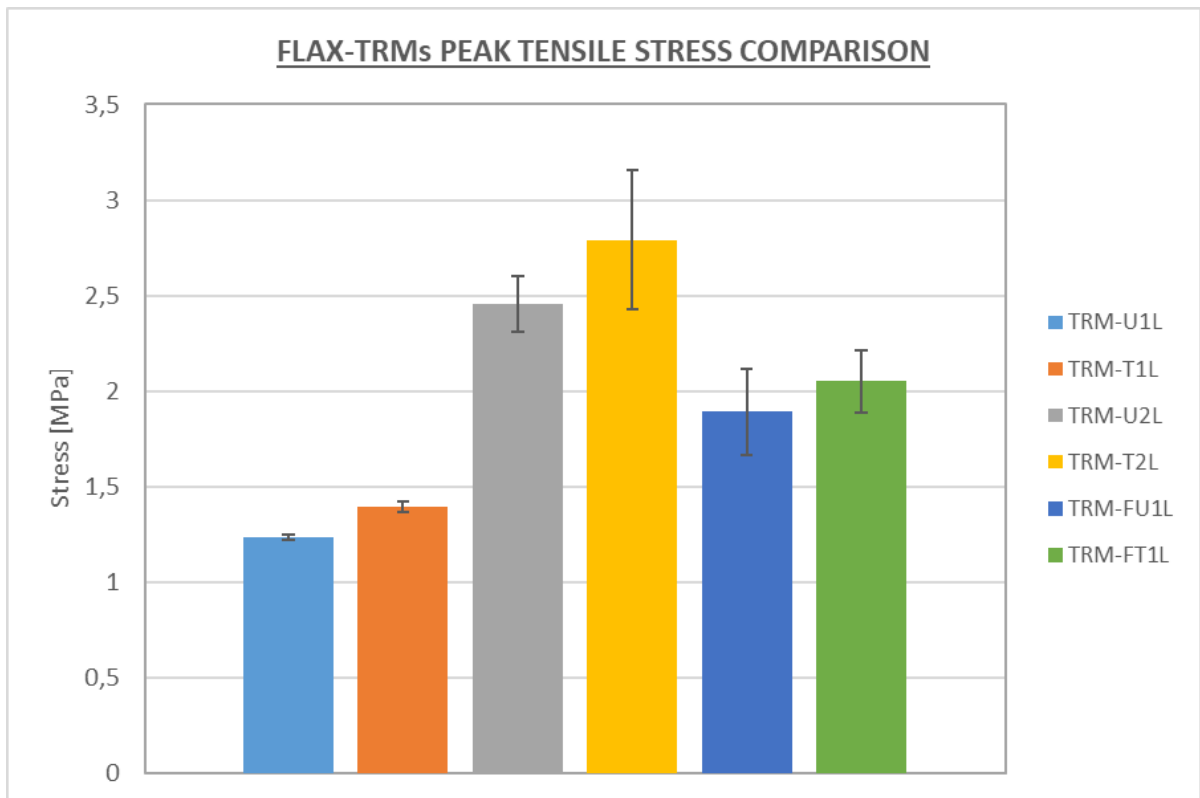


Figure 4.16 - Peak tensile strength comparison of different TRMs

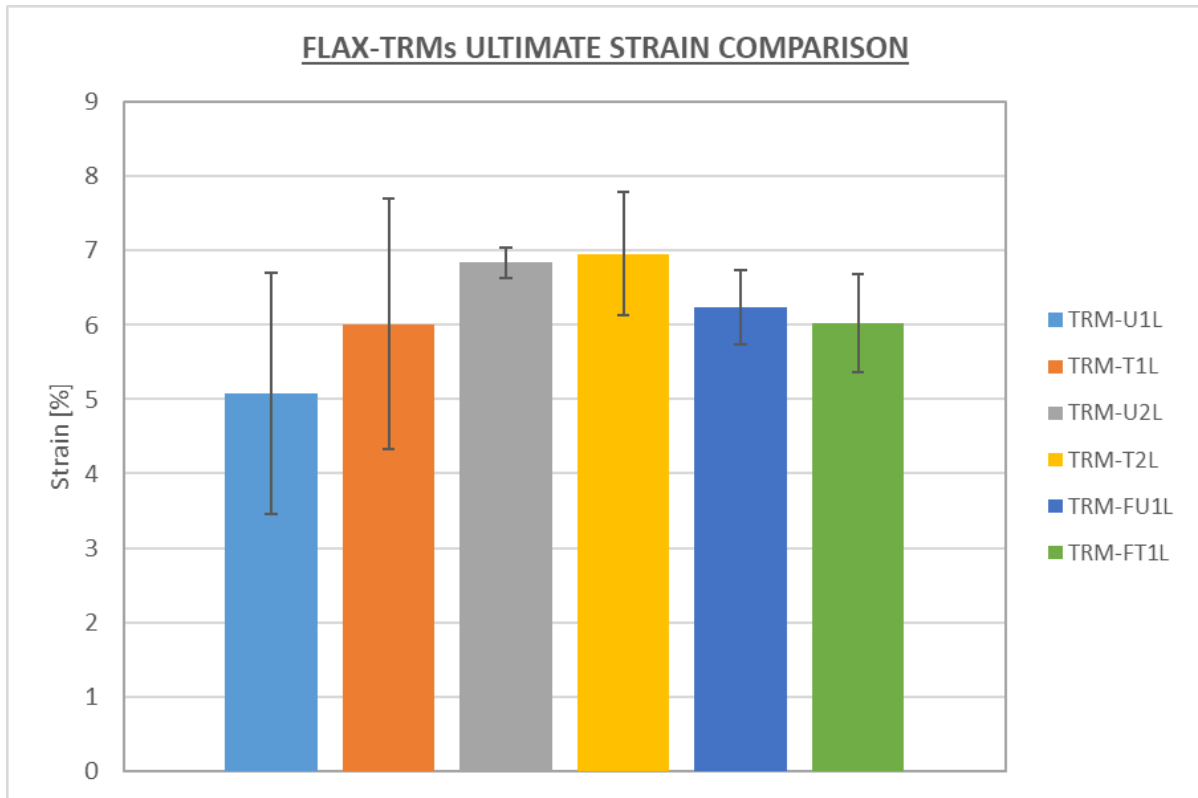


Figure 4.17 - Ultimate strain comparison of different TRMs

4.2. Pull-out Tests on Flax-Mortar Interface

4.2.1. Materials & Methods

To study the bond behavior of pre-treated and untreated flax fabric, pull-out test samples were prepared. The mortar-1 described earlier in this chapter is adapted in preparation of the pull-out samples. Cylindrical plastic molds of 25 mm in diameter and 25 mm in height were prepared in the first trial and representative flax threads extracted from treated and untreated flax textile were embedded in mortar such that they align with the central axis of the cylinders. The first trial experienced breakage of several threads before slippage from the mortar specimens. Hence a second trial was prepared with cylindrical PVC molds of 25 mm in diameter and 20 mm in height to allow for slippage of the threads instead of breakage (Figure 4.18).

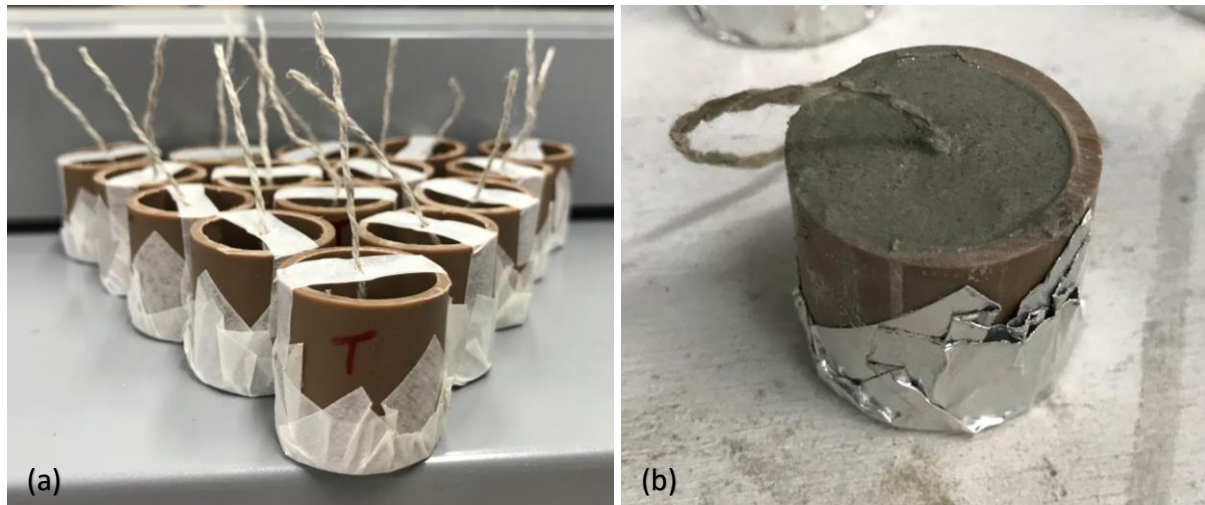


Figure 4.18 - Molds preparation for pull-out samples (a); close-up of a freshly cast sample (b)

Two series of specimens were prepared and cured in a humid chamber for 28 days before testing.

- *Pull-out UT: series of specimens consisting of untreated flax thread embedded uniaxially for a total length of 20 mm in Mortar-1.*
- *Pull-out TT: series of specimens consisting of pre-treated flax thread embedded uniaxially for a total length of 20 mm in Mortar-1.*

At least 10 specimens of each of the series were prepared and cured for 28 days in a humid chamber. The cylindrical specimens were held into place by means of mechanical clamp specifically designed for the purpose. The other end, consisting of the flax textile thread, was first glued to the aluminum tape (commonly known as duct tape, locally sold by the name of Silver Tape in Brazil) with a quick setting glue (TekBond Super Glue 793) for a length of 10 mm to avoid slippage of thread from the machine clamp during testing (Figure 4.19). The specimens were adjusted in the machine clamps such that there is negligible length of thread between the specimen and the clamping so that the elastic elongation of the thread can be ignored. The specimens were tested for pull-out in a microforce testing machine (MTS Tytron 250) with a maximum load cell of 1kN in displacement control rate of 1 mm/minute. The force and corresponding displacement data was recorded.



Figure 4.19 - Pull-out samples (a); test set-up (b)

4.2.2. Results & Discussion

The force-displacement diagram of pull-out samples of both series of specimens is presented in Figure 4.20. The graphs for both series show an initial linear branch till the first slippage of thread occurs in the mortar. An intermediate hardening stage near peak force is observed with eventual pullout of thread from the specimen while experiencing friction resistance of the mortar-thread interface. This behavior is comparable in comparison to similar studies in the past.

The peak force experienced during the test of Pull-out UT series is averaged at 37.5 N with 25% coefficient of variation while for Pull-out TT series is 31.1 N with 11% coefficient of variation. The latter shows a 17% reduction in the shear force capacity while also a reduction in the coefficient of variation of the measured results. A large variability of results is observed for different samples of Pull-out UT series with peak force values varying from 23.8 N up to 56.2 N. Conversely, Pull-out TT series shows a more homogeneous response of peak force varying from 25.3 N up to 35.9 N.

Apart from the peak force, the average response of the Pull-out TT series represents a more homogeneous behavior compared to the Pull-out UT series. Hence, it can be deduced that pretreatment tends to homogenize the flax threads in terms of mechanical response.

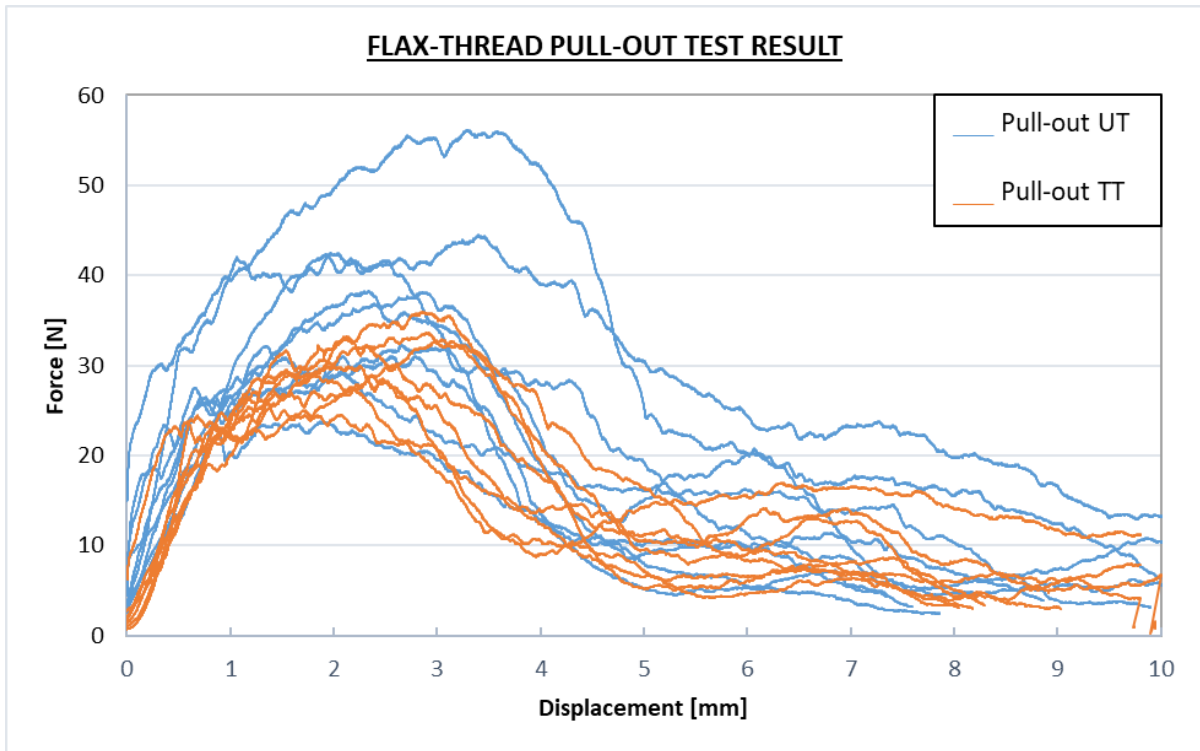


Figure 4.20 – Force versus displacement graph of pull-out test

Chapter 5

5 Mechanical Behavior of Masonry Assemblage Externally Bonded with Flax-TRMs

Mechanical characterization of flax textile and flax-TRMs performed in previous chapters validate their effectiveness for use in strengthening applications. However, there is considerable variability in the results obtained. To better understand the behavior of masonry walls strengthened with flax-TRMs, the experimental campaign is further extended to the application scale. Solid clay-brick masonry walls are prepared and tested in diagonal compression to correlate the response of flax-TRM prisms with wall assemblage and to determine the strengthening design parameters.

5.1. Materials and Methods

The walls are made of solid clay bricks of size 19 x 9 x 5 cm locally purchased in Brazil. The bricks were tested as per ASTM C67-05 for compressive strength and modulus of rupture measured as 32 MPa and 3.2 MPa respectively (Figure 5.1) [43]. Considering the limitations of the universal testing machine, a half-scale model of the brick wall of size 60 x 60 cm was developed as per ASTM 519-15 [42]. The bricks were laid in a running bond pattern with a 1 cm thick mortar between the layers and brick faces (Figure 5.2). The mortar deployed in preparation of the walls was conventional mortar (hereinafter referred to as Mortar-3) with cement to sand ratio of 1:3 and water to cement ratio of 0.65. The compressive strength at 28 days of Mortar-3 was measured as 11.5 MPa (COV 4%). Two samples of reference walls were prepared without application of externally bonded TRM; instead, a 1 cm thick layer of Mortar-1 was applied at both faces of the wall.



Figure 5.1 - Brick compression test set-up (a); test set-up for modulus of rupture (b)



Figure 5.2 - Brick wall during construction (a); fully constructed (b)

The flax textile used for strengthening is the same as characterized in chapter 3. The mortar used for strengthening is the same described as mortar-1 in chapter-4 with a compressive and flexural strength of 12.4 MPa and 1.93 MPa respectively, determined as per EN 196-1. Two specimens of walls were prepared and reinforced for each of the series of TRMs constituting mortar-1 studied in chapter 4. The series of specimens are described below:

- *Wall-Ref*: solid clay-brick wall assemblage of size 60 x 60 cm externally bonded on both faces with mortar-1.
- *Wall-U1L*: solid clay-brick wall assemblage of size 60 x 60 cm externally bonded on both faces with TRM-U1L.

- *Wall-U2L: solid clay-brick wall assemblage of size 60 x 60 cm externally bonded on both faces with TRM-U2L.*
- *Wall-T1L: solid clay-brick wall assemblage of size 60 x 60 cm externally bonded on both faces with TRM-T1L.*
- *Wall-T2L: solid clay-brick wall assemblage of size 60 x 60 cm externally bonded on both faces with TRM-T2L.*

The external strengthening of walls was carried out by applying layers of flax-TRM in following steps:

- 1- Wet the wall surface for better adhesion and then apply a thin layer of mortar and level it with a leveling-bar or trowel (Figure 5.3a).
- 2- Wet the fabric and embed it in the already applied mortar surface while keeping the fabric stretched and remove any possible creases with the help of a roller (Figure 5.3b).
- 3- Apply the second layer of mortar (Figure 5.3c) and smooth it with a trowel in case of single layered TRM or repeat step 1 & 2 in case of double layer and smooth the ultimate mortar layer with the help of a trowel (Figure 5.3d).

Walls were prepared at least 7 days before the application of the flax-TRM strengthening procedure to allow for enough strength gain of the masonry assemblage before TRM application. Walls were intermittently kept wet for 28 days before testing to allow for proper curing of the mortar. Before testing, the walls were painted with a solution of slacked lime for easy identification of development of the cracks and the cracking pattern.



Figure 5.3 - Application of 1st mortar layer (a); embedding of flax-fabric (b); application of 2nd mortar layer (c); smoothed final assemblage (d)

The diagonal compression tests were carried out at NUMATS - Center of Sustainable Materials and Technologies of Federal University of Rio de Janeiro (UFRJ), Brazil. The walls were tested by loading along one vertical diagonal under a universal testing machine (Shimadzu) with a load cell of 500 kN at a displacement control rate of 0.6 mm/minute. Two steel plates (steel angles) were used to adjust the opposite corners of the diagonal for proper load transfer (Figure 5.4). The verticality of the diagonal was ensured by using a laser leveler. The steel shoes/angles/plates were designed in such a way to ensure smooth transfer of the load to the wall diagonal without causing concentration of load at a specific point. The vertical

displacement of the machine's crosshair and the corresponding force were measured during the test.

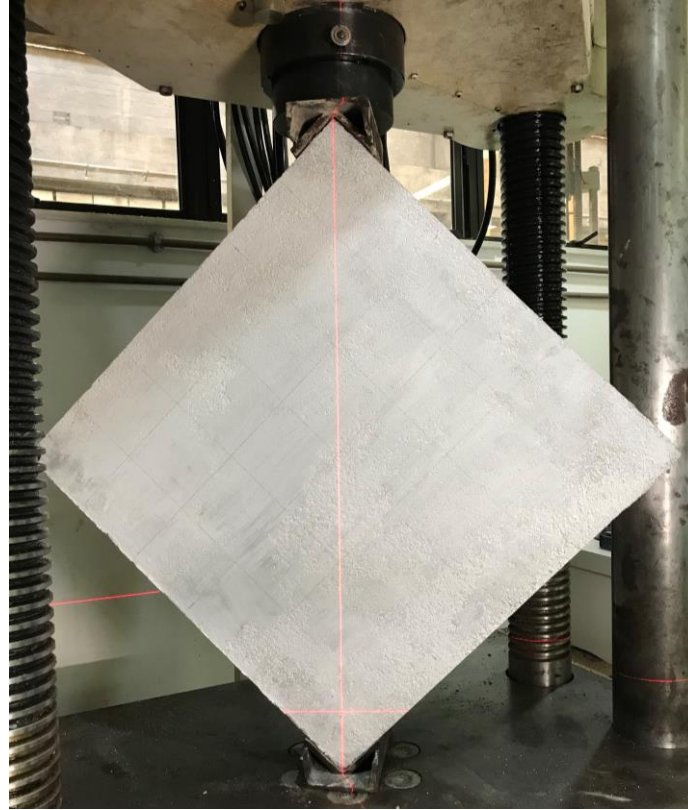


Figure 5.4 - Diagonal compression test set-up

5.2. Results and Discussion

Graph of vertical displacement (diagonal shortening) versus the applied force on the main diagonal of Wall-Ref series is presented in the Figure 5.5. The vertical loading of the wall in diagonal configuration causes a concentration of stresses along the compressed diagonal such that the cracks develop along the vertical direction parallel to the direction of load application.

The Wall-Ref series of samples show a linear load-displacement curve till the maximum load is achieved. However, a brittle failure is observed after achievement of maximum load with abrupt failure at the development of the first crack. The crack develops along the main diagonal either through the brick joints or at splitting of bricks. Due to the brittle failure and splitting of wall along the diagonal into two vertical segments, the Wall-Ref assemblage did not take any load post-peak sudden failure (Figure 5.6). The average peak load taken by the Walls-Ref series is 48.3 kN (COV 9%).

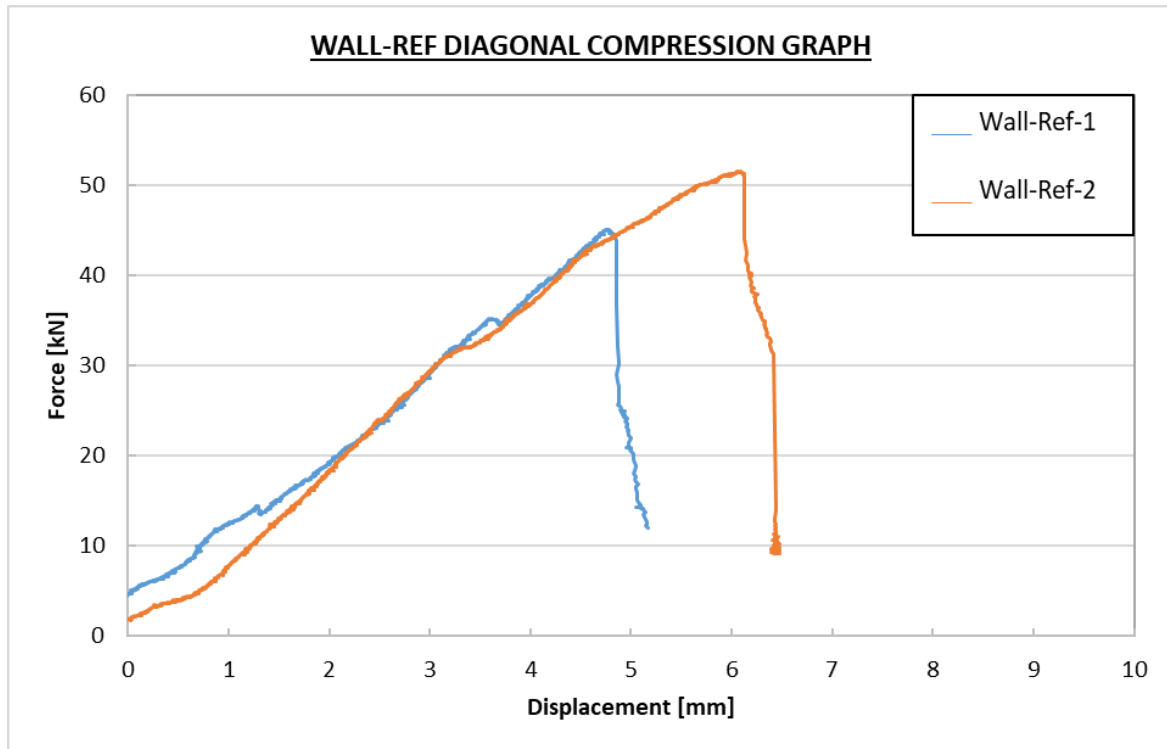


Figure 5.5 - Force versus displacement graph of Wall-Ref series

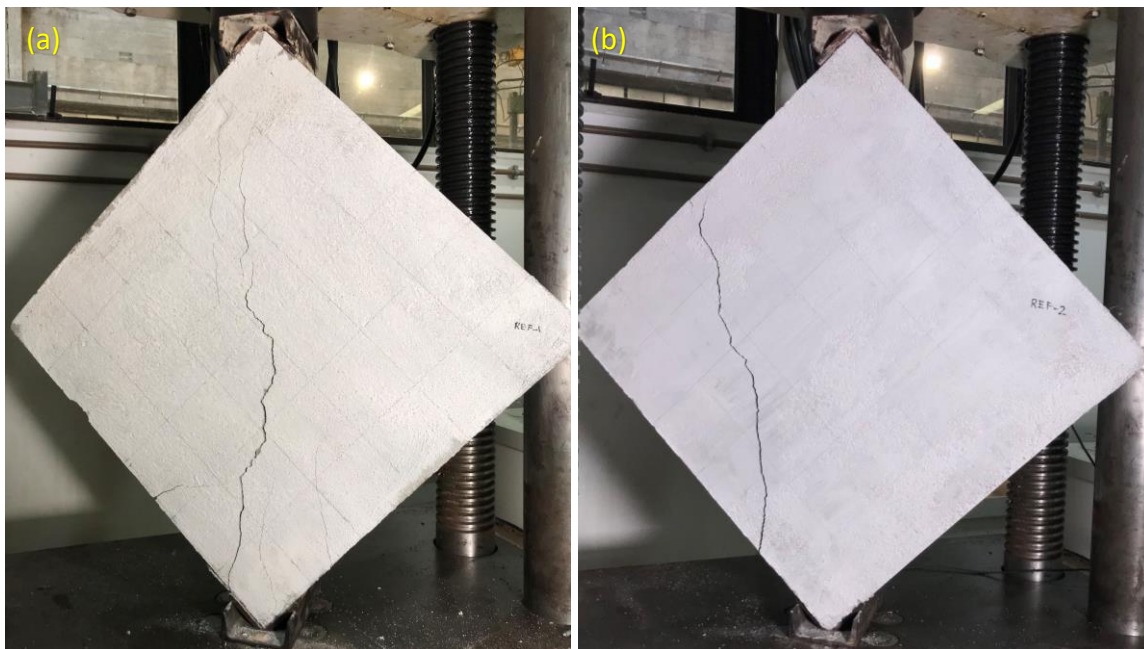


Figure 5.6 - Development of crack in Wall-Ref-1 (a); Wall-Ref-2 (b)

The response of masonry wall assemblages reinforced with flax-TRMs show a similar trend pre-peak as in the case of reference walls except that the peak load taking capacity is significantly enhanced as compared to reference walls. Alternatively, the strengthened walls showed a post peak ductile behavior with a significant load taking capacity in contrast to un-

strengthened walls. This post peak behavior is attributed to textile response after the first crack, and it is relatable to the flax-TRMs response discussed in Chapter 4.

Figure 5.7 and Figure 5.8 represent the force-displacement graphs of Wall-U1L and Wall-T1L series respectively. The Wall-U1L and Wall-T1L series showed a peak load taking capacity of 70 kN (COV 21%) and 72.7 kN (COV 2%) which is 45% and 51% higher than the Wall-Ref series, respectively. The post-peak load bearing capacity of Wall-U1L and Wall-T1L series is measured as 18 kN and 21 kN respectively.

The peak load bearing capacity of Wall-T1L series in comparison to Wall-U1L series is 4% in excess, although significantly less than what was observed in TRM tensile prisms. However, the post-peak load bearing capacity of the former is 17% higher than the latter. This can be related to the more variable nature of masonry substrate on which TRM is applied in comparison to TRM tensile prisms.

A debonding phenomenon has also been observed at fiber-matrix interface in Wall-U1L series of samples in the post-peak phase. While the Wall-T1L series represented a very homogeneous response which again proves that alkaline treatment improves the fiber-matrix bond behavior.

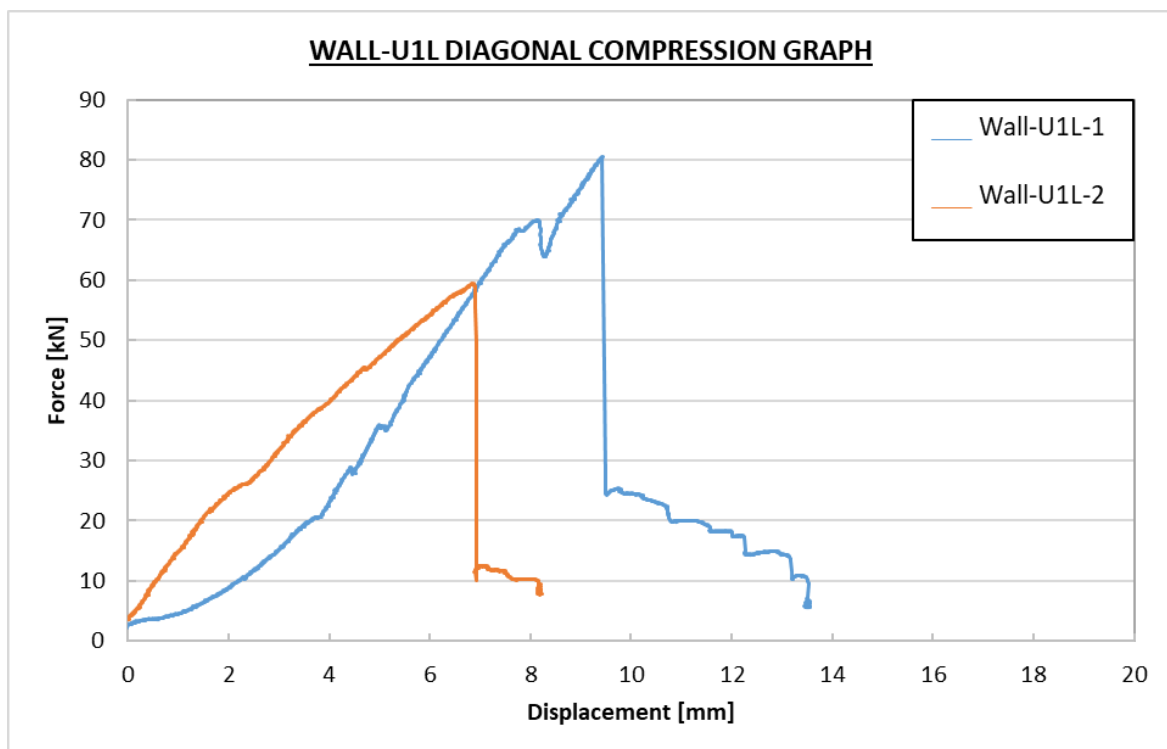


Figure 5.7 - Force versus displacement graph of Wall-U1L series

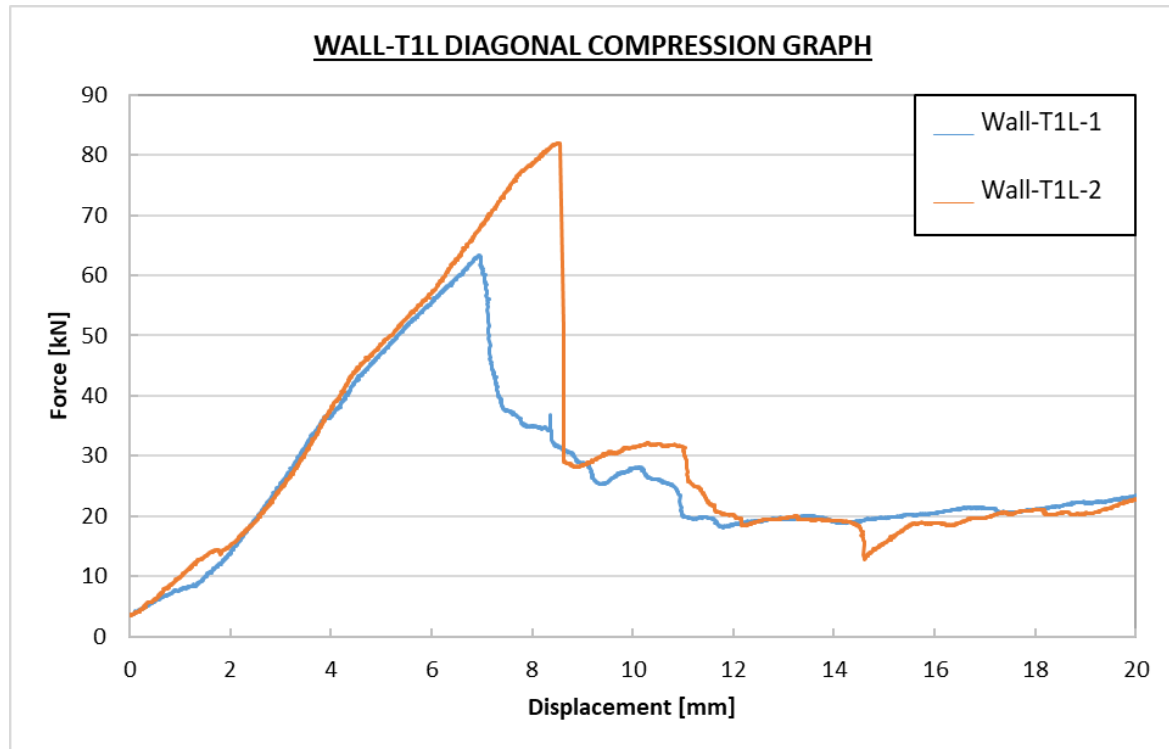


Figure 5.8 - Force versus displacement graph of Wall-T1L series

Figure 5.9 and Figure 5.10 represent the force-displacement graphs of Wall-U2L and Wall-T2L series respectively. The maximum load capacity of the Wall-U2L and Wall-T2L series was recorded as 77.2 kN (COV 2%) and 84.8 kN (COV 9%) which is 60% and 76% higher than the Wall-Ref series respectively. Apart from a significant increase in peak load capacity, a major increase of post peak load gain is observed which is a direct measure of the enhanced ductility of the strengthened walls. The post peak load taking capacity of Wall-U2L and Wall-T2L series is measured as 15 kN and 30 kN respectively.

The Wall-T2L series' load bearing capacity is observed to be 10% higher than Wall-U2L series which is comparable to similar strength enhancement measured in tensile test of TRM prims. This effect is due to better fiber-matrix bond as a result of alkaline treatment of the flax fabric. Similar to Wall-U1L series, the Wall-U2L series experienced debonding at the wall-TRM interface causing a very low post peak strength again signifying the importance of alkaline treatment of flax textile.

The crack development pattern of representative sample of each series of wall assemblage is shown in Figure 5.13.

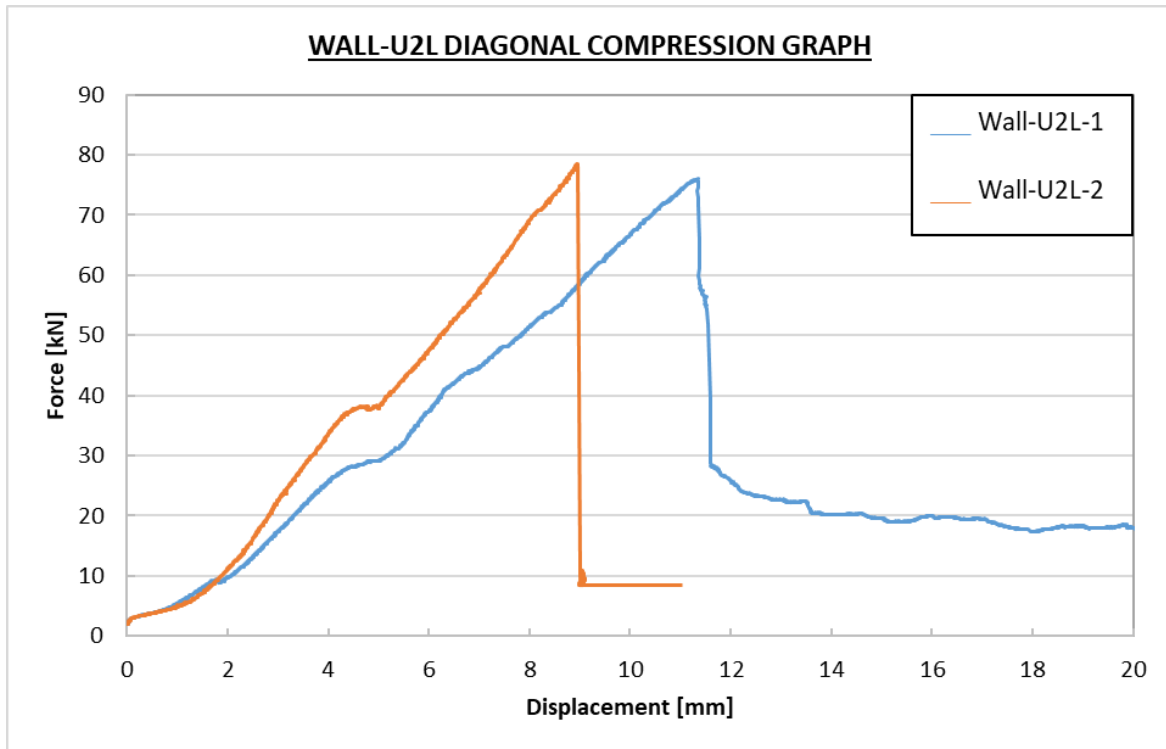


Figure 5.9 - Force versus displacement graph of Wall-U2L series

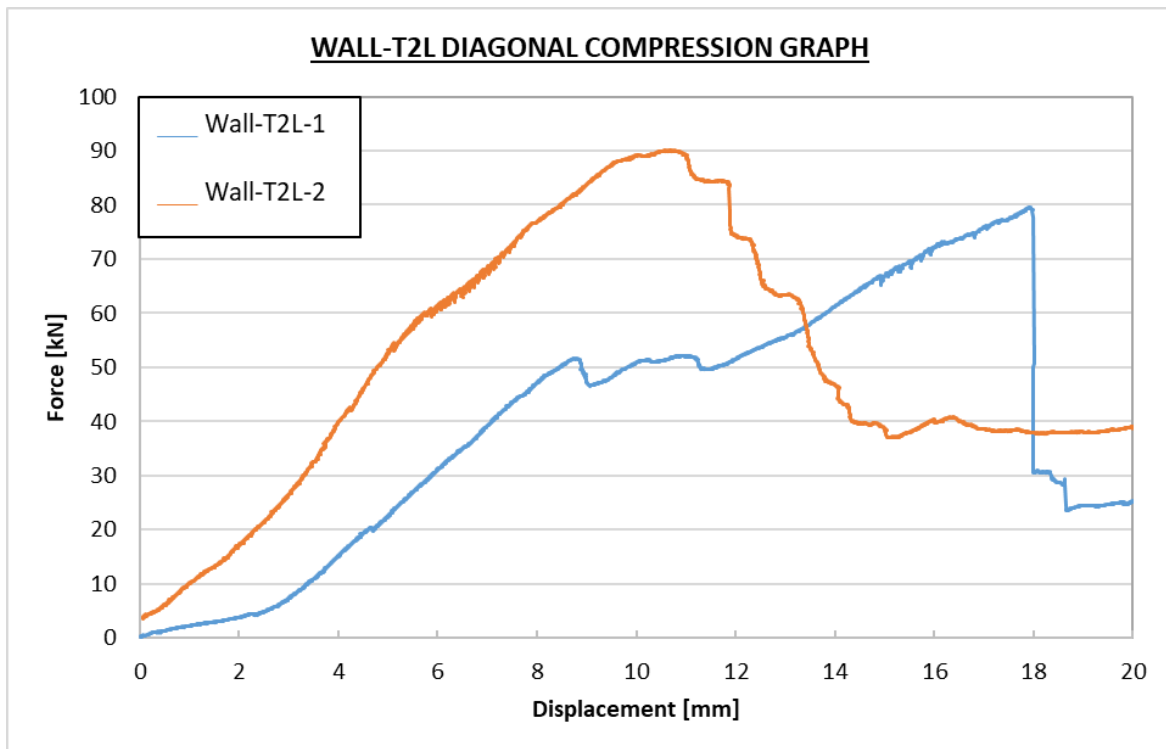


Figure 5.10 - Force versus displacement graph of Wall-T2L series

Figure 5.11 and Figure 5.12 show a comparison of average, peak and post peak load for all series of specimens. The Wall-T2L series represents not only the maximum value of peak strength but also the post peak strength compared to all other series of samples.

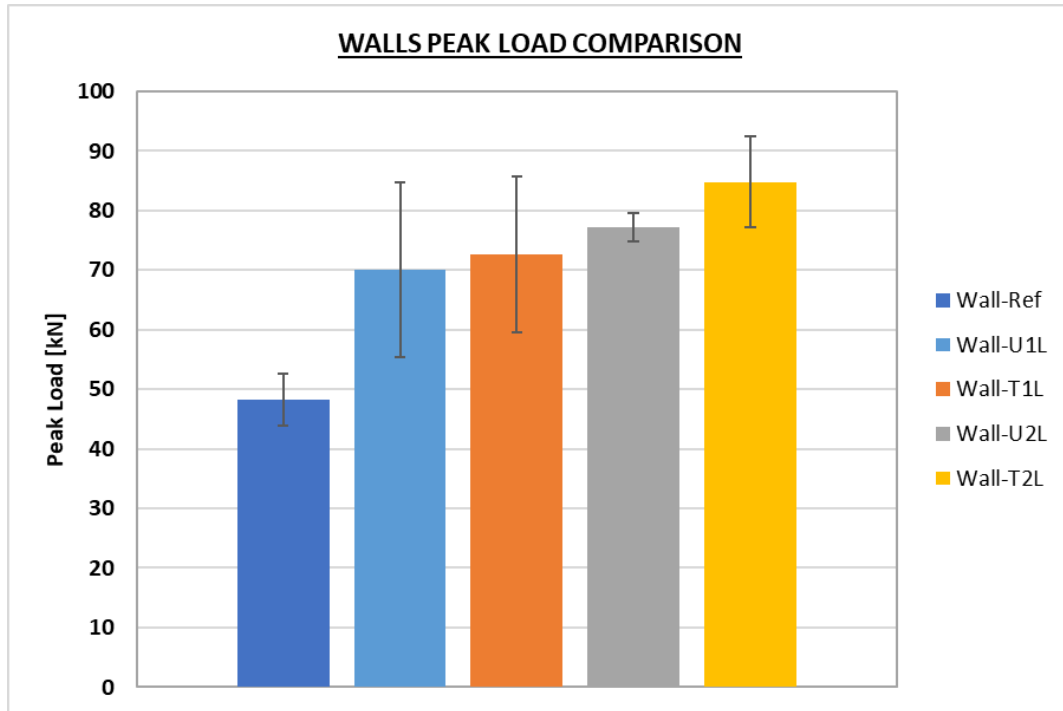


Figure 5.11 - Comparison of peak load bearing capacity of all series of walls.

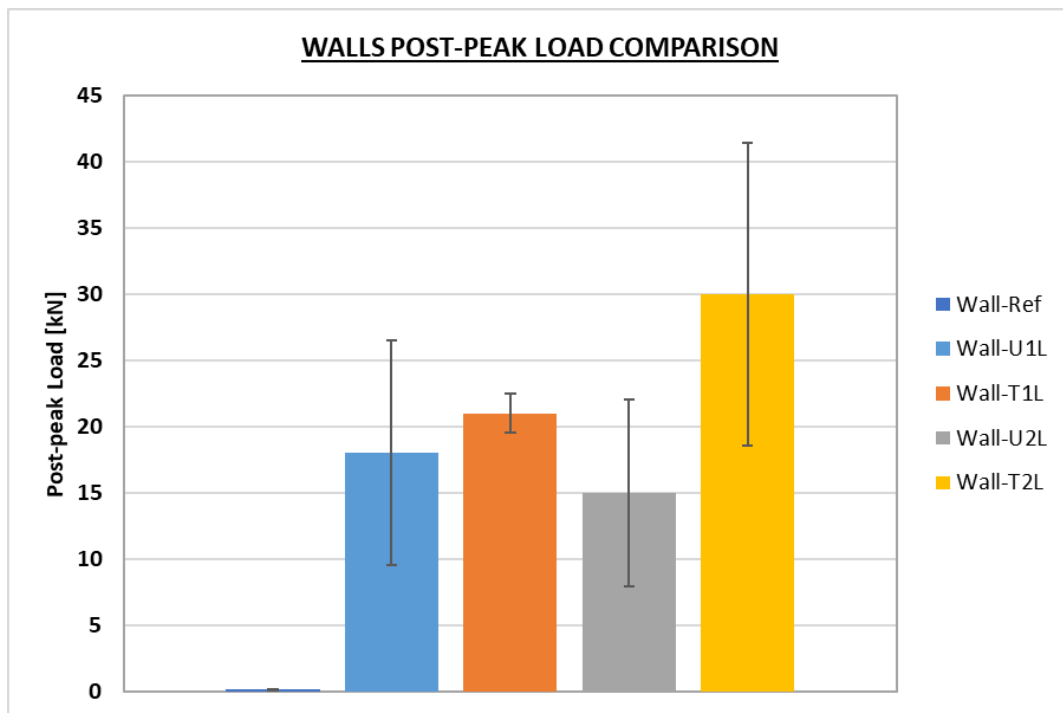


Figure 5.12 - Comparison of post-peak load bearing capacity of all series of walls.



Figure 5.13 - Crack development in representative samples of Wall-U1L (a); Wall-T1L (b); Wall-U2L (c); Wall-T2L (d)

As per the ASTM E519-15 [42], the peak shear stress (τ_0) in the middle of the masonry assemblages can be calculated according to the equation below:

$$\tau_0 = \frac{0.707 * P_{max}}{A_n}$$

Where:

- P_{max} is the peak diagonal load taken by the wall in diagonal compression test.
- A_n is the net resisting area of the wall specimen; calculate as follows:

$$A_n = \frac{(w + h)}{2} * t$$

Where:

- w is the width of the wall specimen (mm).
- h is the height of the wall specimen (mm).
- t is the total thickness of the wall specimen (mm).

The peak shear stress capacity of un-strengthened and strengthened wall series are reported in Table 5.1. A comparison of τ_0 for all series of walls is presented in Figure 5.14. The un-strengthened wall series represented a peak shear stress of 0.51 MPa (COV 9%). In comparison, Wall-T2L series show a maximum shear capacity among all the other series which is 55% and 8% higher than the Wall-Ref and Wall-U2L series respectively. It is also pertinent to note that Wall-T1L series shows a value comparable to Wall-U2L series, once again proving the effectiveness of alkaline treatment of flax fabric employed in wall strengthening.

Table 5.1 - Summary of shear strength of walls.

Sample Type	w (mm)	h (mm)	t (mm)	A_n (mm ²)	P_{max} (kN)	τ_0 (MPa)	τ_0 (MPa) (Avg)	COV (%)
REF-1	60	60	11,2	67200	45,1	0,47	0,51	9
REF-2	60	60	11,2	67200	51,5	0,54		
U1L-1	61	60,5	11,7	71077,5	80,6	0,80	0,70	21
U1L-2	61	60,5	11,6	70470	59,4	0,60		
T1L-1	61	60,5	11,3	68647,5	63,3	0,65	0,74	17
T1L-2	61	60,5	11,5	69862,5	82,0	0,83		
U2L-1	61	61	12,1	73810	76,0	0,73	0,73	1
U2L-2	61	60,5	12,4	75330	78,4	0,74		
T2L-1	61	61	12,1	73810	79,5	0,76	0,79	5
T2L-2	61	60,5	12,8	77760	90,0	0,82		

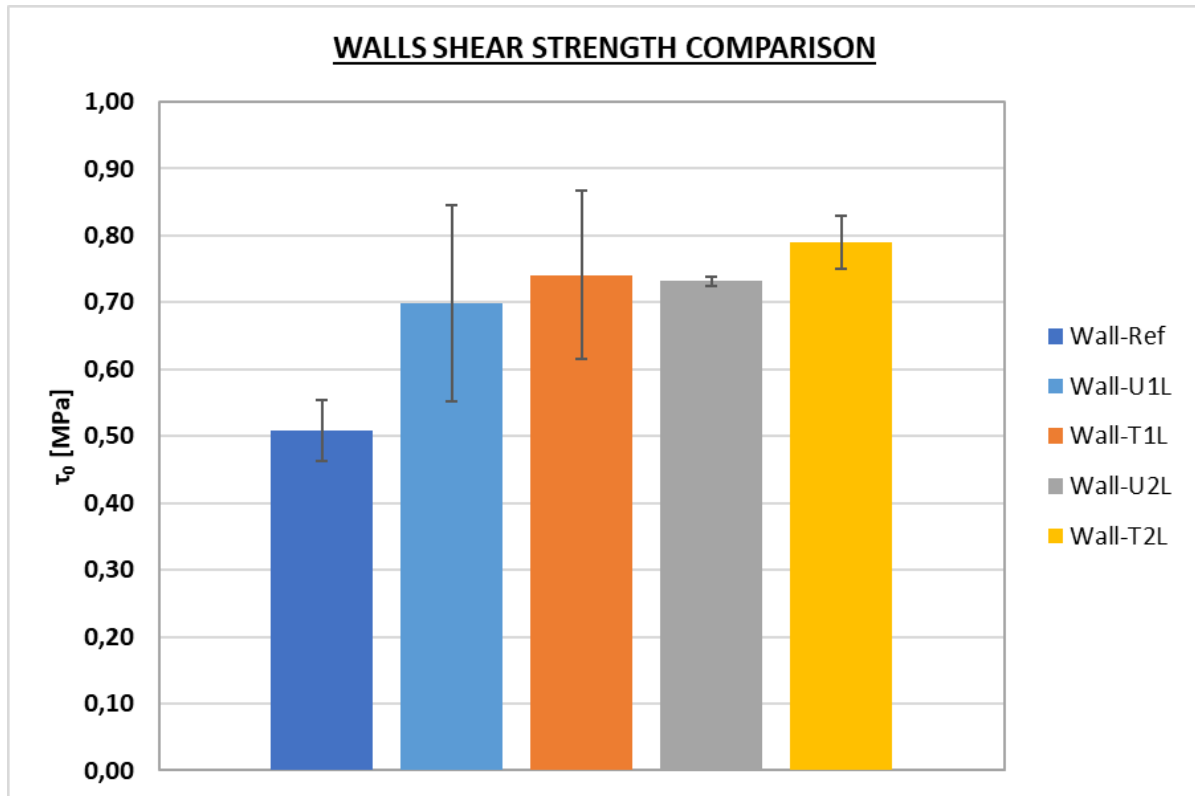


Figure 5.14 - Walls shear strength comparison

The post peak behavior can be analyzed using the procedure proposed by Fantilli et al. [33] as explained in Figure 5.15. The new post-peak diagram presented in Figure 5.15b can be generated by using the $P-d$ curve depicted in Figure 5.15a. This diagram displays the values of normalized load ($y = P/P_{max}$) on the y-axis and the difference x between the actual measured post-peak deflection and d_p (measured deflection at peak load) on the x-axis. The post-peak diagrams are limited to $x = 4 \text{ mm}$, which is the point where the post peak load carrying capacity of unreinforced walls is null. The area A_f , enclosed by the post-peak curves in Figure 5.15b can be used to estimate the walls' fracture toughness [37].

In Figure 5.15b, the post-peak curve can be approximated by a bi-linear relationship as shown in Figure 5.15c. Therefore, the important parameters are P_{max} , which is the wall's peak strength, and its related deformation d_p . The post-peak stage's residual stress can be determined by approximating A_f using the values $[x_1, y_1]$ and $[4 \text{ mm}, y_2]$. The capacity of N-TRM to improve the ductility of the wall can be determined by calculating the value of A_f using the following formula:

$$A_f = \frac{1 + y_1}{2} * x_1 + \frac{y_1 + y_2}{2} * (4 - x_1)$$

Where, y_1 represents the normalized load taken by the wall right before failure; y_2 represents the normalized post-peak load value in presence of large cracks; x_1 (in mm) on x-axis value corresponding to y_1 . A higher value of y_1 and A_f indicates a better N-TRM and

increased toughness of the externally strengthened wall. The corresponding values of these parameters obtained from the most representative wall samples for each series are presented in Table 5.2. The measured A_f values of Wall-T2L series are 115%, 138%, and 219% higher than the corresponding Wall-U2L, Wall-T1L, and Wall-U1L series respectively.

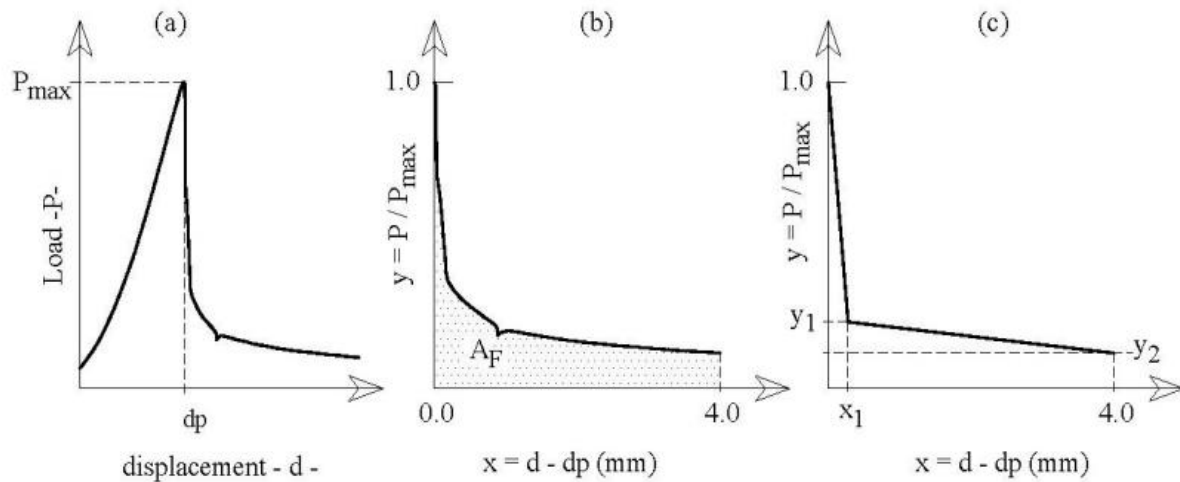


Figure 5.15 - Wall diagonal compression result: a) load vs. displacement (P-d) diagram; b) post-peak curve; c) idealized bilinear post-peak curve to determine TRM effect [37].

Table 5.2 - Summary of fracture toughness parameters of all walls.

Wall Type	P_{max}	d_p	x_1	y_1	y_2	A_f
Wall-Ref	52	6,09	0	0	0	0
Wall-U1L	81	9,43	0,07	0,31	0,13	0,91
Wall-T1L	82	8,49	0,12	0,35	0,23	1,22
Wall-U2L	76	11,35	0,24	0,38	0,25	1,35
Wall-T2L	90	10,56	2,13	0,71	0,44	2,90

Wall fracture toughness parameter A_f , y_1 , y_2 and P_{max} are plotted against number of cracks developed in TRM tensile test specimens (Figure 5.16). More the number of cracks developed in TRM prisms in tensile test corresponds to higher fracture toughness of the wall strengthened with TRM.

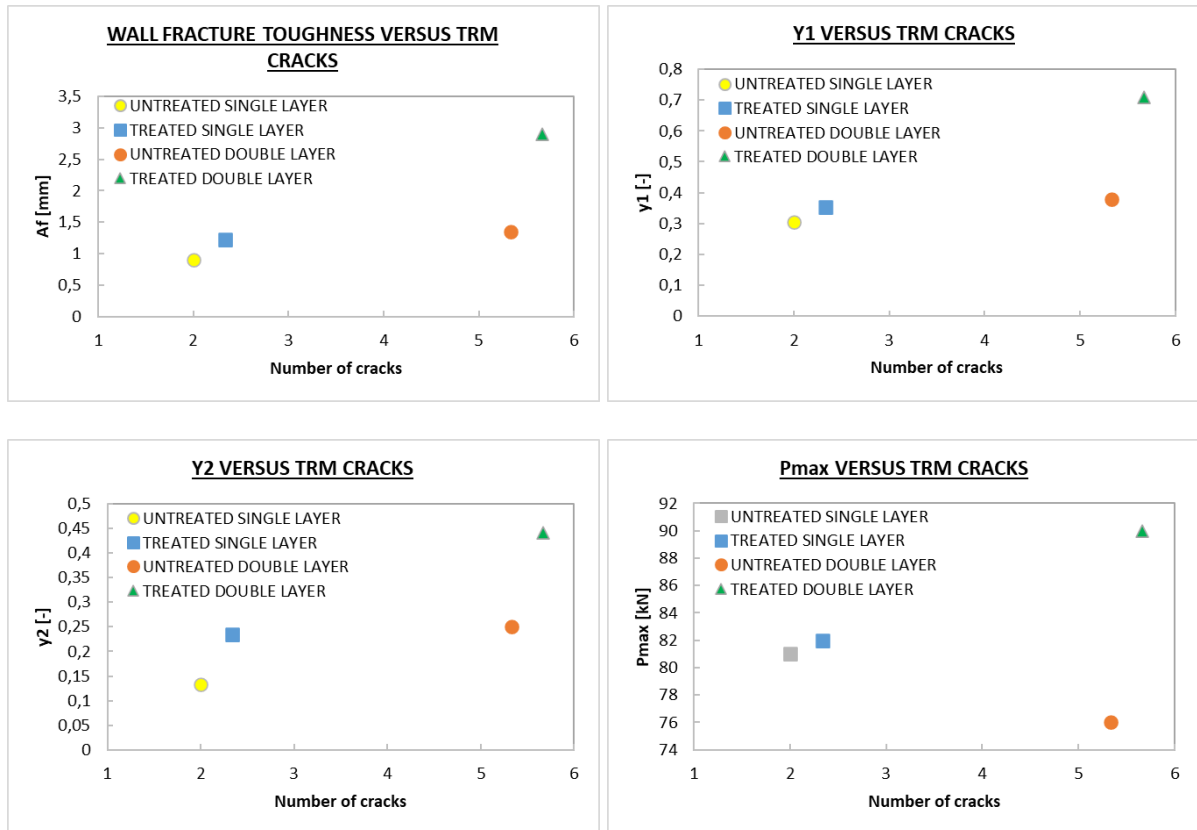


Figure 5.16 - Wall fracture toughness parameter A_f versus number of cracks in TRM (a); y_1 vs number of cracks (b); y_2 vs number of cracks (c); P_{max} vs number of cracks developed in TRM tensile test.

Chapter 6

6 Conclusions and Recommendations

The experimental campaign was conducted to determine the improvement in mechanical properties of masonry structures strengthened with flax-TRMs embedded with flax fabric subjected to alkaline treatment.

6.1. Main Conclusions

Initially, the change in yarn morphology and tensile response of flax yarn, thread and fabric strip was determined and compared with the reference untreated samples. Secondly, the tensile response of TRMs and the pull-out behavior of threads embedded with treated and untreated flax-fabric strips and threads respectively, was investigated and compared. Thirdly, short jute fibers were incorporated in the mortar matrix to prepare fiber-based mortar matrix embedded with flax-fabric and their tensile response was compared with conventional mortar based TRMs.

Lastly, brick masonry wall assemblages were prepared and reinforced with treated and untreated flax based TRMs and tested in diagonal compression test to investigate their mechanical performance and compare the results with reference un-strengthened wall specimens. Following conclusions can be drawn based on the results of the performed experimental investigations:

- Analysis of OM and SEM images represents a considerable change in fiber morphology with an increase in perimeter of the thread cross-section while decreasing the net cross-section area by 4%. Additionally, the dispersion of these physical properties in untreated flax threads is more evident as compared to the treated threads measured with a reduction of coefficient of variation of cross-section area from 11% to 6% from former to latter.
- The tensile strength of flax thread and fabric slightly decreases with alkaline treatment mainly due to the removal of amorphous layers from the fiber structure. While the mean deformability of the individual thread is observed to decrease, the fabric strips experienced an increase in the ultimate strain.
- TRMs prepared with treated flax-fabric represented a better mechanical performance both in terms of higher ultimate strength and corresponding strain at peak. An increase of 13% in the peak strength was observed in TRMs embedded with treated flax-fabric compared to untreated. An increase of 19% and 2% in ultimate strain was observed in TRMs embedded with single and double layer treated flax-fabric respectively, compared to untreated ones.
- A smaller crack opening at any fixed value of stress was observed in treated series of specimens compared to untreated samples.

- Addition of short jute fibers in the mortar matrix results in considerable improvement of mechanical properties of TRMs without changing the mortar mix design. An increase of 48% in peak strength of TRM prepared with addition of 5% jute fibers was observed in comparison to the reference conventional mortar.
- TRMs prepared with fiber-based mortar represent the highest exploitation ratio of the flax fabric compared to the TRMs prepared with reference conventional mortar thus representing the most efficient solution.
- Pull-out tests of treated flax threads show a reduction in peak slip force while also significantly reducing the coefficient of variation compared to untreated flax threads.
- Walls strengthened with TRM embedded with 2 layers of treated flax fabric represented the most promising strengthening solution in terms of peak strength capacity as well as wall fracture toughness A_f compared to untreated (single and double layer) and treated single layer.
- Walls strengthened with untreated flax fabric layers experienced debonding at the fiber-matrix interface.

In conclusion, the experimental campaign highlights the potential of using sustainable materials and practices as a replacement of conventional materials and methods.

6.2. Recommendations

This study details the outcomes of using alkaline treatment on plant-based flax fabric to be employed in seismic strengthening of masonry structures. A preliminary study on the use of fiber-based matrix has also been employed and noteworthy results have been observed. There is, however, a need to perform comprehensive studies aimed at obtaining the optimum fiber-mortar ratio to get the best results. Similar other fabric treatments as reported in literature can be applied to determine the best possible treatment to enhance the TRM properties. A proper fabric stretching procedure needs to be developed to get the best possible results in terms of TRM deformability.

References

- [1] M. Pepe, R. Lombardi, G. Ferrara, S. Agnetti and E. Martinelli, "Experimental Characterisation of Lime-Based Textile-Reinforced Mortar Systems Made of Either Jute or Flax Fabrics," *Materials*, vol. 16, no. 2, p. 709, 2023.
- [2] CNR DT 215/2018, "Istruzioni per la Progettazione, L'esecuzione ed il Controllo di Interventi di Consolidamento Statico Mediante L'utilizzo di Compositi Fibrorinforzati a Matrice Inorganica," Consiglio Nazionale delle Ricerche, Roma, Italy, 2018.
- [3] C. Papanicolaou, T. Triantafyllou and M. Lekka, "Externally bonded grids as strengthening and seismic retrofitting materials of masonry panels," *Construction and Building Materials*, vol. 25, no. 2, pp. 504-514, 2011.
- [4] G. Giacomini, "Innovative strengthening materials for the post-earthquake reconstruction of L'Aquila masonries," in *Proceedings of the 10th international conference on structural analysis of historical constructions*, LEUVEN, 2016.
- [5] F. Giuseppe, B. Coppola, L. Di Maio, L. Incarnato and E. Martinelli, "Tensile strength of flax fabrics to be used as reinforcement in cement-based composites: experimental tests under different environmental exposures," *Composites Part B: Engineering*, vol. 168, pp. 511-523, 2019.
- [6] L. Ascione, G. de Felice and S. De Santis, "A qualification method for externally bonded Fibre Reinforced Cementitious Matrix (FRCM) strengthening systems," *Composites Part B: Engineering*, vol. 78, pp. 497-506, 2015.
- [7] G. Ferrara, *Flax-TRM Composite Systems for Strengthening of Masonry: From Material Identification to Structural Behavior*, Cham, Switzerland: Springer, 2021.
- [8] Technical Committee RILEM and 232-TDT (Wolfgang Brameshuber), "Recommendation of RILEM TC 232-TDT: test methods and design of textile reinforced concrete," *Materials and Structures*, vol. 49, p. 4923-4927, 2016.
- [9] A. Bilotta, F. Ceroni, G. P. Lignola and A. Prota, "Use of DIC technique for investigating the behaviour of FRCM materials for strengthening masonry elements," *Composites Part B: Engineering*, vol. 129, pp. 251-270, 2017.
- [10] S. De Santis, F. Giulia Carozzi, G. de Felice and C. Poggi, "Test methods for Textile Reinforced Mortar systems," *Composites Part B: Engineering*, vol. 127, pp. 121-132, 2017.
- [11] M. Saidi and A. Gabor, "Use of distributed optical fibre as a strain sensor in textile reinforced cementitious matrix composites," *Measurement*, vol. 140, pp. 323-333, 2019.
- [12] M. Del Zoppo, M. Di Ludovico and A. Prota, "Analysis of FRCM and CRM parameters for the in-plane shear strengthening of different URM types," *Composites Part B: Engineering*, vol. 171, pp. 20-33, 2019.

- [13] ASTM E519–2: 2003, "Standard test method for diagonal tension (shear) in masonry assemblages," ASTM committee C15 on manufactured Masonry Units, West Conshohocken, PA, US , 2003.
- [14] L. A. S. Kouris and T. C. Triantafillou, "State-of-the-art on strengthening of masonry structures with textile reinforced mortar (TRM)," *Construction and Building Materials*, vol. 180, pp. 1221-1233, 2018.
- [15] C. Meyer, "The greening of the concrete industry," *Cement and Concrete Composites*, vol. 31, pp. 601-605, 2009.
- [16] L. Coppola and et al., "Binders alternative to Portland cement and waste management for sustainable construction – Part 2," *Journal of Applied Biomaterials & Functional Materials*, vol. 16, no. 4, pp. 207-221, 2018.
- [17] L. Yan, N. Chouw and K. Jayaraman, "Flax fibre and its composites – A review," *Composites Part B: Engineering*, vol. 56, pp. 296-317, 2014.
- [18] A. Komuraiah, N. Shyam Kumar and B. Durga Prasad, "Chemical Composition of Natural Fibers and its Influence on their Mechanical Properties," *Mechanics of Composite Materials*, vol. 50, pp. 359-376, 2014.
- [19] K. Charlet, S. Eve, m. Gomina and J. Breard, "Tensile deformation of a flax fiber," *Procedia Engineering*, vol. 1, no. 1, pp. 233-236, 2009.
- [20] M. P. Dicker, P. F. Duckworth, A. B. Baker, G. Francois, M. K. Hazzard and P. M. Weaver, "Green composites: A review of material attributes and complementary applications," *Manufacturing*, vol. 56, pp. 280-289, 2014.
- [21] D. B. Dittenber and H. V. GangaRao, "Critical review of recent publications on use of natural composites in infrastructure," *Composites Part A: Applied Science and Manufacturing*, vol. 43, no. 8, pp. 1419-1429, 2012.
- [22] S. R. Ferreira, E. Martinelli, M. Pepe, F. d. A. Silva and R. D. T. Filho, "Inverse identification of the bond behavior for jute fibers in cementitious matrix," *Composites Part B: Engineering*, vol. 95, pp. 440-452, 2016.
- [23] M. E. A. Fidelis, R. D. T. Filho, F. d. A. Silva, B. Mobasher, S. Müller and V. Mechtcherine, "Interface characteristics of jute fiber systems in a cementitious matrix," *Cement and Concrete Research*, vol. 116, pp. 252-265, 2019.
- [24] S. R. Ferreira, F. d. A. Silva, P. R. L. Lima and R. D. T. Filho, "Effect of fiber treatments on the sisal fiber properties and fiber–matrix bond in cement based systems," *Construction and Building Materials*, vol. 101, pp. 730-740, 2015.
- [25] M. Aly, M. Hashmi, A. G. Olabi, K. Y. Benyounis, M. Messeiry, A. Hussain and E. F. Abadir, "Optimization of Alkaline Treatment Conditions of Flax Fiber Using Box–Behnken Method," *Journal of Natural Fibers*, vol. 9, no. 4, 2012.
- [26] I. Bonfanti, A. P. Fantilli, R. D. T. Filho and Y. G. d. S. Mendonca, "An Experimental Campaign on the Use of Natural Fibre-Reinforced," *Key Engineering Materials*, vol. 916, pp. 457-464, 2022.

- [27] R. Olivito, O. Cevallos and A. Carrozzini, "Development of durable cementitious composites using sisal and flax fabrics for reinforcement of masonry structures," *Materials & Design*, vol. 57, pp. 258-268, 2014.
- [28] O. Cevallos and R. Olivito, "Effects of fabric parameters on the tensile behaviour of sustainable cementitious composites," *Composites Part B: Engineering*, vol. 69, pp. 256-266, 2015.
- [29] G. Ferrara and E. Martinelli, "Tensile behaviour of textile reinforced mortar composite systems with flax fibres," in *Proceedings of the 12th fib international PhD symposium in civil engineering*, Prague, 2018.
- [30] L. Mercedes, L. Gil and E. Bernat-Maso, "Mechanical performance of vegetal fabric reinforced cementitious matrix (FRCM) composites," *Construction and Building Materials*, vol. 175, pp. 161-173, 2018.
- [31] G. Ferrara, M. Pepe, R. D. T. Filho and E. Martinelli, "Mechanical Response and Analysis of Cracking Process in Hybrid TRM Composites with Flax Textile and Curauá Fibres," *Polymers*, vol. 13, no. 5, 2021.
- [32] G. Ferrara, M. Pepe, E. Martinelli and R. D. T. Filho, "Influence of an Impregnation Treatment on the Morphology and Mechanical Behaviour of Flax Yarns Embedded in Hydraulic Lime Mortar," *Fibers*, vol. 7, no. 4, 2019.
- [33] A. P. Fantilli, S. Sicardi and F. Dotti, "The use of wool as fiber-reinforcement in cement-based mortar," *Construction and Building Materials*, vol. 139, pp. 562-569, 2017.
- [34] M. Ramesh, K. Palanikumar and K. H. Reddy, "Plant fibre based bio-composites: Sustainable and renewable green materials," *Renewable and Sustainable Energy Reviews*, vol. 79, pp. 558-584, 2017.
- [35] R. Codispoti, D. V. Oliveira, R. S. Olivito, P. B. Lourenço and R. Fangueiro, "Mechanical performance of natural fiber-reinforced composites for the strengthening of masonry," *Composites Part B: Engineering*, vol. 77, pp. 74-83, 2015.
- [36] G. Ferrara, C. Caggegi, E. Martinelli and A. Gabor, "Shear capacity of masonry walls externally strengthened using Flax-TRM composite systems: experimental tests and comparative assessment," *Construction and Building Materials*, vol. 261, no. 120490, 2020.
- [37] I. Bonfanti, Sviluppo e caratterizzazione di sistemi di rinforzo in fibra naturale per il miglioramento e l'adeguamento sismico delle strutture in muratura, Torino: Politecnico di Torino, 2019.
- [38] EN 196-1:1994, "Methods of Testing Cement-Part 1: Determination of strength," European Committee of Standardization, Brussels, Belgium, 1994.
- [39] EN 1015-3:2004, "Methods of test for mortar for masonry - Part 3: Determination of consistence of fresh mortar (by flow table)," European Committee for Standardization, Brussels, Belgium, 2004.

- [40] ACI 549.4R-13, "Guide to Design and Construction of Externally Bonded Fabric Reinforced Cementitious Matrix (FRCM) Systems for Repair and Strengthening Concrete and Masonry Structures," American Concrete Institute, Michigan, USA, 2013.
- [41] AC434, "Acceptance criteria for masonry and concrete strengthening using Fiber-Reinforced Cementitious Matrix (FRCM) composite systems," International Code Council Evaluation Service, 2011.
- [42] ASTM E519-15, "Standard Test Method for Diagonal Tension (Shear) in Masonry Assemblages," ASTM International, Pennsylvania, USA, 2015.
- [43] ASTM C67-05, "Standard Test Method for Sampling and Testing Brick and Structural Clay Tile," ASTM International, Pennsylvania, USA, 2005.